BELL TELEPHONE LABORATORIES
INCORPORATED

COVER SHEET FOR TECHNICAL MEMORANDUM

TITLE Active RC Filter Building Blocks Using Frequency Emphasizing Networks Part I

MM 67-5316-1

CASE CHARGED— 38763

DATE— January 3, 1967

FILING CASES— 38763-17

AUTHOR— G. S. Moschytz

FILING SUBJECTS— Hybrid Integrated Circuits
Linear Filter Design for Microminiaturization
Thin Film Circuit Design

ABSTRACT

An engineering approach to integrated active RC filter design is described. Complex filter networks are broken down into a small family of cascadable second order filter building blocks consisting of tantalum thin film RC networks and semiconductor integrated operational amplifiers. The same building blocks are used for any desired filter configuration such as low-, high-, or bandpass filters, notch filters, etc. They therefore possess the uniformity necessary for high production quantities, batch processing and the economical advantages that go with these methods.

A series of three memoranda will describe the filter design method in detail. In the present memorandum (Part I), the circuit design considerations leading to the second order building blocks are discussed, and their hybrid integrated implementation briefly described. In Part II the sensitivity and stability characteristics of the networks will be analyzed and predicted performance compared with measurements made on some laboratory models. Some practical filter design examples will also be described in detail. Finally, in Part III the development of the ceramic substrates presently being prepared, that combine the tantalum thin film resistors and capacitors with semiconductor integrated operational amplifiers will be discussed.

DISTRIBUTION

(REFER G.E.I. 13.9-3)

COMPLETE MEMORANDUM TO

CORRESPONDENCE FILES:

OFFICIAL FILE COPY (FORM E-7770) — PLUS ONE WHITE COPY FOR EACH ADDITIONAL CASE REFERENCED

REPRODUCIBLE COPY (FORM E-1328)

REFERENCE COPIES (10)

PATENT DIVISION (2) IF MEMORANDUM HAS PATENT SIGNIFICANCE

H. W. Augustadt - WR
W. M. Bacon - HO
W. L. Brune - WL
G. K. Burns - HO
H. O. Burton - HO
A. Busala - IN
R. E. Cardwell - HO
J. R. Davey - HO
W. H. D'Zio - HO
A. C. Ekvall - WL
B. E. Epting - GR
D. Feldman - WH
W. O. Fleckenstein - HO
R. D. Fracassi - HO
F. E. Froehlich - HO
A. M. Gerrish - HO
H. A. Henning - HO
D. Hirsch - HO
H. J. Jones - WL
N. Knapp, Jr. - HO
M. C. Kolibaba - HO
J. T. Koo - AL
E. R. Kretzmer - HO
J. J. Lang - MV
W. J. Lawless - HO
S. C. Lee - WH
O. Loosme - HO
G. H. Lovell - WL
R. W. Lucky - HO
G. Malek - HO
D. G. Marsh - HO
J. E. Mazo - HO
D. A. McLean - AL
D. G. Medill - HO
C. R. Moster - HO
W. H. Orr - AL
G. Pasternack - HO
B. K. Peele - BU
G. A. Porter - MV

COVER SHEET ONLY TO

CORRESPONDENCE FILES:

THREE COPIES—PLUS ONE COPY FOR EACH ADDITIONAL FILING SUBJECT

Complete Memorandum to (Cont'd)

G. A. Pullis - HO
D. W. Rice - HO
J. W. Schaefer - HO
P. L. Schmidt - WL
P. O. Schuh - IN
N. E. Snow - HO
J. Salz - HO
S. G. Student, Jr. - HO
W. Thelen - MV
R. N. Watts - HO
T. J. West - MH
R. L. Whalin - HO
F. J. Witt - MV
R. W. Wyndrum, Jr. - WH
R. M. Zeigler - HO
H. M. Zydney - HO

E-1328 (11-63)

DATE FILE

BELL TELEPHONE LABORATORIES
INCORPORATED

SUBJECT: Active RC Filter Building Blocks Using Frequency Emphasizing Networks Part I - Case 38763-17

DATE: January 3, 1967

FROM: G. S. Moschytz
MM67-5316-1

MEMORANDUM FOR FILE

I. INTRODUCTION

Transmission filters have always occupied a relatively large proportion of the overall equipment volume in communication systems. The main reason for the large size of these filters is the size of the inductors. Inductor size (and cost) increases with decreasing frequency which is one reason for the excessive space occupied by filters in low frequency and voiceband communication systems. As more and more of the remaining circuitry, in particular the digital circuitry, in these systems is being microminiaturized using semiconductor integrated devices, the discrepancy between filter size and overall equipment size is becoming increasingly apparent. Because this discrepancy is widespread in communication systems today, much effort is presently being devoted to filter size reduction. The seemingly obvious approach to attaining this objective would be to microminiaturize inductors. Unfortunately, this cannot be done for a variety of technological reasons [1,2,3]. The only alternative

is to build inductorless filters. This is possible by combining passive RC components with active devices such as feedback amplifiers, negative impedance converters, gyrators and the like.

Engineering has been defined as the application of scientific principles and knowledge to produce an economic solution to problems. Thus the subject discussed in this memorandum may be considered as an attempted engineering approach to integrated filter design. That such an approach, whether it be the one discussed here or another, is called for at the present time is evident from the disparity between the abundance of literature on active RC filter designs for microminiaturization and the almost total absence of any commercial implementations. One reason for this is that active RC filters are generally designed individually for the wide variety of applications, such as exists in the communications field. The individual production quantities are therefore invariably too low to absorb the high tooling and handling costs that go with integrated circuit production [4]. Thus integrated active filter networks have remained far too costly for commercial use.

To overcome the problem of economical feasibility, we have taken the same approach with integrated linear circuits that has proven to be highly successful with integrated

digital circuits. It consists of reducing the number of filter varieties by breaking complex filter networks up into a small family of basic second-order building blocks. If these building blocks can be designed to be sufficiently versatile to cover a large range of low-runner applications, then they will be required in large enough quantities as to justify the high costs involved in integrated circuit production. This concept of circuit standardization is vital to the economical success of any type of integrated circuit and introduces design guidelines that differ fundamentally from those pertaining to conventional circuit design [5]. Thus integrated circuits designed with the fewest number of components to satisfy a particular requirement may be very much less economical than a more complex design that covers a larger variety of applications, thereby increasing the total production volume.

It has been shown recently [6] that hybrid active networks, consisting of tantalum thin film passive networks and semiconductor integrated active networks are ideally suited for the design of low sensitivity active RC filters. Also the building block design approach, besides being economical, is particularly suitable for low sensitivity networks. This is because network sensitivity increases rapidly with the order of the network. Since sensitivity is a particularly critical parameter in RC active networks, it becomes

impractical to design high Q networks with more than one pair of conjugate complex poles per active section.* Higher order networks then result as a composite combination of the separate active sections, i.e., building blocks, each realizing one pair of conjugate complex poles and the required transmission zeros. For ease of implementation it is desirable to have building blocks possessing inherent isolating characteristics so that there is negligible interaction between them. In this way the transmission poles and zeros can be individually realized by the corresponding separate sections.

This memorandum describes the design of second-order† hybrid integrated filter sections consisting of tantalum thin film RC networks and semiconductor integrated operational amplifiers. The sections display excellent isolating properties and thus lend themselves particularly well to cascade design. Other configurations, such as parallel connections of the single building blocks are also practicable. The same building blocks are used for any desired filter

---

* Negative real poles may be added without detrimental effects on the sensitivity, as they can be realized by passive RC networks.

† The network order here refers to the number of conjugate complex poles.

configuration such as low-, high-, or bandpass filters, notch filters, etc. They therefore possess the uniformity necessary for high production quantities, batch processing and the economical advantages that go with these methods. Amongst other things the filter design approach described here is a result of making full use of the design features afforded by operational amplifiers such as ideal summing points (i.e., virtual ground), very high input and very low output impedances. Operational amplifiers in themselves are attractive economically since their versatility ensures them a very wide field of applications outside that of active filters.

In the filter design method described here, the required second-order network is decomposed into two separate sections in cascade. The first consists of a passive RC approximation of the desired transfer characteristic. It provides the asymptotic response of the desired filter transfer function. The second is an active RC correcting network, consisting essentially of an RC null network and two operational amplifiers. This is required to provide a frequency emphasizing response in the vicinity of the natural frequencies of the preceding passive RC network. Connected in tandem the two sections provide the initial filter characteristic accurately.

The big advantage of this scheme is that all basic second-order networks can be obtained by simple variations of the passive RC configuration only. But for changes in the RC time constant of the null network, the active RC correcting network following remains essentially the same for all filter applications. As will be shown, even these circuit changes can be minimized by fully utilizing the circuit peculiarities inherent in thin film circuit technology. It should be emphasized again here that it was precisely with a view to this circuit standardization at the cost, perhaps, of circuit simplicity, that the filter design method described here evolved. Thus, for example, a medium damped second-order low-pass filter could certainly be designed using a simpler active RC network than is suggested here. On the other hand, however, that same simpler circuit could not be used to obtain a high Q second-order bandpass network.

For convenience to the reader, this memorandum has been broken up into three parts. In Part I the circuit design considerations leading to the second-order filter building blocks are discussed. The hybrid integrated implementation of these networks is also briefly described. In Part II the sensitivity and stability characteristics of the networks will be analyzed and predicted performance compared with measurements made on laboratory models. Practical filter design examples will also be described in detail.

Finally, in Part III the ceramic substrates presently being prepared that combine tantalum thin film resistors and capacitors with semiconductor integrated operational amplifiers will be discussed in detail.

II. PRINCIPLE OF ACTIVE RC FILTER DESIGN USING FREQUENCY EMPHASIZING NETWORKS

1. Decomposition of Nth Order Networks

The transmission function of an Nth order Linear, Lumped-Parameter, Finite (LLF) Network can always be obtained as the ratio of two polynomials with real coefficients in the variable s, namely:

$$T_o(s) = \frac{y}{x} = \frac{b_m s^m + b_{m-1} s^{m-1} + \ldots + b_1 s + b_o}{a_n s^n + a_{n-1} s^{n-1} + \ldots + a_1 s + a_o} . \qquad (1)$$

where: x = input signal

y = output signal

$n \geq m$

and the roots of the numerator and denominator polynomials are either real or occur in conjugate complex pairs.

In the active RC realization of this type of function it has invariably been found impractical to design higher than second-order networks at a time. This is primarily due to the relatively high transmission sensitivity to component variations of active linear networks and to the fact that this sensitivity increases rapidly with the order of the network. Another reason is that active linear

networks are potentially unstable inasmuch as their transmission poles are not inherently constrained from crossing the $j\omega$-axis into the right-half plane. Therefore networks of higher order are also more difficult to stabilize. Thus it has become common practice in active filter design to realize any given Nth order transmission function by a cascade of first and second-order networks. The corresponding second-order transmission functions are obtained by factoring the given Nth order characteristic into simple and biquadratic terms each having real coefficients. The transmission function then has the form:

$$T_o(s) = K \frac{\prod_{i=1}^{m/2} \left(s^2 + 2\sigma_{z_i} s + \omega_{z_i}^2 \right)}{\prod_{j=1}^{n/2} \left(s^2 + 2\sigma_{p_j} s + \omega_{p_j}^2 \right)} \qquad (2)$$

for m and n even, and

$$T_o(s) = K \frac{(s-z) \prod_{i=1}^{\frac{m-1}{2}} \left(s^2 + 2\sigma_{z_i} s + \omega_{z_i}^2 \right)}{(s-p) \prod_{j=1}^{\frac{n-1}{2}} \left(s^2 + 2\sigma_{p_j} s + \omega_{p_j}^2 \right)} . \qquad (3)$$

for m and n odd. Because the coefficients of each term are real, the corresponding roots are either real or conjugate complex.

2. Decomposition of Second-Order Networks

From the foregoing remarks it follows that inductorless filter design generally consists of designing cascadable active RC networks to realize transmission functions whose most general form is given by:

$$T(s) = K \frac{s^2 + \frac{\omega_z}{q_z} s + \omega_z^2}{s^2 + \frac{\omega_p}{q_p} s + \omega_p^2} \qquad (4)$$

where

$$q = \frac{\omega}{2\sigma} \qquad (5)$$

q is called the inverse damping factor and the subscripts z and p stand for "zero" and "pole" respectively. In general, Equation (4) defines a pair of conjugate complex zeros and poles as shown in Figure 1.

It is in the design of active RC equivalents to the basic second-order networks generally required, that available active synthesis methods differ. In general,

different active RC configurations are used for each basic network. In the method to be described here, the required second-order network is decomposed into two separate sections in cascade. The first provides a passive RC approximation of the desired transfer characteristic. The second is an active RC correcting network such that the two sections in tandem provide the initial characteristic accurately. By following this approach, basic second-order networks can be obtained by simple variations of the passive RC configuration only. Furthermore, the active RC correcting network provides isolation between section pairs so that complex filter configurations can be obtained by cascading second-order stages without the need for buffer amplifiers.

We first consider the passive RC approximation of Equation (4). Theoretically the RC realization of the numerator is not restricted in any way, i.e., the roots of this polynomial may be located anywhere in the complex frequency plane. If we confine ourselves to three terminal RC networks, however, then the zeros of Equation (4) are excluded from the positive real axis. It is in the realization of the denominator that the major limitation imposed by passive RC networks becomes apparent. The roots of the denominator are the natural frequencies or the transmission poles of the network. They are therefore restricted to the negative real axis of the complex frequency plane

(including the origin and infinity) and they must be simple, i.e., of first order.

The roots of the denominator of Equation (4) are defined by an equation of the form:

$$s^2 + \frac{\omega}{q} s + \omega^2 = 0 \qquad (6)$$

Figure 2 shows the locus of the roots of Equation (6) for q varying from zero to infinity. As q is increased from zero, the two poles approach each other on the negative real axis starting at zero and minus infinity, respectively. The two poles coincide at

$$s_{1,2} = -\omega \qquad (7)$$

where

$$q = q_{cr} = 0.5 \qquad (8)$$

For $q > 0.5$ the two poles become conjugate complex and lie on a semicircle of radius ω. For infinitly high q the two poles finally end up on the $j\omega$-axis at a distance of $\pm\omega$ from the origin.

From the foregoing discussion, it follows that Equation (4) can only be realized accurately by a passive RC network so long as q_p is smaller than 0.5. In general,

the specified inverse damping factor will exceed this limiting value, i.e., the required transmission poles will be conjugate complex. This is the case to be considered here, since from a practical point of view it is the starting point for active RC network synthesis.

For the general case that q_p is larger than 0.5 Equation (4) can be approximated by selecting a new parameter q_R in the denominator such that it is realizable by a passive RC network. Therefore,

$$q_R < 0.5 \quad . \tag{9}*$$

and the corresponding passive RC transmission function is given by:

$$T_R(s) = K_R \frac{s^2 + \frac{\omega_z}{q_z} s + \omega_z^2}{s^2 + \frac{\omega_p}{q_R} s + \omega_p^2} \tag{10}$$

where K_R is a scaling factor determined by the impedance level of the RC network. The pole-zero diagram of $T_R(s)$ is shown in Figure 3a.

To obtain the characteristic originally specified by Equation (4) $T_R(s)$ must now be multiplied by a correcting function $T_A(s)$ such that:

---

* q_R may not <u>equal</u> 0.5 since the negative real poles of an RC network must be simple.

$$T_A(s) = \frac{T(s)}{T_R(s)} = K_A \cdot \frac{s^2 + \frac{\omega_p}{q_R} s + \omega_p^2}{s^2 + \frac{\omega_p}{q_p}(s) + \omega_p^2} \qquad (11)$$

where

$$K_A = \frac{K}{K_R} \qquad (12)$$

and by definition:

$$q_p > q_R \qquad (13)$$

Since the inverse damping factor in the denominator of this function is larger than 0.5, it can only be realized by an active RC network when inductors are not to be used.

At this point it is of interest to examine the active correcting function $T_A(s)$ more closely. Since we are restricting ourselves to second-order networks the expression given by Equation (11) is the most general to occur. By definition, the zeros of $T_A(s)$ are negative real, the poles conjugate complex. They are geometrically related as shown by the corresponding pole-zero diagram in Figure 3b. Introducing the normalized angular frequency

$$\Omega = \frac{\omega}{\omega_p} \qquad (14)$$

the amplitude response of the correcting function is given by:

$$| T_A(\Omega) = K_A \left[\frac{\left(\frac{1}{\Omega} - \Omega \right)^2 + \frac{1}{q_R^2}}{\left(\frac{1}{\Omega} - \Omega \right)^2 + \frac{1}{q_p^2}} \right]^{1/2} \tag{15}$$

For $\Omega >> 1$:

$$| T_A(j\Omega) |_{\Omega \to \infty} = K_A \tag{16}$$

and for $\Omega = 0$:

$$| T_A(j\Omega) |_{\Omega=0} = K_A \tag{17}$$

Thus the response approaches the constant value K_A at high and low frequencies and is symmetrical to the normalized angular frequency $\Omega = 1$. The peak response occurs at this frequency and is given by

$$\hat{T}_A = | T_A(j\Omega) |_{\Omega=1} = \frac{q_p}{q_R} \cdot K_A \tag{18}$$

As a result of the expressions given by Equations (13), (16), (17), and (18), it is clear that the correction function $T_A(s)$ defines a frequency emphasizing characteristic as shown qualitatively by the plot of Equation (15) in Figure 4. Thus frequency emphasis is required of the active correcting network in the vicinity of the undamped natural frequency ω_p of Equation (4). In effect it simulates the resonance or energy storage properties common to LC, but unobtainable with passive RC networks.

The frequency selectivity of a Frequency Emphasizing Network (hereafter referred to as an FEN) can be defined in the conventional way namely by the quality factor Q (see Appendix A). This is the ratio of the normalized center frequency ($\Omega = 1$) and the bandwidth corresponding to the two -3 db frequencies. Referring to Figure 4, the lower of these two frequencies is

$$\Omega_\ell = \sqrt{\frac{1}{4q_A^2} + 1} - \frac{1}{2q_A} \tag{19}$$

where

$$q_A = \sqrt{q_p^2 - 2q_R^2} \tag{20}$$

Since the two -3 db frequencies are geometrically symmetrical to the center frequency $\Omega = 1$, the higher frequency results as

$$\Omega_h = \frac{1}{\Omega_\ell} \tag{21}$$

and

$$Q_{FEN} = \frac{1}{\Omega_h - \Omega_\ell} = q_A = \sqrt{q_p^2 - 2q_R^2} \tag{22}$$

The proposed method of active network design can now be summarized as follows:

1) A given nth-order transmission function $T_o(s)$ is partitioned into a product of second-order characteristics with real coefficients:

$$T_o = \prod_{i=1}^{n/2} T_i(s) \tag{23}$$

If n is odd a first-order factor will be present in this product.

2) Each second-order term $T_i(s)$ is in turn decomposed into the product of two second-order functions. The first is realized by a passive RC 3-terminal network

that determines the basic, i.e., the asymptotic filter characteristics of $T_i(s)$. The second is a universal active RC FEN that is independent of the filter type specified by $T_i(s)$ and provides frequency emphasis or LC resonance properties in the vicinity of the undamped natural frequencies of $T_i(s)$.

These two steps are represented symbolically in Figure 5. By following this procedure we shall see later how active filters can be realized by a family of general-purpose integrated circuits. They can be obtained by simple modifications of a single universal filter building block. First, however, the decomposition of some representative second-order networks is illustrated.

III. ILLUSTRATIVE EXAMPLES OF SECOND-ORDER NETWORK DESIGN

It may already be clear to the reader, at this point, that the only network synthesis involved in the procedure described here is the passive RC realization of the transfer function $T_R(s)$. Since we are initially restricting ourselves to second-order networks, this is not a very formidable problem. It becomes still less so if $T_R(s)$ can be selected as a transfer immitance. In this case, the passive RC networks can be synthesized without having to consider their driving-point properties. As can be seen from Figure 6, this is possible, if for example, the input impedance to the FEN is negligibly small. In this case,

$$T_R(s) = \left.\frac{I_0}{E_1}\right|_{E_0=0} = -[y_{21}]_R \qquad (24)$$

If this expression is valid, a passive RC 2-port must be designed to realize a specified short circuit transfer admittance. Numerous synthesis techniques exist for this purpose [7,8,9]. RC ladder networks are obtained for transmission zeros on the negative real axis including zero and infinity. When imaginary transmission zeros are required, balanced networks with more than one transmission path between input and output invariably result [10,11]. Applying some

of the circuit configurations resulting from these synthesis methods, in particular those suggested by Balabanian and Cinkilie [12],* the short circuit transfer admittances of a number of representative second-order RC networks were calculated in Appendix B. The results are compiled in Table 1.

To obtain a specified voltage transfer function T(s), the transfer function of the active correcting network to be cascaded with the passive RC 2-port, characterized by Equation (24), results as:

$$T_A(s) = \left.\frac{E_2}{I_0}\right|_{I_2=0} = [Z_{21}]_A \qquad (25)$$

where the designations refer to Figure 6.

The decomposition will now be illustrated by some examples. Equations (24) and (25) have been assumed to apply. We first consider a second-order low-pass filter whose voltage transfer function is given by:

$$T(s) = \frac{1}{s^2 + \frac{\omega_p}{q_p} + \omega_p^2} \qquad (26)$$

---

* These configurations were derived using the synthesis method advanced by Hakimi and Seshu.

where

$$q_p > 0.5$$

and

$$K = 1 .$$

The amplitude response defined by this transfer function depends on the parameter q_p as shown by the plotted curves in Figure 7a.

The decomposition into two sections first consists of finding the corresponding passive RC network to approximate the response specified by Equation (26). Any one of the three networks under (1) in Table 1 can be used. With the configuration (1c) and assuming $\rho = 1$ we obtain:

$$T_R(s) = [y_{21}]_R = \frac{\omega_p^2}{3R} \cdot \frac{1}{s^2 + 2.66\omega_p s + \omega_p^2} \qquad (27)$$

where $q_R = 0.375$. The amplitude response for this value of q_R is shown in Figure 7a.

The response of the FEN results as:

$$T_A(s) = [Z_{21}]_A = \frac{T(s)}{T_R(s)} = \frac{3R}{\omega_p^2} \cdot \frac{s^2 + 2.66\omega_p s + \omega_p^2}{s^2 + \frac{\omega_p s}{q_p} + \omega_p^2} \qquad (28)$$

The amplitude response of $T_A(s)$ can be obtained from Figure 7a by substracting the curve for $q_R = 0.375$ from the curve for the particular value of q_p required and subsequently scaling it to obtain a peak value of $8q_pR/\omega_p^2$. Cascading the RC network with an appropriate FEN, the second-order low-pass filter specified by Equation (26) can thus be realized by the low-pass configuration shown in Table 2.

The other examples shown in Table 2 were derived by using Table 1 and following precisely the same procedure as described above. The normalized characteristics of the first four are shown in Figures 7a to 7d for a limited range of the parameter q_p.

The poles of the RC networks were chosen arbitrarily in these examples. The considerations determining their choice will be discussed later. Amongst other things it will be shown that for simplicity of FEN design, they should always be chosen with the same inverse damping factor q_R.

IV. THE DESIGN OF FREQUENCY EMPHASIZING NETWORKS

In this section the design of the active correcting network whose response is specified by Equation (11) will be discussed. As was pointed out earlier, this response is invariably that of a Frequency Emphasizing Network (FEN). Depending on the application in question, the main difference between FENs, beside the particular frequency of operation,

is in the degree of frequency emphasis required. Highly selective networks, such as high Q bandpass sections, will require very much more frequency emphasis at the "resonant" frequency than say a critically damped low-pass network. FEN design will therefore be considered separately for these two different types of applications. It will be shown later, however, that the design of the one is very similar to that of the other - so that both configurations can be simply derived from one and the same network.

The analysis in this section is made assuming idealized active devices and passive components. It is intended primarily to show the circuit design principles with which the FENs can be obtained. A detailed analysis will follow in the sections on FEN sensitivity and stability, in Part II of this memorandum.

1. Medium Selectivity FENs (MSFENs)

Consider the block diagram shown in Figure 8. It consists of an inverting Voltage Controlled Voltage Source (VCVS) μ, a noninverting VCVS β, and a feedback network $T_N(s)$. The transmission function of this network is given by:

$$T_F(s) = \frac{E_2}{E_1}(s) = -\frac{\mu}{1+\mu\beta \cdot T_N(s)} . \qquad (29)$$

If $T_N(s)$ is the transfer response of an infinite null network as given by

$$T_N(s) = K_N \frac{s^2 + \omega_n^2}{s^2 + \frac{\omega_n}{q_N} s + \omega_n^2} \tag{30}$$

then Equation (29) becomes

$$T_F(s) = K_F \frac{s^2 + \frac{\omega_n}{q_N} s + \omega_n^2}{s^2 + \frac{\omega_n}{q_F} s + \omega_n^2} \tag{31}$$

where

$$K_F = - \frac{\mu}{1+\mu\beta K_N} \tag{32}$$

and

$$q_F = (1+\mu\beta K_N) q_N. \tag{33}$$

It is shown in Appendix D that a passive RC Twin-T network has the voltage transfer response given by Equation (30). For the potentially symmetrical Twin-T shown in Figure 9, we then get

$$\omega_n = \frac{1}{RC} \tag{34}$$

$$q_N = \frac{1}{2} \cdot \frac{\rho}{1+\rho} \tag{35}$$

and

$$K_N = 1 \tag{36}$$

The factor ρ gives a measure of the Twin-T symmetry. For values of ρ between zero and infinity, q_N varies between zero and 0.5. The upper limit, of course, coincides with the constraint on q for passive RC networks as expressed by Equation (6). Furthermore, it is clear from Equations (30) and (33) that when $\mu\beta$ is larger than zero, q_F will be larger than q_N. Thus, as discussed in Section II, the transmission function given by Equation (31) is that of a Frequency Emphasizing Network.

Setting Equation (31) equal to the desired correction function given by Equation (11) we require that

$$q_N = q_R \tag{37a}$$

$$q_F = q_p \tag{37b}$$

$$\omega_n = \omega_p \tag{37c}$$

and

$$K_F = K_A. \tag{37d}$$

The required overall loop-gain of the FEN in terms of the specified correcting function $T_A(s)$ then follows from Equations (33), (36), and (37), namely:

$$\mu\beta = \frac{q_p}{q_R} - 1 \ . \tag{38}$$

It will be shown later that as a feedback network the FEN must be stabilized by frequency compensation networks to avoid parasitic oscillations. This process can be greatly simplified if the gain of the amplifier β in the feedback loop does not exceed unity. This leaves the forward gain μ (see Figure 8) to satisfy Equation (38). This equation indicates that q_R should be chosen as closely to its upper limit value 0.5 as possible to economize on the required gain μ. Equation (35) shows that q_R can be made to approach 0.5 by using an asymmetrical Twin-T for the notch filter $T_N(s)$ in which ρ is much larger than 1. This, however, brings both a technological and a circuit problem with it. In any available microminiaturization technique, high resistor values are difficult to produce with any precision. When

using tantalum thin film resistors, for instance, it becomes increasingly difficult to realize values in the order of 250 KΩ or higher for reasons of resistor stability and required surface space. Furthermore, we have implied by our derivation of Equation (31) that the noninverting VCVS β in Figure 8 does not load down the preceding notch filter $T_N(s)$. This is desirable so as to be independent of variations of the input impedance of β. It is only true, however, as long as the series resistor $R(1+\rho)$ (see Figure 9) is negligibly small compared to the input impedance of β. This, of course, limits the maximum permissible value of ρ. In any event, the most that can be achieved by going to extreme asymmetry in the Twin-T is a factor of two, since q_N increases from 0.25 to 0.5 as ρ is increased from unity to infinity. If we consider the maximum gain that can be obtained from the forward amplifier μ, with say, no more than 1 percent drift in gain, it will be typically in the order of 40 db. Thus, from Equation (38), the maximum obtainable value of q_p would only be increased from 25 to 50 by going to very large values of ρ. This is still much too low for most high selectivity applications. We shall see in the next section that there is a much more effective way of increasing the maximum available value of q_p than to use an asymmetrical Twin-T. This method, incidentally, will actually require the Twin-T to be symmetrical, i.e., $\rho = 1$.

From the above discussion, it follows that the circuit configuration shown in Figure 8 is only suitable for medium values of q_p. In this class of applications the grounded unity gain VCVS β can be realized by an emitter-follower or a Darlington pair. The forward gain stage μ should have a summing point at which the input and feedback signals can be added independently. Its gain should be well controlled and easily adjustable and it should invert the incoming signal. These requirements can be satisfied close to ideally by an operational amplifier in the inverting mode. The practical FEN circuit is therefore realizable by the configuration shown in Figure 10. The corresponding transmission function is given by

$$T_A(s) = -\frac{\frac{R_F}{R_G}}{1 + \frac{R_F}{R_Q}} \frac{s^2 + \frac{\omega_p}{q_R} s + \omega_p^2}{s^2 + \frac{\omega_p}{q_p} s + \omega_p^2} \tag{39}$$

where

$$q_p = \left(1 + \frac{R_F}{R_Q}\right) \cdot q_R \tag{40}$$

From Equations (18), (39), and (40) the transmission at the peak frequency $s = j\omega_p$ is given by

$$\hat{T}_A = \left| T_A(j\omega) \right|_{\omega=\omega_p} = \frac{R_F}{R_G} . \qquad (41)$$

The response at high and low frequencies is given by Equations (16) and (17) respectively, and equals

$$\left| T_A(j\omega) \right|_{\omega\to\infty} = \left| T_A(j\omega) \right|_{\omega=0} = \frac{R_F}{R_G} \cdot \frac{R_Q}{R_F+R_Q} \approx \frac{R_Q}{R_G} . \qquad (42)$$

The approximation in Equation (42) is valid when $R_F >> R_Q$.

A noninverting unity gain operational amplifier represents a closer approximation to an ideal grounded VCVS than a Darlington pair. The assumptions of zero input admittance and output impedance made in the above derivations are satisfied more accurately for this case and the gain is closer to unity. The corresponding circuit configuration is shown in Figure 11. The same transmission functions as those derived above hold for this circuit; in fact the approximations made in them are satisfied more accurately.

There are some important advantages inherent in the FEN configurations shown in Figures 10 and 11 when using operational amplifiers. Due to the virtual ground at the input to the inverting amplifier in the forward transmission path, the signals from the passive RC network and from the

feedback path can be added independently of each other. Because of this and the isolation afforded by the voltage amplifier in the feedback path, the basic parameters of the network can be adjusted for very simply and independently of one another. This follows directly from the transmission functions of the network. Equation (40) shows that the inverse damping factor q_p which determines the selectivity of the FEN can be adjusted for by varying the resistor R_Q. Neither the frequency nor the peak forward gain of the network are thereby effected. Similarly the peak gain is independently determined by the resistor R_G [see Equation (41)] and the peak frequency by the RC product of the notch filter in the feedback loop [see Equation (34)]. We shall see later that this latter parameter will be adjusted for by selecting the corresponding capacitors so that the resistors and with them the dc operation of the network can be maintained invariant. Due to the very low output impedance of operational amplifiers, another advantage obtained with the FENs shown in Figures 10 and 11 is that the 2-section circuits shown in Figures 5b and 6 can be cascaded with essentially no interaction between individual circuits.

In the sections on FEN stability and sensitivity it will be useful to know the root locus of the FEN transmission function given by Equation 39. This is particularly

simple to obtain. We recall first the geometric interdependence of the zeros and poles of the FEN, which was illustrated in Figure 3b. By inspection of Equation (30) we find the same interdependence between the zeros and poles of the notch filter $T_N(s)$. We recall that the poles of $T_N(s)$ are the open loop poles of the FEN at which the root locus must begin (i.e., for $\mu = 0$) and that the zeros of $T_N(s)$ are the open loop zeros of the FEN at which the root locus must end (i.e., for $\mu = \infty$). It is easy to see then that the root locus starts at the negative real transmission zeros of the FEN and then follows the semicircle with radius ω_p about the origin. The root locus is shown in Figure 12 and, as is to be expected, corresponds exactly to the construction shown in Figure 3b.

2. High Selectivity FENs (HSFENs)

As a result of the expression given by Equation (38) the required loop gain $\mu\beta$ of the circuit shown in Figure 8 is proportional to the specified value of q_p and inversely proportional to q_R. Since q_R is the inverse damping factor of a passive RC network, it is restricted to values between 0.25 and the upper limit 0.5. Thus typically the required loop gain $\mu\beta$ is approximately three to four times q_p. For high Q bandpass networks $\mu\beta$ may therefore be required to take on very high values. It was pointed out in the previous

section that this results in stability problems with the FEN. One way of alleviating the stability problem is to restrict the gain of the amplifier in the feedback loop to unity. This in turn introduces sensitivity problems, because all the gain required for high selectivity must be obtained from the forward amplifier μ. The larger μ is chosen, the less it can be desensitized to ambient variations by feedback and the more the gain will drift.

A solution to this problem that avoids critical stability is to use an active null network for $T_N(s)$ in Equation (29) whose inverse damping factor q_N can be chosen arbitrarily but whose forward gain is unity. In effect, this means adding a second feedback loop in the configuration of Figure 8 without altering the loop conditions of the original feedback network. Instead of looking at the new configuration as a double feedback loop, however, it is simpler to consider it as a single feedback loop with an active unity gain null network in the feedback loop.

The active null network is shown in Figure 13a. From Appendix E, Equations (E-12), (E-31), (E-32), and (E-33) we obtain the following transmission function for this network:

$$T_{Na}(s) = \frac{1}{\beta} \cdot \frac{E_{out}}{E_{in}} = K_{Na} \frac{s^2 + \omega_n^2}{s^2 + \frac{\omega_n}{q_{Na}} s + \omega_n^2} \tag{43}$$

where:

$$K_{Na} = \frac{1}{1+r} = \frac{R_L}{(1+\rho)R+R_L} \tag{44}$$

$$\omega_n = \frac{1}{RC} \tag{45}$$

$$q_{Na} = \frac{1}{2} \frac{\rho(1+r)}{(1-\beta)\cdot(1+\rho) + r\rho} \tag{46}$$

and

$$r = (1+\rho) \frac{R}{R_L} \tag{47}$$

For the case that $\beta = 1$ (i.e., unity-gain voltage amplifier),

$$q_{Na}\Big|_{\beta=1} = \frac{1}{2} \frac{1+r}{r} \tag{48}$$

Expression (48) is plotted as a function of r in Figure 14. Clearly for large values of q_{Na}, r must be made as small as possible. From Equation (47) it follows then that R_L should be made as large as possible. However, similar considerations to those restricting the maximum value of ρ in the preceding

section (see discussion of Equation (35)) impose an upper limit on R_L here. The input impedance of the voltage amplifier following the passive RC null network is in parallel with R_L. To be sure that the ratio r is determined by passive resistors only, R_L must remain very much smaller than this input impedance. Furthermore, when realized as a semiconductor or thin film integrated resistor, the maximum value of R_L is limited in value to about 250 KΩ. On the other hand, contrary to the case of the passive infinite null network used in the preceding section [see Equation (35)] nothing is to be gained in this case by making ρ larger than unity. In fact, the required R_L for a given q_{Na} can be decreased by actually making ρ smaller than unity. (See Figure 47.) To accommodate both the passive and the active infinite null network cases, it therefore becomes practical to use a symmetrical Twin-T network in the FEN with $\rho = 1$. With values of $r \ll 1$

$$q_{Na}\Big|_{\beta=1} \approx \frac{1}{2r} \qquad (49)$$

Referring to the network in Figure 8, but substituting the transfer function of the passive null network $T_N(s)$ by the active network $T_{Na}(s)$ (see Figure 13b), we obtain the new closed loop transfer function:

$$T_{Fa}(s) = \frac{E_2}{E_1}(s) = -\frac{\mu}{1 + \mu\beta T_{Na}(s)} \tag{50}$$

Substituting Equations (43) to (47) into Equation (50) we obtain:

$$T_{Fa}(s) = \frac{E_2}{E_1}(s) = K_{Fa}\frac{s^2 + \frac{\omega_n}{q_{Na}}s + \omega_n^2}{s^2 + \frac{\omega_n}{q_{Fa}}s + \omega_n^2} \tag{51}$$

where:

$$K_{Fa} = -\frac{\mu}{1 + \frac{\mu\beta}{1+r}} \tag{52}$$

$$q_{Fa} = \left(1 + \frac{\mu\beta}{1+r}\right)\cdot q_{Na} \tag{53}$$

With (46), Equation (53) can be written as:

$$q_{Fa} = \frac{\rho}{2}\cdot\frac{1+r+\mu\beta}{(1-\beta)(1+\rho) + \rho r} \tag{54}$$

For $\beta = 1$ this simplifies to:

$$q_{Fa}\Big|_{\beta=1} = \frac{1+r+\mu}{2r} \tag{55}$$

With $r \ll 1$ and $\mu \gg 1$ this becomes:

$$q_{Fa}\Big|_{\beta=1} \approx \frac{\mu}{2r} \tag{56}$$

whereby $r = \frac{2R}{R_L}$ when the Twin-T is symmetrical.

With a unity gain noninverting operational amplifier ($\beta = 1$) and a symmetrical Twin-T ($\rho = 1$) we obtain the configuration shown in Figure 15. For this case the coefficients of the transmission function given by Equation (51) become:*

$$K_{Fa} = - \frac{(1+r) \cdot \frac{R_F}{R_G}}{1 + r + \frac{R_F}{R_Q}} \tag{57}$$

$$q_{Fa} = \frac{1 + r + \frac{R_F}{R_Q}}{2r} \tag{58}$$

where

$$r = \frac{2R}{R_L} \tag{59}$$

---

* Strictly speaking Figure 8 is not the accurate equivalent diagram for the network shown in Figure 15 because in Figure 8 the forward gain μ is entirely within the feedback loop. Thus Equations (57) and (58) can only be derived directly from Equations (52) and (53) if μ is assumed to represent the forward gain of the network and the symbol "$\mu\beta$" represents its loop gain. Thus by inspection of Figure 15 $\mu = R_F/R_G$ and $\mu\beta = \beta . R_F/R_Q$. The same comments apply to Figure 8 with respect to Figures 10 and 11.

and q_{Na} is given by Equation (48). Since in general:

$$\frac{R_F}{R_Q} >> 1$$

and

$$r << 1$$

Equations (57) and (58) can be simplified as follows:

$$K_{Fa} \approx - \frac{R_Q}{R_G} \tag{60}$$

and

$$q_{Fa} \approx \frac{1}{2r} \cdot \frac{R_F}{R_Q} \tag{61}$$

For this case q_{Na} is given by Equation (49).

The peak transmission occurs at the frequency $s = j\omega_n$ and equals:

$$T_{Fa} = K_{Fa} \cdot \frac{q_{Fa}}{q_{Na}} = \frac{R_F}{R_G} \tag{62}$$

At high and low frequencies the response approaches the constant value K_{Fa}, i.e.:

$$T_F(j\omega)\Big|_{\omega\to 0} = T_F(j\omega)\Big|_{\omega\to\infty} = \frac{\left(1+\frac{2R}{R_L}\right)\frac{R_F}{R_G}}{1+\frac{2R}{R_L}+\frac{R_F}{R_Q}} \qquad (63)$$

In general this value is approximately equal to $\frac{R_Q}{R_G}$.

At this point it is instructive to consider the root locus of the FEN with an active null network in the feedback loop. It can be derived from the transfer function given by Equation (50). The root locus starts at the open loop poles and ends at the open loop zeros, which in this case are identical to the poles and zeros respectively of $T_{Na}(s)$. The zeros of $T_{Na}(s)$ result directly from the numerator of Equation (43). The poles depend only on the resistor ratio r when, as assumed here, $\beta = 1$. The root locus for this particular case was derived in Appendix E and shown in Figure E.2. The zeros and poles of $T_{Na}(s)$ for a specific value of r can therefore be assumed as in Figure 16a. The root locus of the poles of $T_{Fa}(s)$ (see Equation 50) as a function of μ (since $\beta = 1$) then lies between these two pairs of critical frequencies as also shown in Figure 16a. A typical pole pair for $T_{Fa}(s)$ for a given value of r and μ is shown in Figure 16b. The zero pair, which coincides with the poles of $T_{Na}(s)$ is also shown.

From Equation (53) it follows that

$$q_{Fa} > q_{Na} \tag{64}$$

Therefore the expression given for $T_{Fa}(s)$ [see Equation (51)] and the corresponding pole-zero diagram shown in Figure 16b define the frequency characteristic of an FEN as required. The next step therefore is to equate $T_{Fa}(s)$ with the required active correcting network $T_A(s)$ given by Equation (11). To do so we should list a set of four required identities such as those given by Equations (37a to d). However, in this case only three are possible, namely:

$$q_{Fa} = q_p \tag{65a}$$

$$\omega_n = \omega_p \tag{65b}$$

and

$$K_{Fa} = K_A \tag{65c}$$

The fourth, namely that $q_{Na} = q_R$ is, of course, not possible since we have generated conjugate complex FEN zeros (i.e., conjugate complex open loop poles) with the active null network. These cannot accurately cancel out the negative real poles introduced by the approximating RC network preceding the FEN. Therefore, when cascading an RC network whose general short circuit transfer admittance is of the form given by

Equation (10), with a high selectivity FEN characterized by Equation (51) an error in the overall response is introduced of the form:

$$T_E(s) = \frac{s^2 + \frac{\omega_p}{q_{Na}} s + \omega_p^2}{s^2 + \frac{\omega_p}{q_R} s + \omega_p^2} \qquad (66)$$

Since q_{Na} is larger than q_R, $T_E(s)$ defines a Frequency Attenuating Network of medium selectivity. Its response approaches unity at high and low frequencies and is symmetrical to the normalized frequency $\Omega = 1$. [See Equation (14).] Minimum transmission occurs at this frequency, namely:

$$\hat{T}_E = |T_E(j\Omega)|_{\Omega=1} = \frac{q_R}{q_{Na}} \qquad (67)$$

Assuming $q_R = 0.25$ and the unity gain amplifier in the feedback loop (i.e., $\beta = 1$) the maximum transmission error can be expressed with Equation (48) as:

$$\hat{T}_E = \frac{1}{2} \cdot \frac{r}{1+r} \qquad (68)$$

A qualitative plot of the frequency response defined by $T_E(s)$ is shown in Figure 17.

The frequency selectivity of a Frequency Attenuating Network (hereafter referred to as an FAN) can be defined in the same way as for an FEN (see Appendix A). Referring to Figure 17 we find the same expressions for the -3 db frequencies as those given by Equations (19) and (21) except that here:

$$q = q_E = \frac{q_R q_{Na}}{\sqrt{q_{Na}^2 - 2q_R^2}} \tag{69}$$

Therefore:

$$Q_E = \frac{1}{\Omega_h - \Omega_\ell} = q_E = \frac{q_R q_{Na}}{\sqrt{q_{Na}^2 - 2q_R^2}} \tag{70}$$

In many highly selective filtering applications, in particular those involving single high-Q bandpass sections only, the error $T_E(s)$ can be ignored. Generally such applications require the filtering of a particular frequency or group of frequencies (e.g., "tone pickoff filters") or the exclusion of others and are not concerned with the detailed shape of the frequency response. In those cases, however, where an accurate amplitude or phase response is required and specified by a particular transfer function, then the addition of what might be termed the parasitic zero-pole pair defined by Equation (66) will be unacceptable. It must then be compensated for by

cascading an MSFEN of the type described under IV.1. The response of the MSFEN will, of course, be the inverse of that given by Equation (66). An example of a high Q bandpass network whose response is accurately given by:

$$T(s) = K \frac{s}{s^2 + \frac{\omega_p}{q_p} s + \omega_p^2} \qquad (71)$$

where

$$q_p >> 0.5$$

is shown in Figure 18. As shown in Appendix A, Equation (A.41) the Q corresponding to this transmission function is equal to q_p. Without the compensating MSFEN network the Q is a more complicated expression and is given by Equation (A.84) in Appendix A, if we let:

$$q_1 \equiv q_R$$

$$q_2 \equiv q_{Na}$$

and

$$q_3 \equiv q_p$$

Assuming given values of q_R and q_{Na} the required value q_p corresponding to a specified frequency selectivity Q is solved for in Equation (A.86). This expression is plotted in the Appendix in Figures A.7 and A.8.

In general, a double FEN section will only be required for the dominant poles of a high selectivity, precision filter. In some cases it might even be possible to utilize the parasitic pole-pair defined by Equation (66) to realize part of a desired frequency response in which case no double FENs would be necessary.

The same advantages of independent network parameter adjustment that are obtainable with the MSFEN configurations shown in Figures 10 and 11 apply to the HSFEN configuration of Figure 15. In fact, as a comparison of the two network types shows, the only difference in the HSFEN configuration is the added feedback loop and the RC network loading the Twin-T. Beside using R_Q for independent FEN selectivity adjustment, we now also have the variable r for this purpose. The choice of these two variables for a given value of q_p will be discussed in the sections on FEN sensitivity and stability in Part II of this memorandum.

V. FREQUENCY REJECTION NETWORKS (FRNs)

Theoretically there is no justification for picking out second order Frequency Rejection Networks (hereafter

referred to as FRNs) from the family of networks realizable by cascading an RC network with an FEN. As was shown under Section III in Tables 1 and 2 they can be realized in precisely the same way as any of the other second order networks listed there. Practically, however, there is an important reason for doing so. FRNs require transmission zeros as close to the $j\omega$ axis as possible. The RC approximating networks that will supply these conjugate complex zeros are invariably networks with more than one transmission path between input and output terminals. The Twin-T is an example of such a network. Transmission zeros are obtained by critically balancing the two parallel signal paths for zero transmission at the desired frequency. This entails high precision trimming of the network components - generally of the resistors. Methods of efficiently performing this tuning process are available [13,14]. Nevertheless, due to the high degree of precision required the procedure is always relatively time consuming and therefore expensive in production.* It is, therefore, desirable to restrict this type of balanced network to a minimum.

---

* Unless very high quantities (yearly business in excess of one million dollars) justify full automation, the tuning process is a manual one priced at approximately 20 cents per minute.

Since a precision tuned Twin-T is already incorporated in the FEN, the question naturally arises whether it alone could not be used to realize the general transmission function of an FRN, which has the form:

$$T(s) = K \frac{s^2 + \omega_{n_1}^2}{s^2 + \frac{\omega_{n_2}}{q_p} s + \omega_{n_2}^2} \tag{72}$$

instead of cascading a second Twin-T with an FEN as shown for instance in Example (4) of Table 2. Fortunately this is indeed possible with the active null network used in the HSFEN as shown in the following.

FRN With Active HSFEN Null Network

a. Voltage Amplifier With Gain Larger than Unity

We consider here a network configuration that is more general than that discussed in Section IV.2 (see Figure 13a). It is shown in Figure 19. The difference between the two networks is that here:

$$r \neq c \tag{73}$$

and

$$\beta > 0 \tag{74}$$

From Appendix E we can readily find the network parameters required for a specified transmission function of the type given by Equation (72). From Equations (E. 20) and (E. 21) we find:

$$\frac{1}{RC} = \omega_{n_1} \tag{75}$$

$$\frac{1+r}{1+c} = \left(\frac{\omega_{n_2}}{\omega_{n_1}}\right)^2 \tag{76}$$

From Equation (E. 30) the necessary gain β is given by

$$\beta = 1 + \tfrac{1}{2}\frac{\rho}{1+\rho}\left\{(1+c)\left[\left(\frac{\omega_{n_2}}{\omega_{n_1}}\right)^2 \frac{-1}{q_p}\left(\frac{\omega_{n_2}}{\omega_{n_1}}\right)\right] + c - 1\right\} \tag{77}$$

If a noninverting operational amplifier is to be used to provide the gain β, then one of the following two inequalities must be satisfied:

$$r \leq \frac{q_p\left[\left(\frac{\omega_{n_2}}{\omega_{n_1}}\right)^2 - 1\right] + \frac{\omega_{n_2}}{\omega_{n_1}}}{q_p\left[\left(\frac{\omega_{n_2}}{\omega_{n_1}}\right)^2 + 1\right] - \frac{\omega_{n_2}}{\omega_{n_1}}} \tag{78}$$

$$c \geq \frac{q_p \left[1 - \left(\frac{\omega_{n_2}}{\omega_{n_1}} \right)^2 \right] + \frac{\omega_{n_2}}{\omega_{n_1}}}{q_p \left[\left(\frac{\omega_{n_2}}{\omega_{n_1}} \right)^2 + 1 \right] - \frac{\omega_{n_2}}{\omega_{n_1}}} \qquad (79)$$

These constraints guarantee the required value of β to be larger or equal to unity.

The modifications required of the active null network used in the HSFEN to provide the general FRN transfer function given by Equation (72) are not very extensive. The fact that the resistor ratio r and the capacitor ratio c need not be equal does not affect the circuit configuration but only the actual resistor and capacitor values. A slight change in configuration is necessary when β is required to be larger than unity (assuming that one of the inequalities given by Equations (78) and (79) is satisfied), since the HSFEN is designed with β equal to unity for stability reasons. Referring to the HSFEN network shown in Figure 15, the gain of the noninverting operational amplifier designated A_n can be increased from unity by adding an appropriate resistor from the inverting input terminal to ground. Since this may effect the dc offset voltage of A_n, some adjustment of the feedback resistor may subsequently be necessary.

It is shown next that if a unity gain amplifier is used so as to retain the HSFEN active null network exactly, the realizable transmission functions will be limited.

b. Voltage Amplifier With Unity Gain

Setting $\beta = 1$ in the network shown in Figure 19 does not affect Equations (75) and (76). From Appendix E, [see Equation (E. 34)] the inverse damping factor however now becomes:

$$q_p \Big|_{\beta=1} = \frac{[(1+r)(1+c)]^{\frac{1}{2}}}{r+c} \tag{80}$$

i.e., it depends only on the resistance ratio r and on the capacitance ratio c. Furthermore from Equations (E.35) and (E.36) of the Appendix, these ratios are no longer independent but related by the two requirements that:

$$r = \frac{q_p \left[\left(\frac{\omega_{n_2}}{\omega_{n_1}} \right)^2 - 1 \right] + \frac{\omega_{n_2}}{\omega_{n_1}}}{q_p \left[\left(\frac{\omega_{n_2}}{\omega_{n_1}} \right)^2 + 1 \right] - \frac{\omega_{n_2}}{\omega_{n_1}}} \tag{81}$$

and

$$c = \frac{q_p \left[1 - \left(\frac{\omega_{n_2}}{\omega_{n_1}} \right)^2 \right] + \frac{\omega_{n_2}}{\omega_{n_1}}}{q_p \left[\left(\frac{\omega_{n_2}}{\omega_{n_1}} \right)^2 + 1 \right] - \frac{\omega_{n_2}}{\omega_{n_1}}} \qquad (82)$$

For physical realizability, r and c must remain positive. As can be readily derived from the results given in Appendix E this limits the range of realizable frequency ratios $\omega_{n_2}/\omega_{n_1}$ as a function of q_p, as follows:

$$\frac{1}{2q_p} \left\{ \sqrt{4q_p^2 + 1} - 1 \right\} < \frac{\omega_{n_2}}{\omega_{n_1}} < \frac{1}{2q_p} \left\{ \sqrt{4q_p^2 + 1} + 1 \right\} \qquad (83)$$

These limits are plotted on semilogarithmic paper in Figure 20. Clearly the range of obtainable frequency ratios decreases rapidly with increasing q_p. Thus the configuration shown in Figure 19 with $\beta = 1$ is only of general use in realizing transfer functions of the type given by Equation (72) when low values of q_p are required.

VI. HYBRID INTEGRATED CIRCUIT TECHNIQUES

In the preceding sections, the circuit techniques with which to realize the proposed method of active RC filter design have been discussed. We will now consider the device techniques at our disposal with which to realize these networks in microminiaturized form.

The two most important considerations that determine the choice of a particular integrated circuit technique are the cost of production and the required degree of circuit insensitivity to ambient variations. For sufficiently high production quantities, however, production costs will not differ appreciably with the integrated circuit technique applied. In this case the circuit sensitivity requirements decide the approach to take. This is particularly true in the field of active linear networks which often have to compete in performance with the low transmission sensitivity of high quality passive LC networks. It has been shown [see Reference 6] that hybrid integrated circuits, in which semiconductor integrated active devices are combined with tantalum thin film resistors and capacitors, are very well suited for the microminiaturized implementation of linear active networks, provided that circuit characteristics can be made to depend almost exclusively on the tantalum thin film components.

Highly stable circuits then result, due to the high quality of presently available tantalum thin film components (see Table 3). In fact if indeed it is possible to design networks whose characteristics are determined by the thin film characteristics, then the resulting network may actually exhibit less sensitivity to ambient temperature variations than is obtainable with high quality passive LC networks. This is evident from Table 4 in which the frequency drift with respect to temperature of tantalum thin film RC networks is compared with that of standard and high quality LC networks. Due to the capability of matching thin film resistor and capacitor temperature coefficients, the maximum frequency drift of a second order network will not drift by more than 0.15 percent over a temperature range of 50°C. Furthermore, again assuming that pole stability is determined by the thin film components only, the Q of a second order network will remain essentially constant with temperature variations.

The method of desensitizing active RC networks that affords the most versatility in network design is to minimize separately the active and passive sensitivity coefficients making up the pole sensitivity of a second order network [see Reference 6, Section III.2]. In the present context this specifically means stabilizing the active devices of the FEN individually with high precision thin film feedback networks to the extent that the closed loop gain is determined

by these networks only. For this to be possible high open loop gain devices are required. Fortunately, they are also available and at reasonable cost in the form of semiconductor integrated operational amplifiers. As was pointed out earlier the use of operational amplifiers also provides the isolation within the FEN to provide independent parameter adjustability and, between building-block stages, to provide independent cascadability.

An important advantage of tantalum thin film resistors is that they can be very accurately adjusted after deposition by trim anodization [15]. This provides a one-way resistor vernier adjustment by converting the top layer of the metal (e.g., tantalum nitride) resistor film into an insulating film of tantalum oxide. Thus, individual resistors that determine either the frequency, gain or Q of a network can be adjusted while it is in its normal mode of operation [16]. This process of resistor adjustment is limited to within approximately 50 percent of the initial resistance value. To provide initial coarse resistor adjustments, scratchpad techniques are used. For this purpose the resistor is tapped at given intervals by a short circuiting shunt path. The resistor can then be increased to the desired amount by scribing open a particular shunt path. The taps on the resistor can for instance be distributed to give a binary series of resistor values (see Figure 21).

The possibility of scribing open thin film conduction paths can be further utilized to increase the versatility of thin film networks. Multiple conducting paths corresponding to a variety of circuit configurations can be initially deposited on a ceramic substrate. Subsequently, all paths excluding those required for a particular application can be scribed open and thus made inoperative. This approach is used extensively in the design of the hybrid active filter networks described here.

In developing the hybrid integrated TOUCH-TONE Generator the "piggyback" circuit construction, using separate resistor and capacitor substrates, was found to offer a useful solution to two technological problems [17]. The first is the fact that tantalum thin film capacitors require some degree of protection as they are sensitive to humidity and cannot withstand physical abrasion. Therefore, with the "piggyback" construction the capacitors are deposited on one substrate and a protective substrate placed on top of it with a .003 to .006 inch gap between the two. This gap is filled with a polyethylene-polybutene compound by a vacuum impregnation process which has been shown to improve the humidity sensitivity of the capacitors appreciably. The thin film resistors are then deposited on the exposed surface of the upper substrate onto which the semiconductor integrated

active devices are also either bonded or beam-leaded. This leaves the resistors accessible for final precision adjustment by trim anodization. It also simultaneously alleviates the second problem, namely that the fabrication of thin film resistors requires a processing sequence that is different from that required by thin film capacitors. By depositing the capacitors on a separate substrate a high yield of resistors and capacitors can thus be maintained.

For the same reasons as those mentioned above, the "piggyback" construction is being adopted for the development of the hybrid active filter networks. At the same time, however, this approach lends an added degree of versatility to their design. Since the FEN circuit is essentially a dc-coupled feedback network, it is desirable to maintain essentially the same dc resistance level in it for all applications. This is also desirable to insure minimum offset voltages due to the operational amplifiers. By using a separate capacitor substrate, the RC products determining the frequency of operation can be varied by selecting an appropriate capacitor substrate without affecting the dc operation of the network. This does not, however, involve manufacturing a completely new capacitor substrate for each required frequency. This can be seen by considering the physical configuration of a thin film capacitor as shown in Figure 22a. The narrower of the two capacitor

electrodes determines its capacitance. Thus the range of capacitor values required for a given frequency range can be covered by making the lower (larger) electrode large enough to produce the largest required capacitor value. All the remaining (smaller) capacitors are then obtained by appropriately narrowing the upper electrode. Thus only a variety of upper-electrode production masks are required to cover a given frequency range. For a given application requiring a limited number of operating frequencies the corresponding capacitors can be obtained in a very much simpler way. This is illustrated in Figure 22b. The upper electrode consists of as many interconnected sections as the number of frequencies required. By scribing open, i.e., disconnecting specific sections, the capacitors can be coarse adjusted to the frequency of operation. Fine adjustments are then obtained as before by trim anodization of the corresponding resistors.

VII. ALL PURPOSE FEN/FRN BUILDING BLOCKS

By affectively utilizing the above mentioned hybrid integrated circuit techniques, basic second-order circuits can now be obtained with one and the same resistor-capacitor substrate pair. A multipurpose RC ladder network can be realized by the configuration shown in Figure 23. The conducting paths corresponding to the various filter options required are initially deposited on the upper of the two substrates. Subsequently to obtain a specific filter characteristic, the appropriate paths are opened as indicated.

The multipurpose network shown covers only the first four transfer admittances listed in Table 1. By adding two resistors and one capacitor together with the corresponding conducting path options, the remaining transfer admittances listed under 5) and 6) of Table 1 can also be obtained as shown in Figure 23b. To prevent a substrate from becoming too crowded with conducting path options, two basic substrate pairs designated Types I and II respectively are foreseen, which cover the applications 1 to 4 and 5 and 6 listed in Table 1, separately.

In Figure 24a the combination of the multipurpose RC network with the active correcting network as deposited on a single substrate pair is shown. Again, all conducting paths are deposited allowing for the various filter options mentioned earlier. Also, although not shown in the figure, the conducting paths leading to the noninverting VCVS β are arranged in such a way that either an operational amplifier or a beam-leaded Darlington transistor pair can be directly bonded onto the filter substrate. The terminal connections required for the various filter options and the methods of adjusting the parameters of the network which were discussed under Section IV are summarized in Table 5.

The RC notch filter incorporated in the FEN/FRN is shown in Figure 24b. As discussed in conjunction with Equation 48, the Twin-T used is symmetrical. This choice constitutes a compromise between the requirements of the MSFEN and the HSFEN. As a result the inverse damping ratio corresponding to the RC notch filter [see Equation (35)] is equal to 0.25. As a direct consequence [see Equation (37a)] the inverse damping factor of the RC networks $T_R(s)$ must have the same value, thus in all cases:

$$q_N = q_R = 0.25 \tag{84}$$

Operational amplifiers have very low output impedances. This means that when used as an FEN, in which case the terminals are connected as shown in Figure 24a, the output impedance of the total building block is very low. Similarly, when applied as an FRN with the terminals connected as shown, we again have an operational amplifier at the output of the network and the output impedance is very low. In both cases there is essentially no interaction between a cascade of filter building blocks. Due to these isolating properties, complex filters can be built by cascading appropriate building blocks. Typical filter configurations might thus look like those shown in Figure 25. The network

configuration of a sixth order maximally flat low-pass filter with a single rejection frequency is shown in Figure 25a. It consists of an RC ladder network interspersed with two FENs and an FRN to give the rejection frequency. Similarly a typical fourth order equiripple bandpass filter would also consist of an RC ladder network with two FENs as shown in Figure 25b. In Part II of this memorandum some practical design examples of complex filter configurations are given in detail.

G. S. Moschytz

G. S. MOSCHYTZ

HO-5316-GSM-SAN

Att.
Appendices A-E
Tables 1-5
Figures
References
References to Appendices

REFERENCES

[1] Rand, A., Inductor Size versus Q: A Dimensional Analysis, IEEE Trans. Comp. Parts, CP-10, March, 1963, pp. 31-35.

[2] Newell, W. E., The Frustrating Problem of Inductors in Integrated Circuits, Electronics, Vol. 37, March, 1964, pp. 50-52.

[3] Liebsch, H., Miniaturisierung von Induktivitaetsbauelementen, Nachrichtentechnik, Vol. 12, November, 1962, pp. 409-413. Also: BTL Translation, Nr. TR-64-63, March, 1964.

[4] Padwick, G. C., and Matthewman, R., the Economics of Integrated Circuits, Symposium on "Applications of Microelectronics," University of Southampton, IEE Conference Publication No. 14, 21-23 September, 1965, pp. 33/1-33/8.

[5] Mammano, R. A.,: Basic Rules Simplify Linear IC Design, E.D.N., January 4, 1967, pp. 24-32.

[6] Moschytz, G. S., Linear Active RC Networks, MM-66-5316-8, August 17, 1966.

[7] Truxall, J. G., Automatic Feedback Control System Synthesis, McGraw Hill, 1955, pp. 191-218.

[8] Hakimi, S. L., Seshu, S.: Realization of Complex Zeros of Transmission by Means of RC Networks, Proc. National Electronics Conf., Vol. 13, 1957, pp. 1-13.

[9] Hakimi, S. L., Cruz, J. B.: On Minimal Realization of RC Two-Ports, Proc. NEC, Vol. 16, 1960, pp. 258-267.

[10] Guillemin, E. A., Synthesis of RC Networks, J. Math. and Phys., Vol. 28, No. 1, 1949, pp. 22-42.

[11] Dasher, B. J., Synthesis of RC Transfer Functions as Unbalanced Two Terminal - Pair Networks, IRE Trans. PGCT, Vol. CT-1, December, 1952, pp. 20-34.

[12] N. Balabanian, J. Cinkilie: Expansion of an Active Systhesis Technique, IEEE Trans. PGCT, Vol. CT, June, 1963, pp. 290-298.

[13] Moschytz, G. S., Two-Step Precision Tuning of Twin-T Notch Filter, Proc. IEEE, Vol. 54, No. 5, May, 1966, pp. 811-812.

[14] Orr, W. H., Precision Tuning of a Thin Film Notch Filter, 1964 ISSCC Digest of Tech. Papers, Vol. 7, February, 1964, pp. 56-57.

[15] Buse, L. C., Tuning of Thin Film RC Networks by Wick Anodization, MM-64-2634-11, October 21, 1964.

[16] Moschytz, G. S., RC FSK Modulator for the 103E Data Set, MM-65-5323-16, October 22, 1965.

[17] Moore, R. J., Thin Film Tone Generator for TOUCH-TONE Dialing, MM-66-2624-4, February 21, 1966.

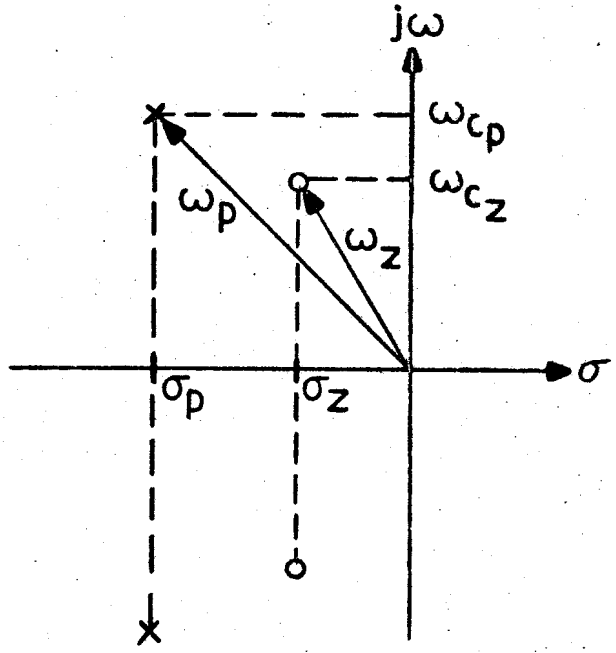

FIGURE 1

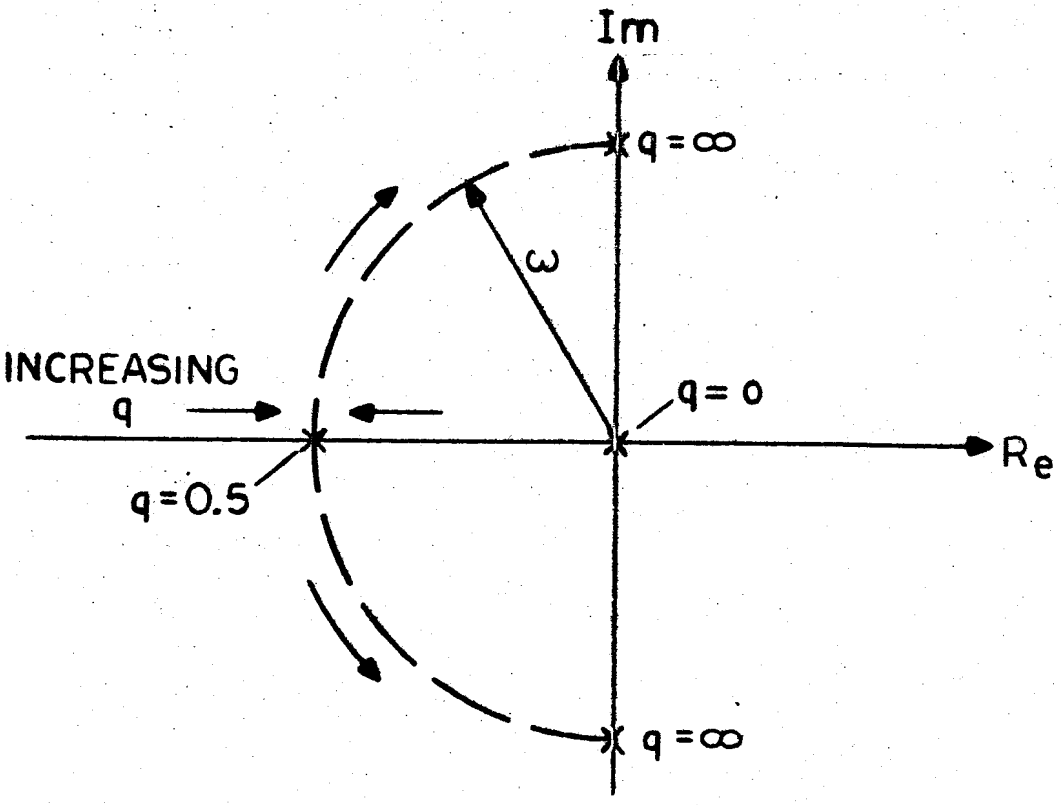

FIGURE 2

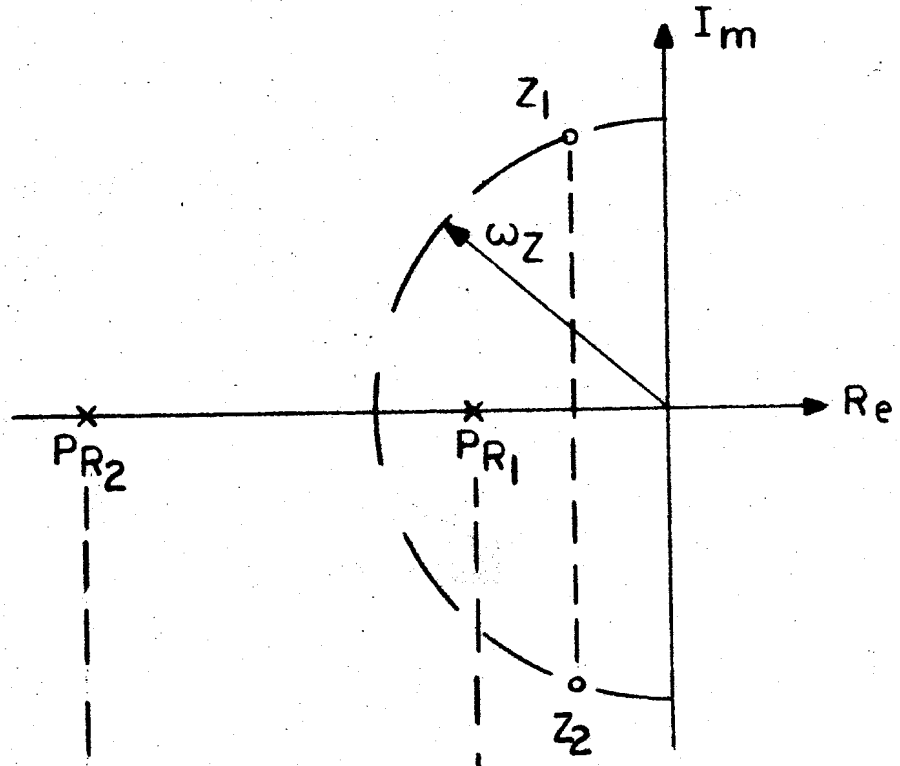

FIGURE 3a

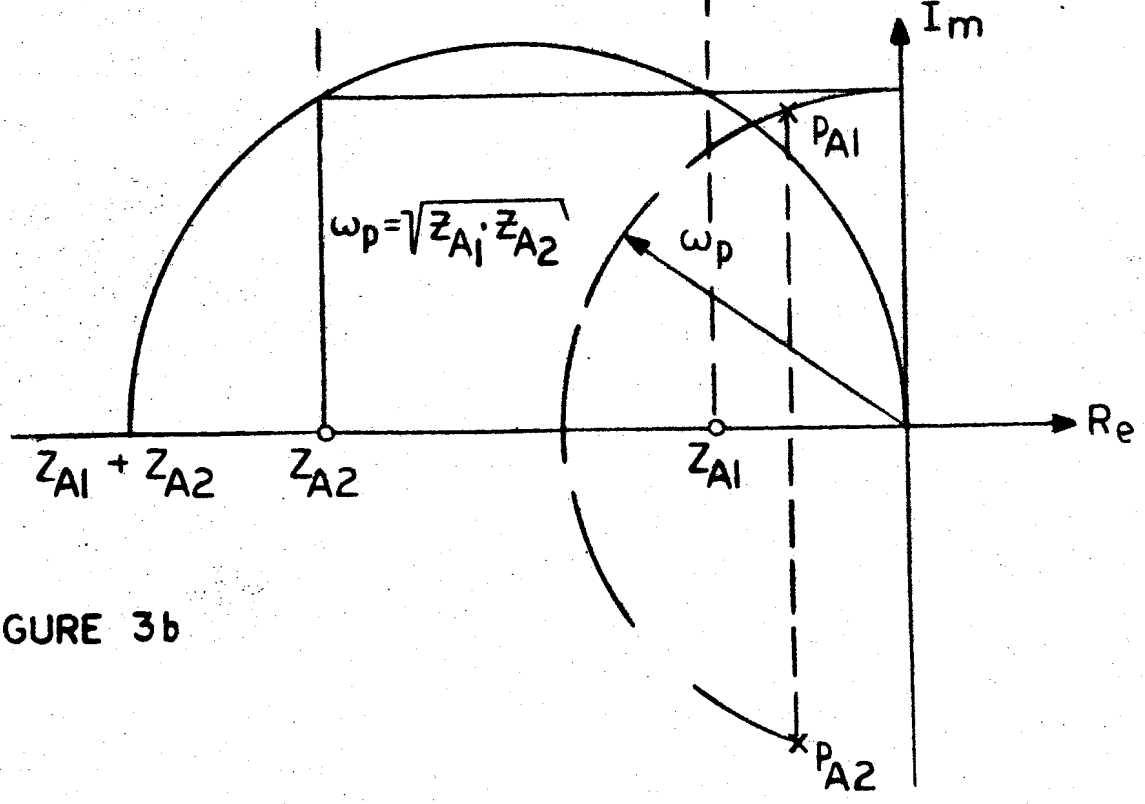

FIGURE 3b

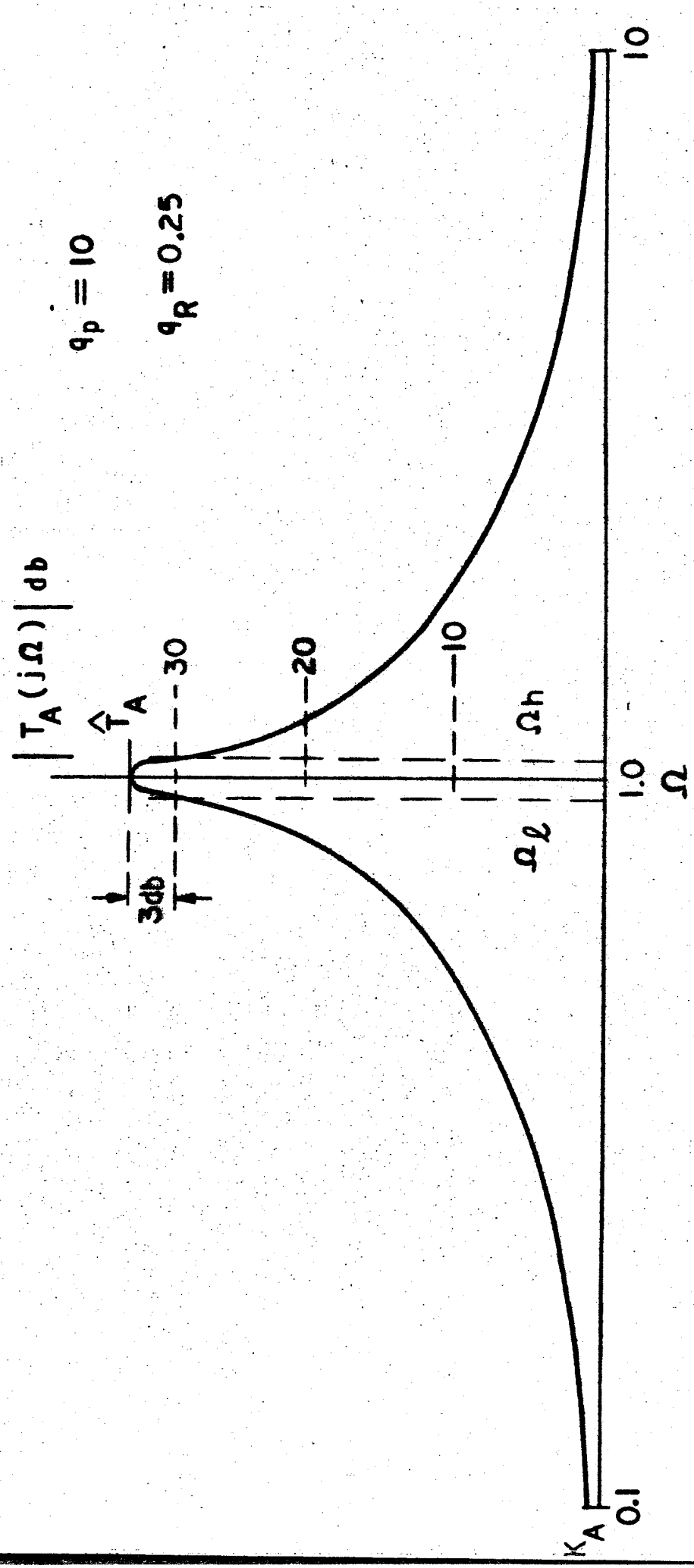
$q_p = 10$
$q_R = 0.25$
$|T_A(j\Omega)|$ db
$\hat{T}_A$
30
20
10
Ω_h
1.0
Ω
Ω_ℓ
3db
10
K_A
0.1

FIGURE 4

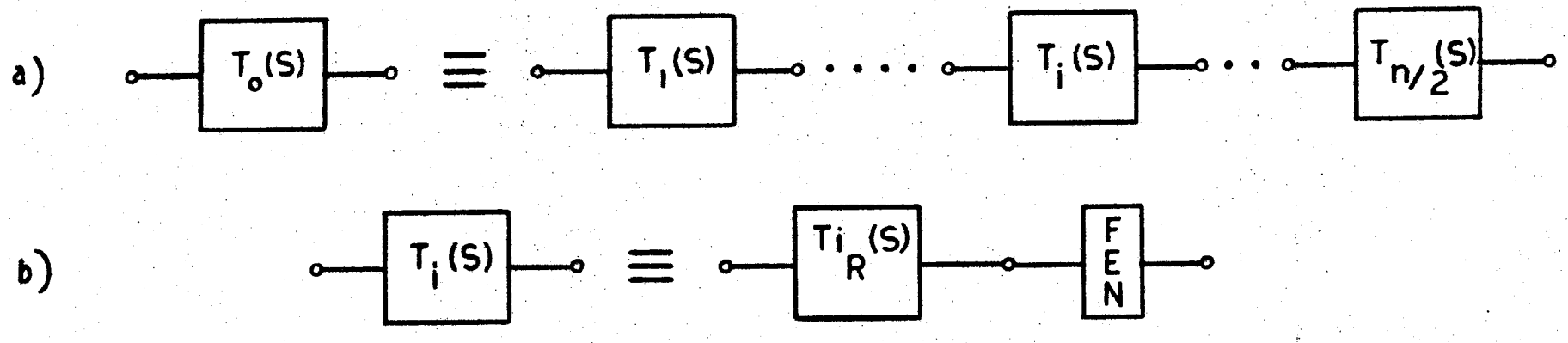

FIGURE 5

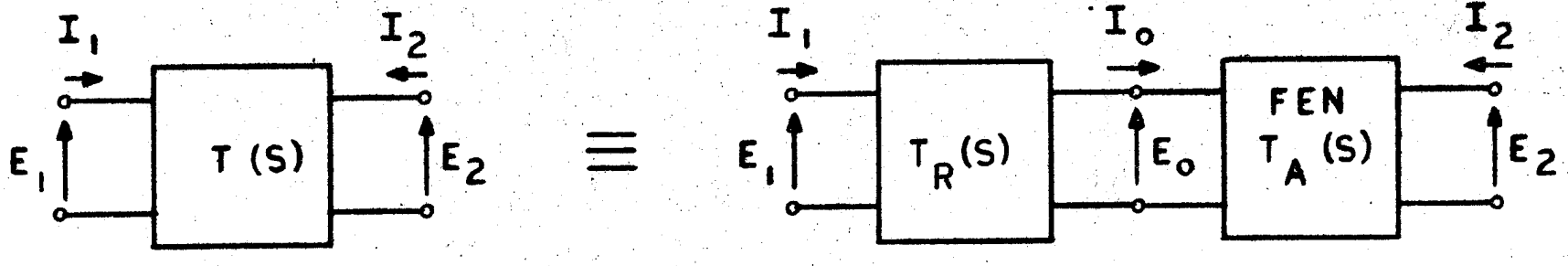

FIGURE 6

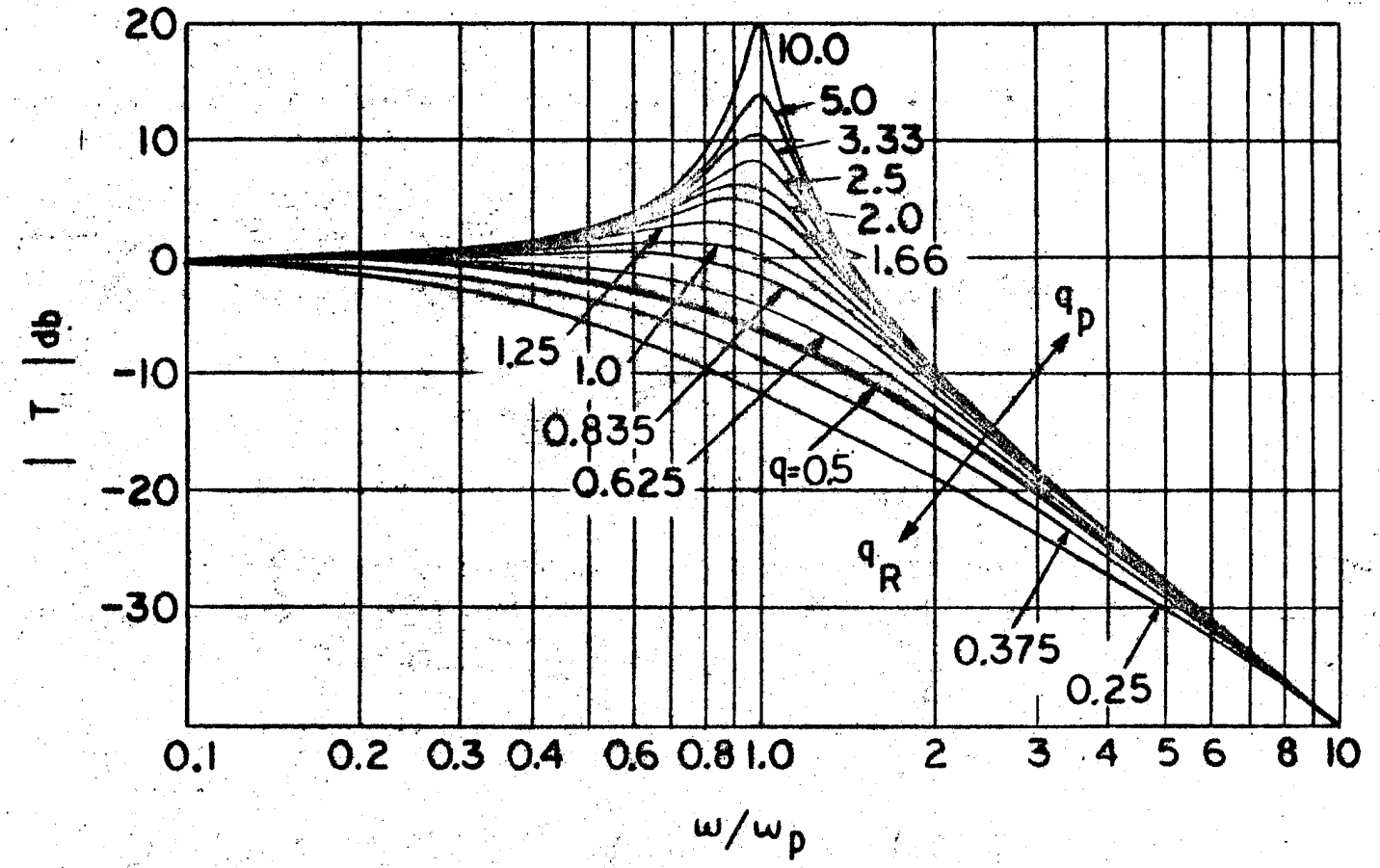
20
10
0
-10
-20
-30
| T | db
10.0
5.0
3.33
2.5
2.0
1.66
1.25
1.0
0.835
0.625
q=0.5
q_p
q_R
0.375
0.25
0.1
0.2
0.3
0.4
0.6
0.8
1.0
2
3
4
5
6
8
10
ω/ω_p

FIGURE 7a

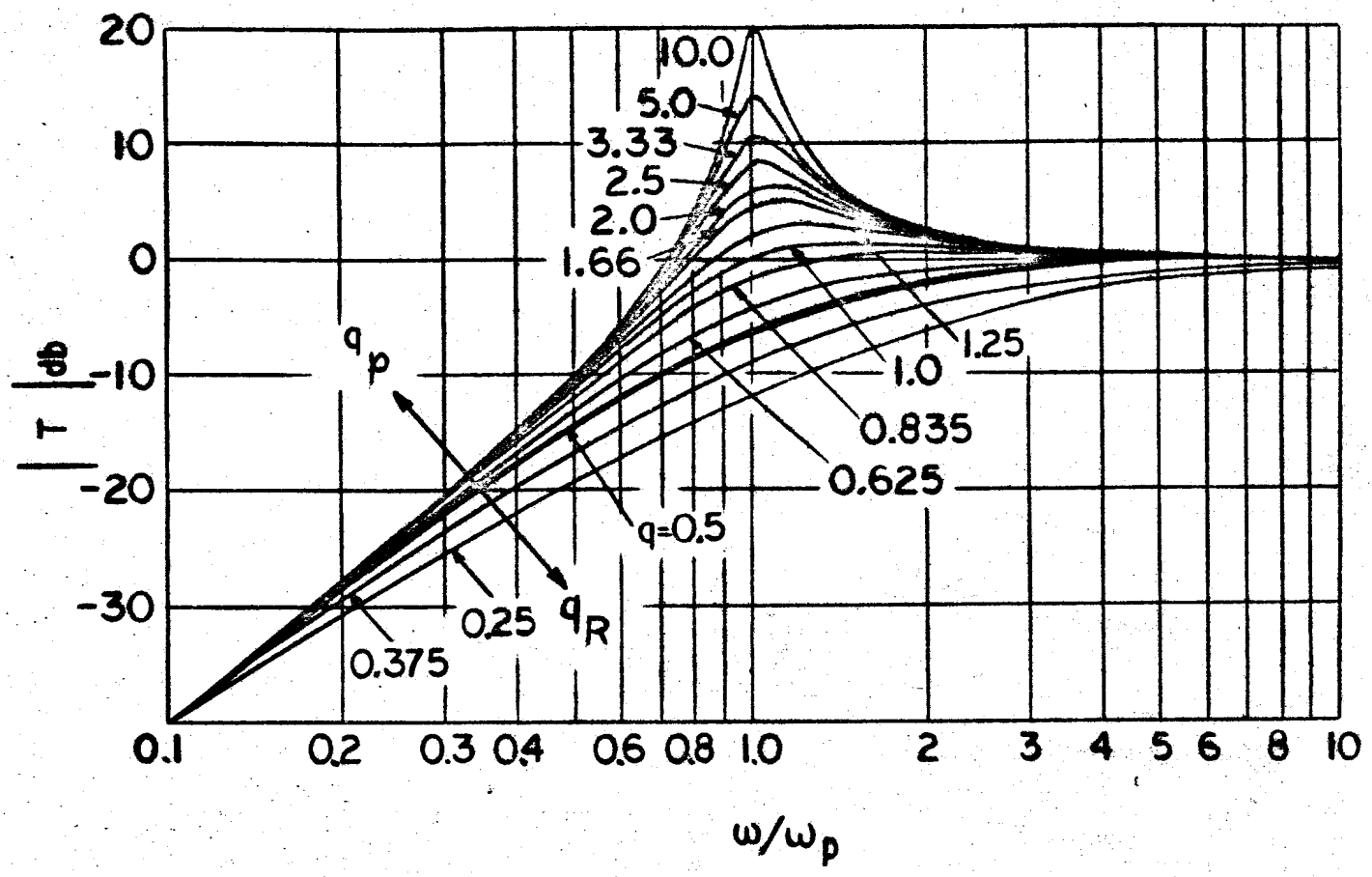
20
10
0
-10
-20
-30
$\frac{dB}{T}$
10.0
5.0
3.33
2.5
2.0
1.66
1.25
1.0
0.835
0.625
q_p
q_R
q=0.5
0.25
0.375
0.1
0.2
0.3
0.4
0.6
0.8
1.0
2
3
4
5
6
8
10
ω/ω_p

FIGURE 7b

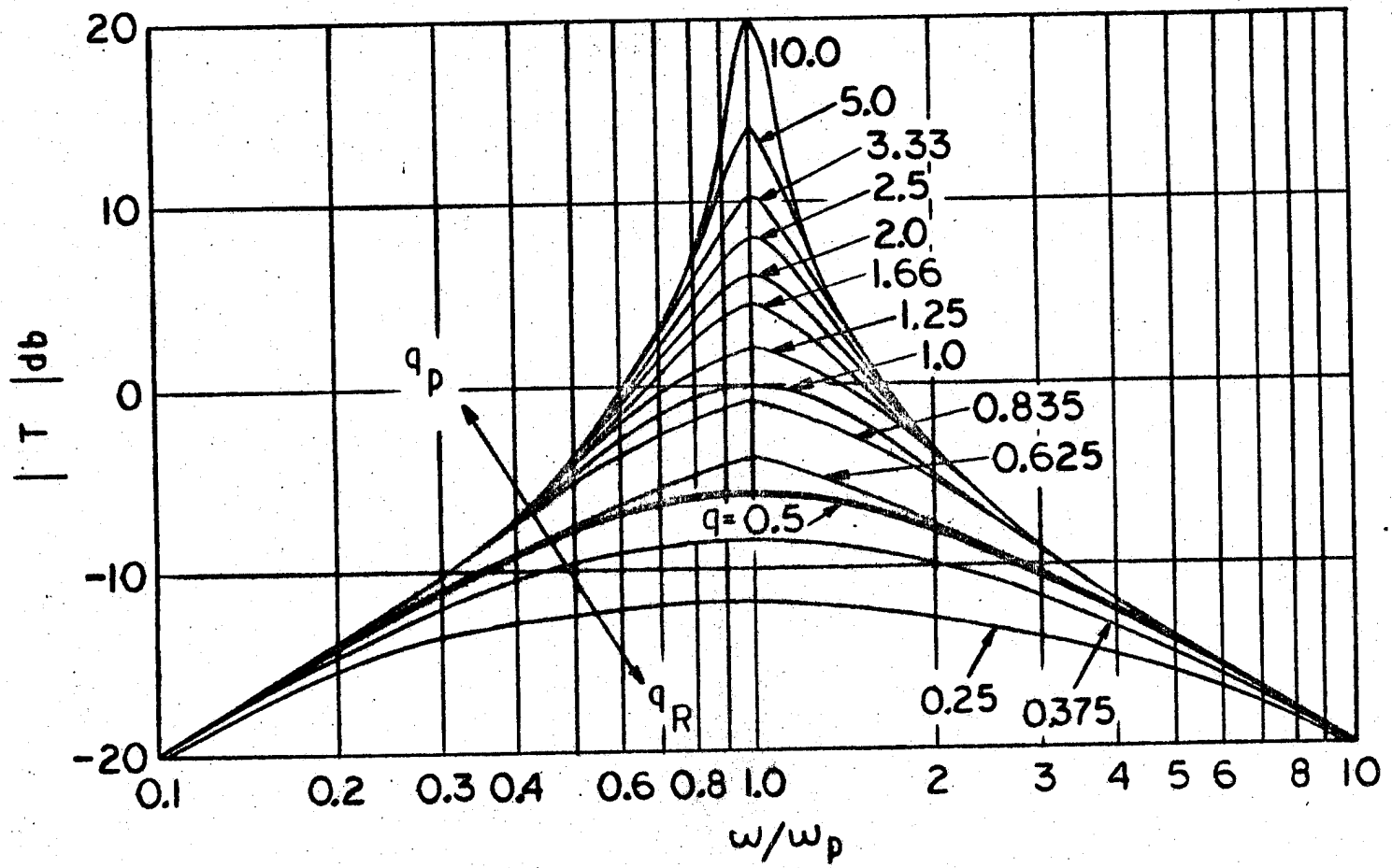

FIGURE 7c

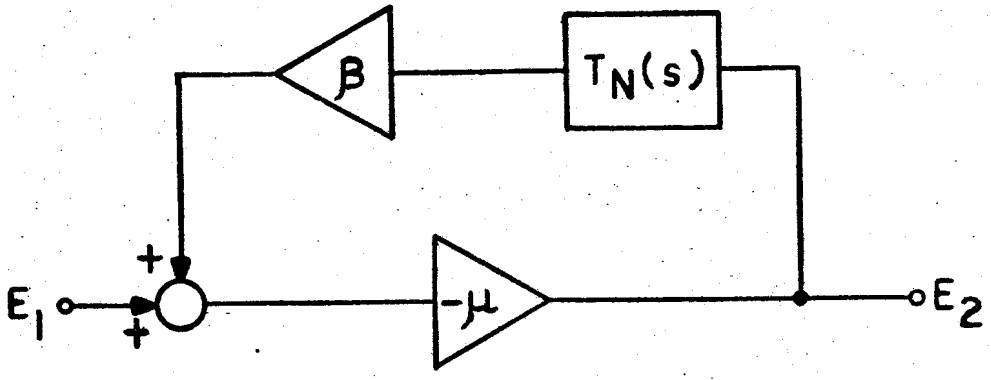

FIGURE 8

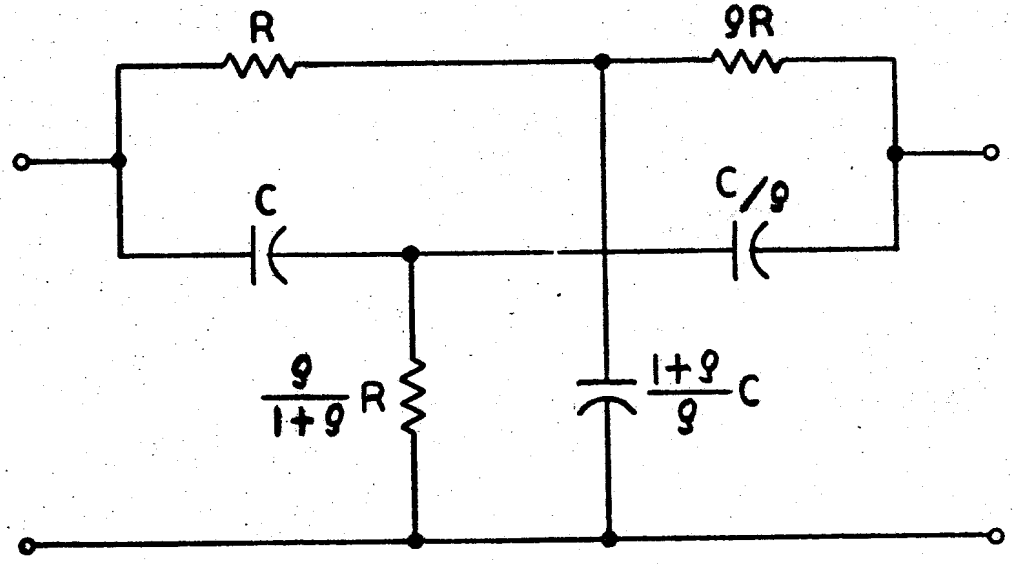

FIGURE 9

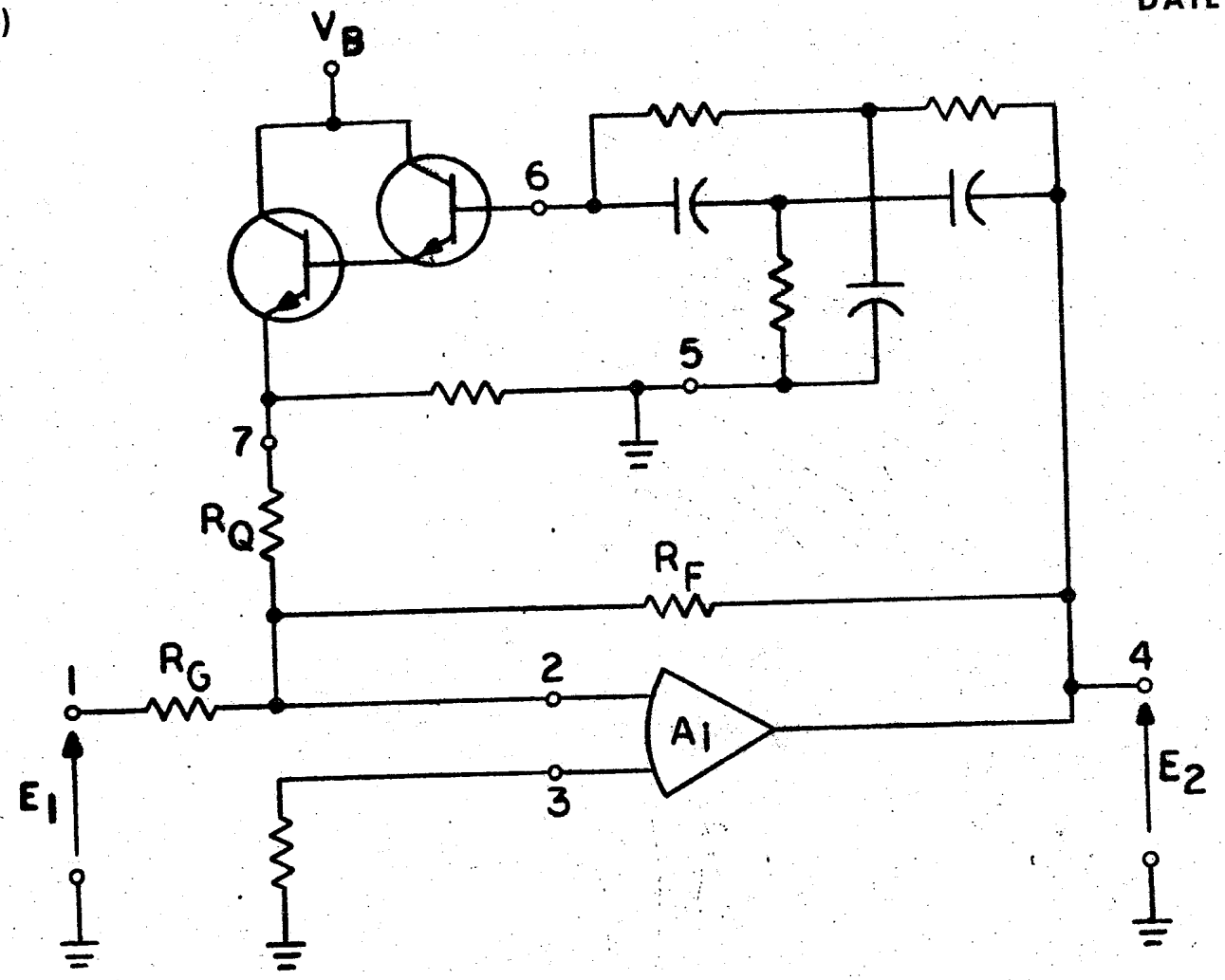

FIGURE 10

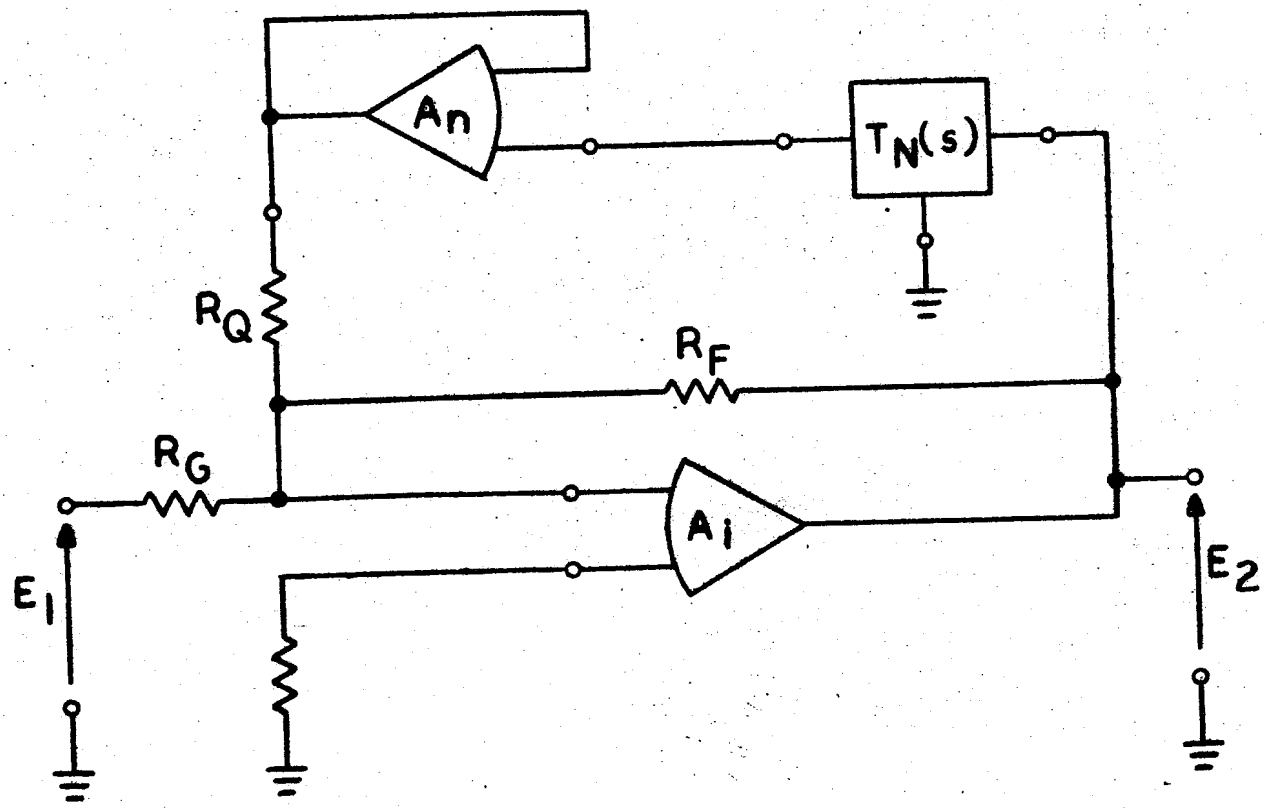

FIGURE 11

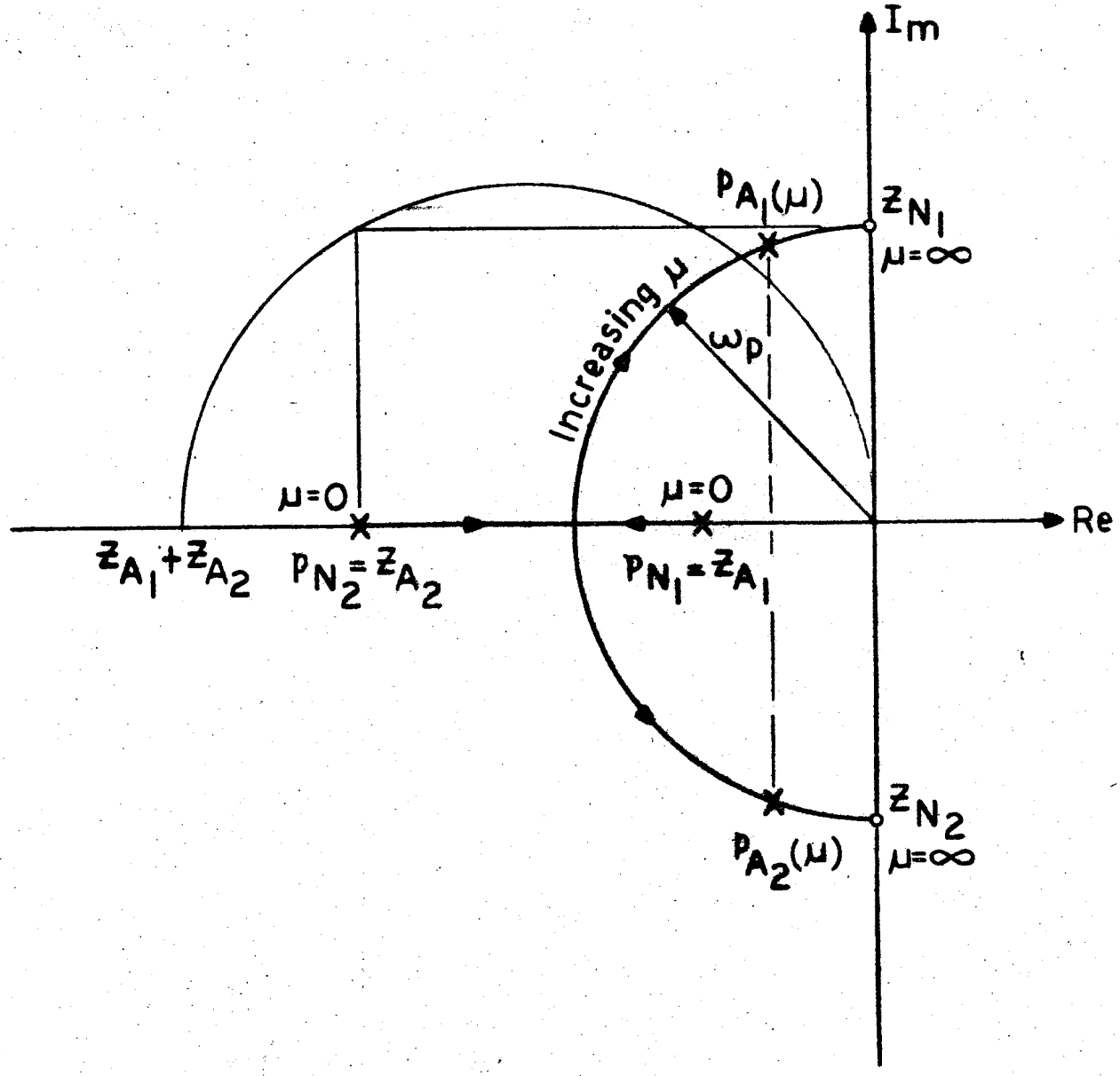
Im
Re
$p_{A_1}(\mu)$
z_{N_1}
$\mu=\infty$
Increasing μ
ω_p
$\mu=0$
$\mu=0$
$z_{A_1}+z_{A_2}$
$p_{N_2}=z_{A_2}$
$p_{N_1}=z_{A_1}$
z_{N_2}
$p_{A_2}(\mu)$
$\mu=\infty$

FIGURE 12

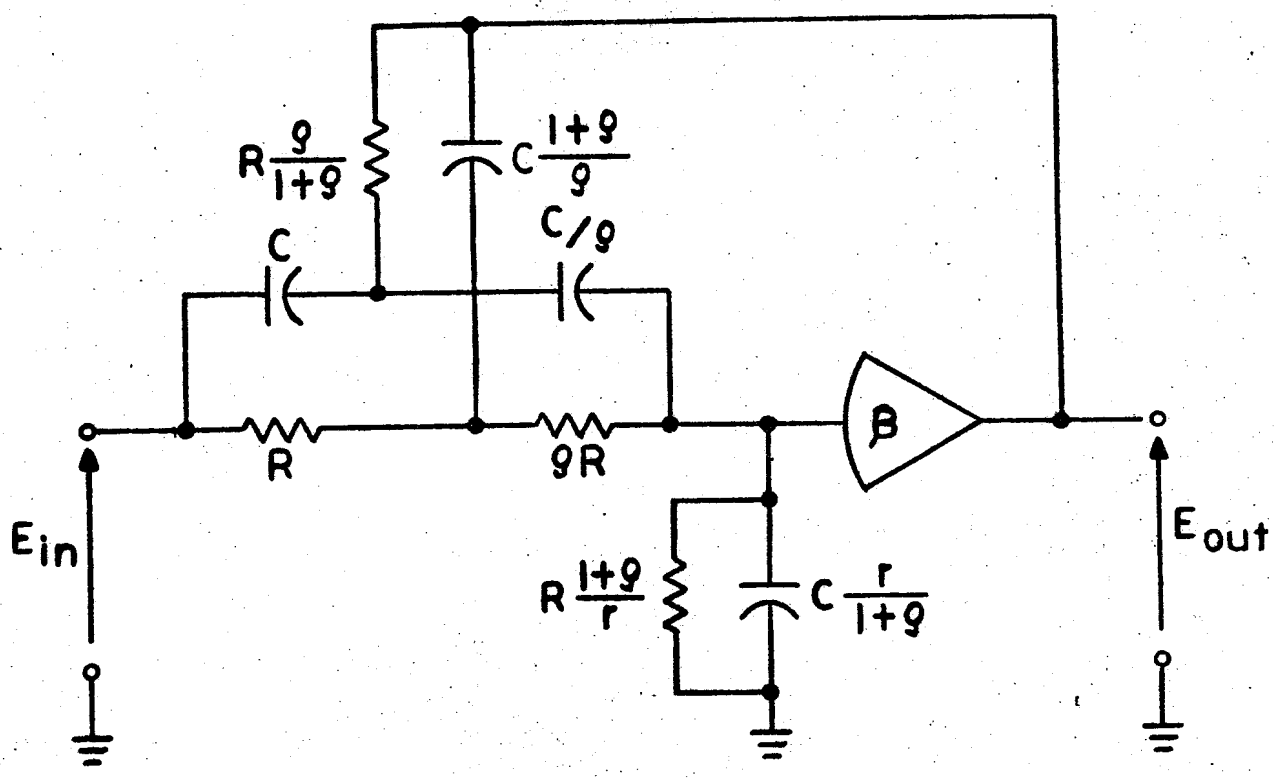

FIGURE 13a

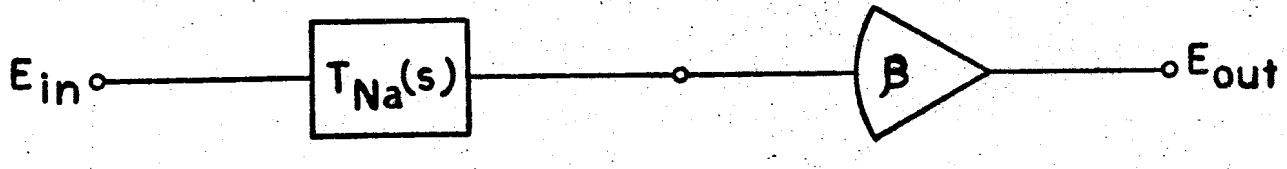

FIGURE 13b

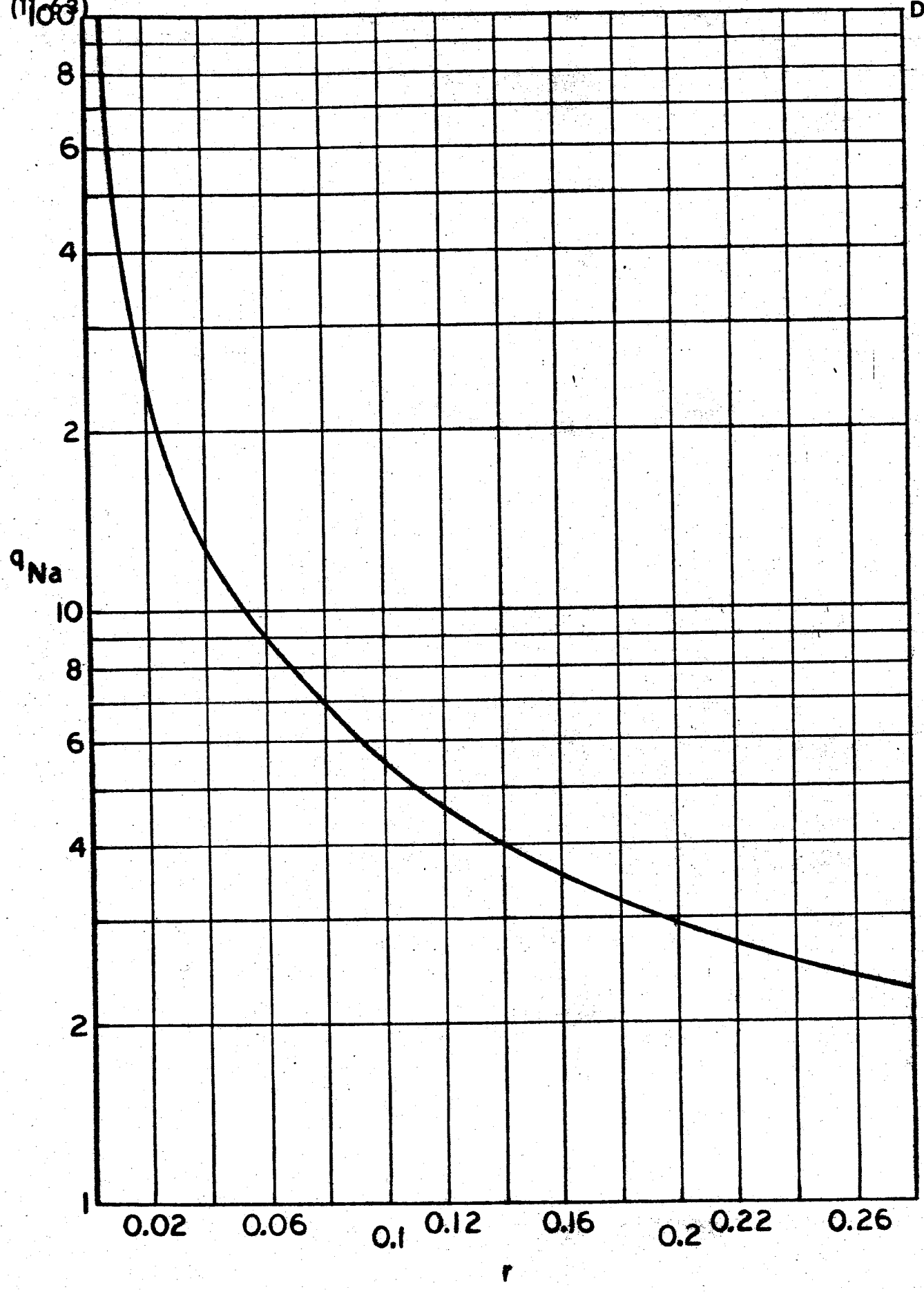

FIGURE 14

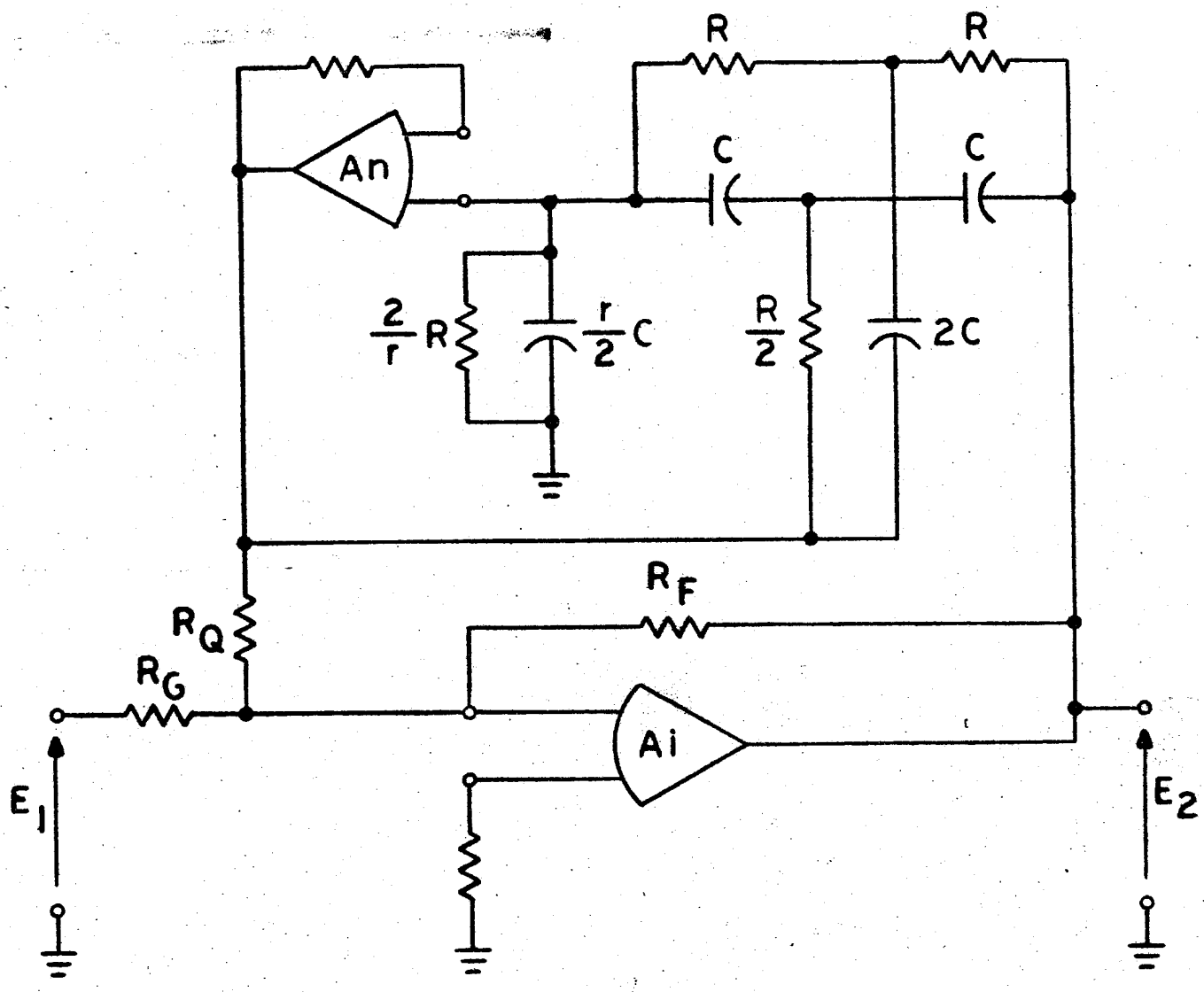

FIGURE 15

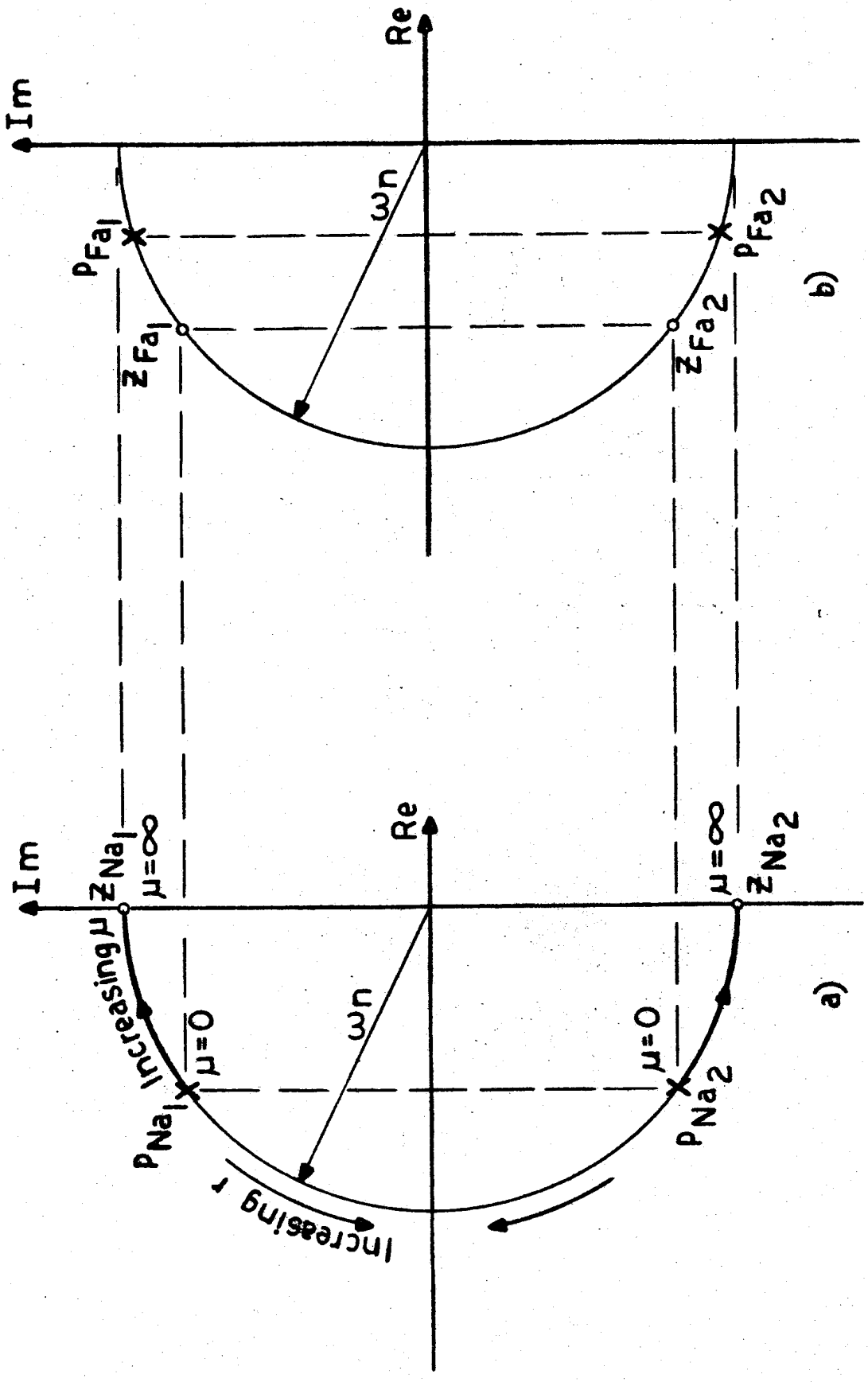
Im
Re
ω_n
p_{Fa1}
p_{Fa2}
z_{Fa1}
z_{Fa2}
b)
Im
Re
z_{Na1}
z_{Na2}
$\mu=\infty$
$\mu=\infty$
$\mu=0$
$\mu=0$
p_{Na1}
p_{Na2}
Increasing μ
Increasing r
a)

FIGURE 16

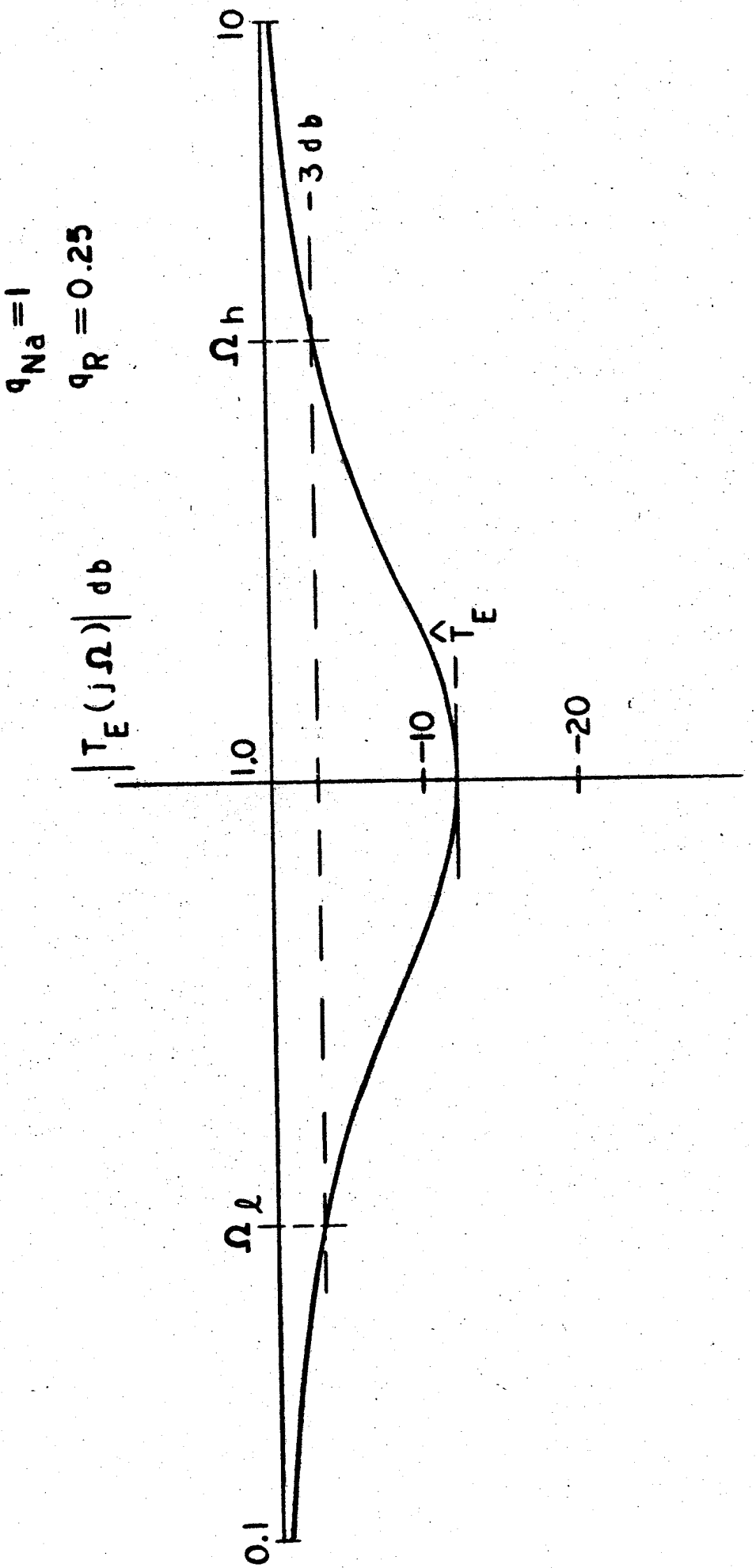

FIGURE 17

FIGURE 18

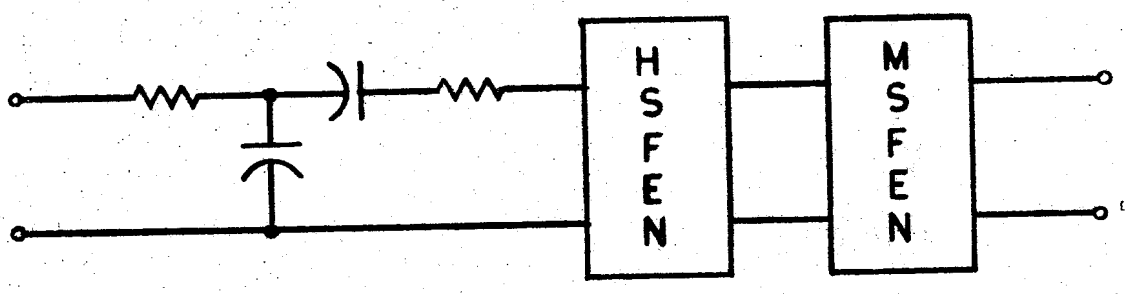

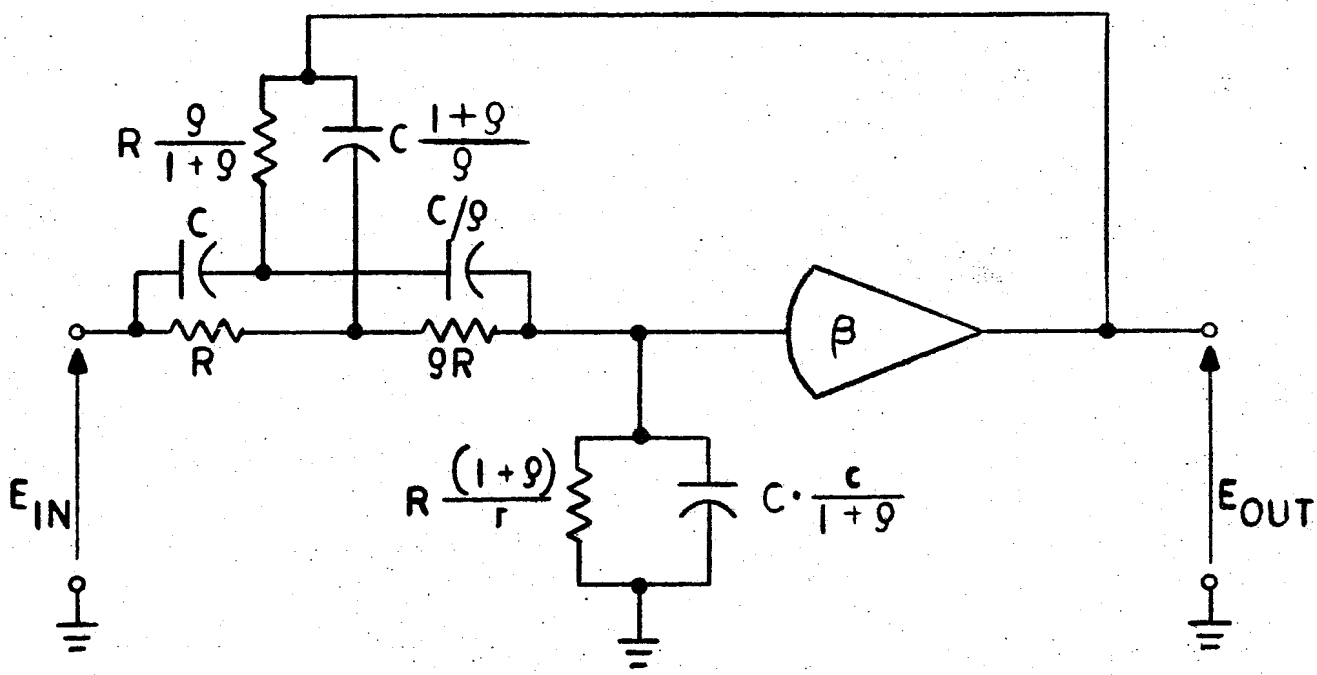

FIGURE 19

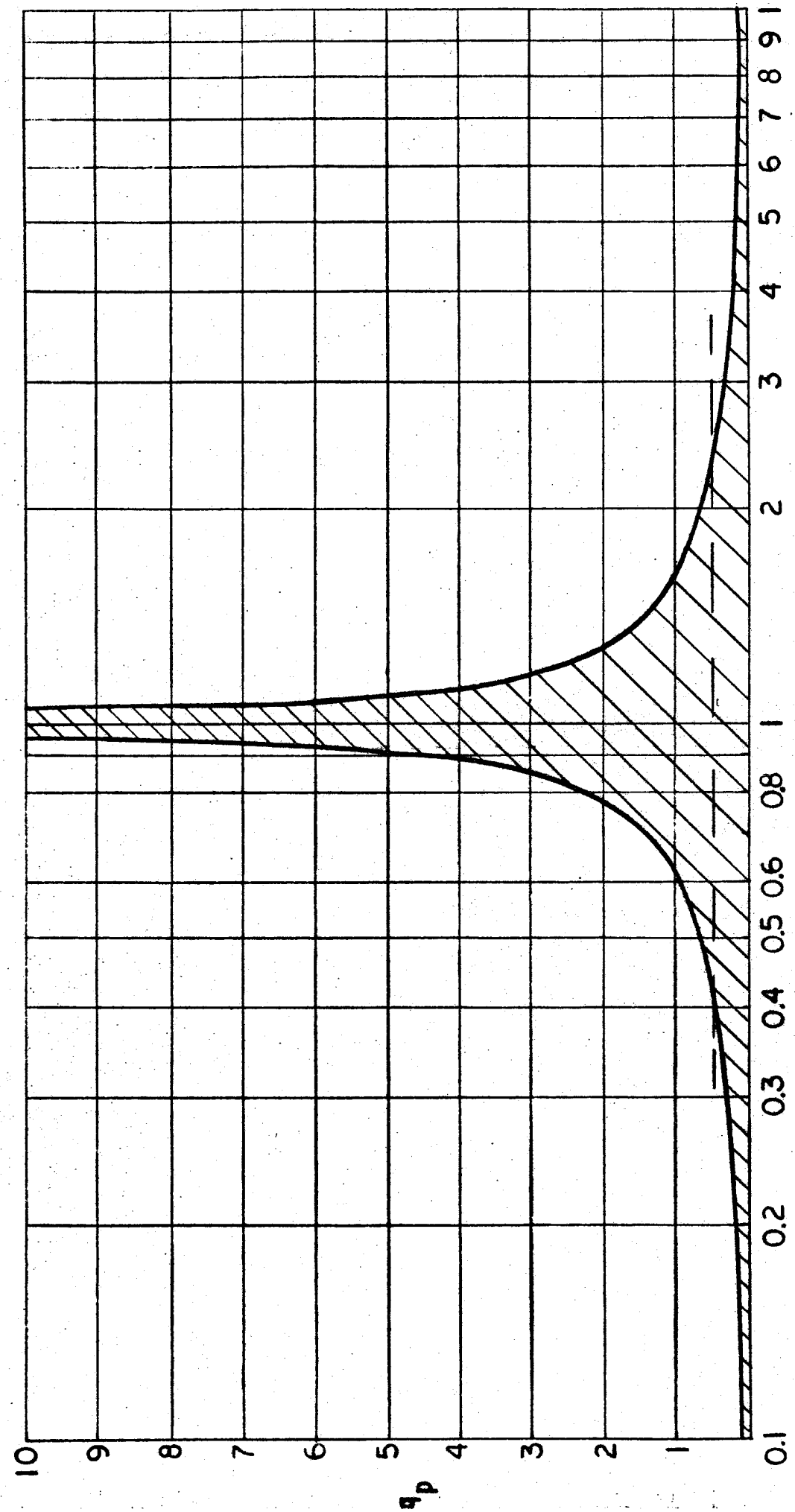
10
9
8
7
6
5
4
3
2
1
0.1
q_p
0.2
0.3
0.4
0.5
0.6
0.8
1
2
3
4
5
6
7
8
9
1
$\omega_{n_1}/\omega_{n_2}$

FIGURE 20

FIGURE 21

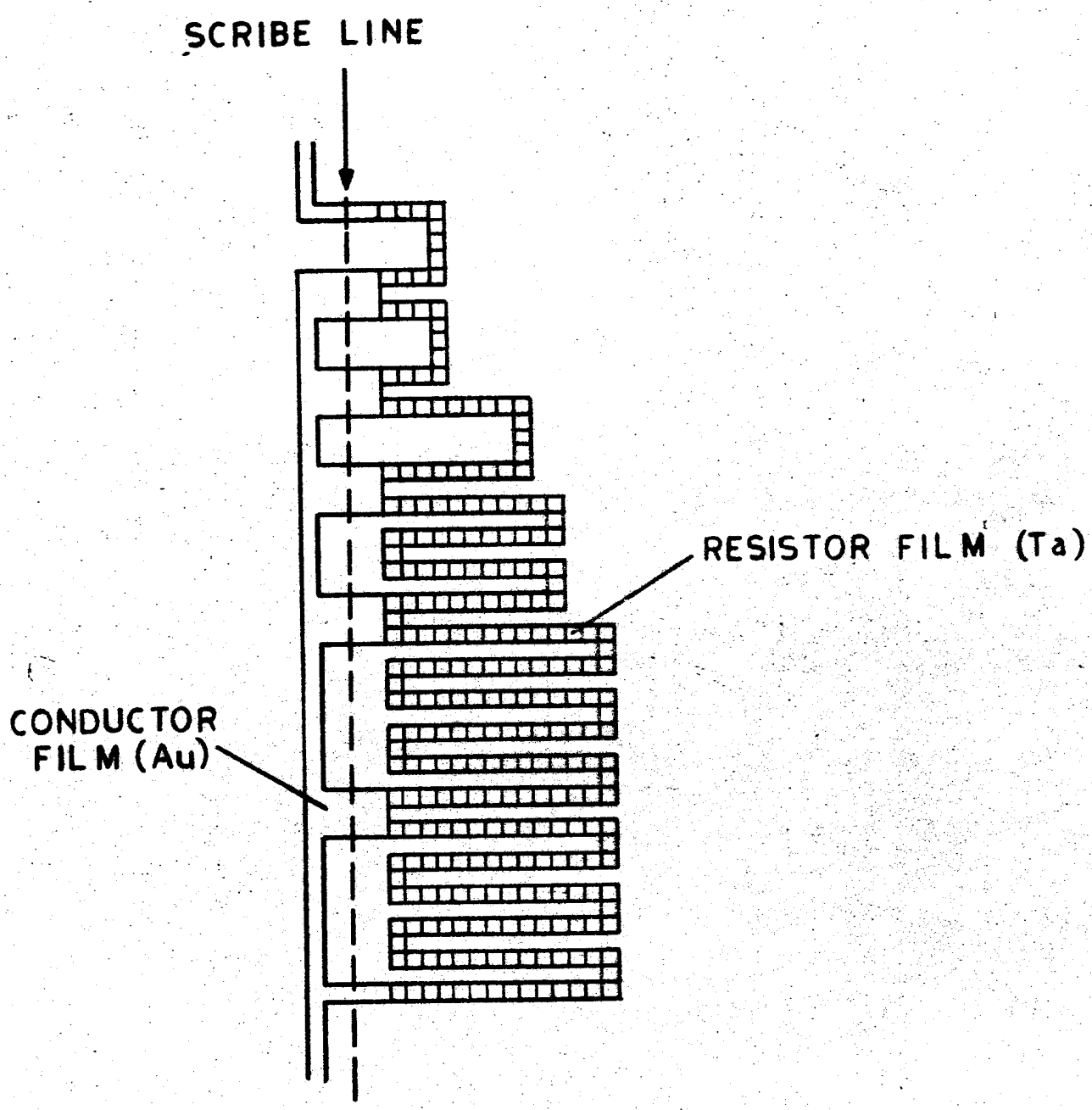

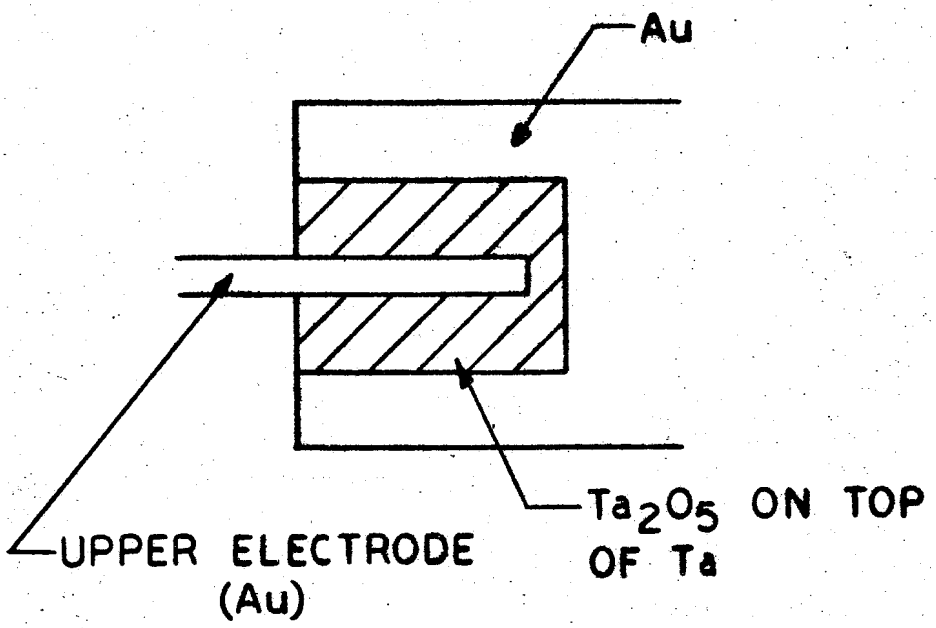

FIGURE 22a

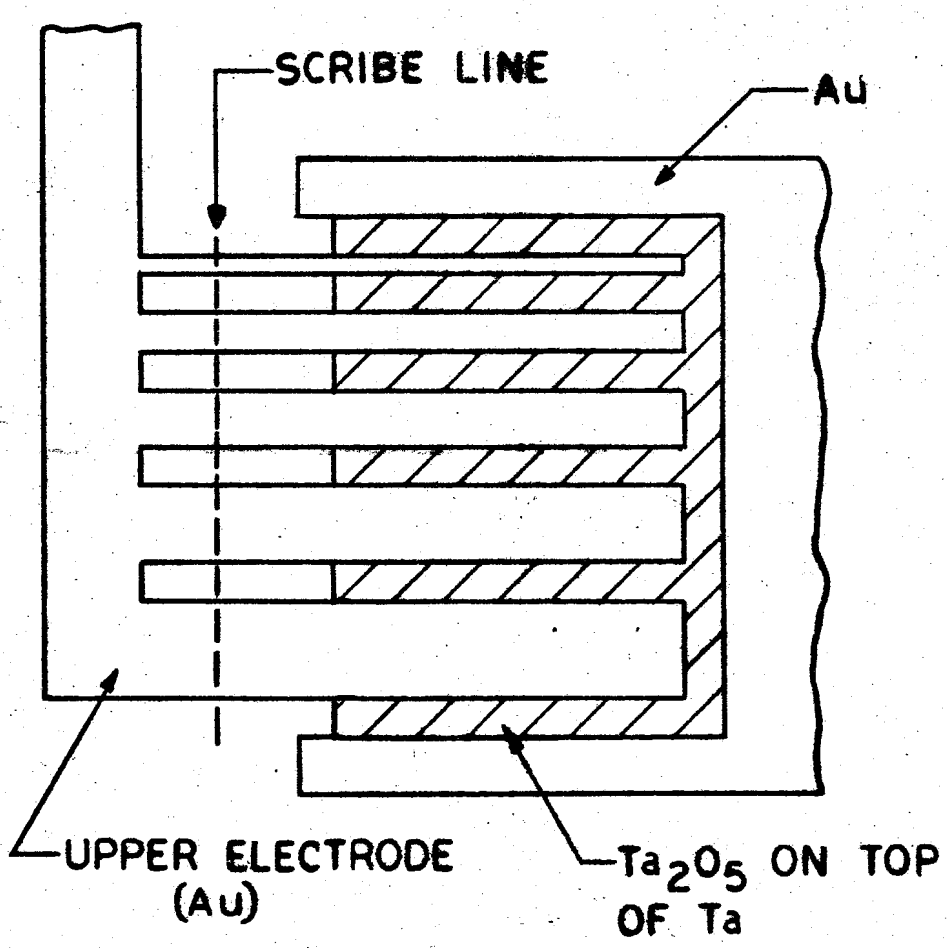

FIGURE 22b

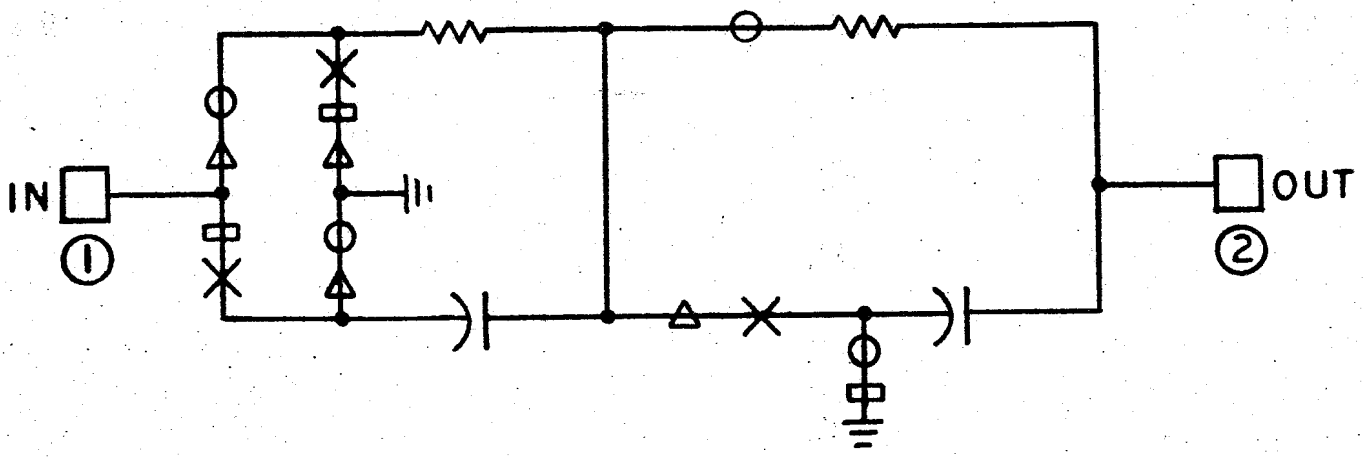

×: OPEN PATHS FOR LPF
○: OPEN PATHS FOR HPF
△: OPEN PATHS FOR BPF
▭: OPEN PATHS FOR RESONATOR

FIGURE 23a

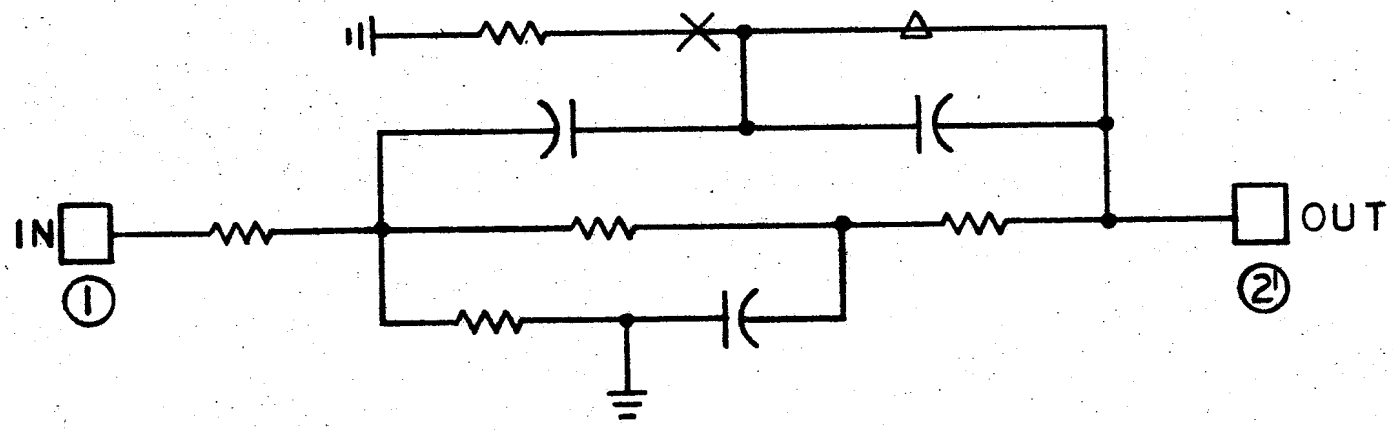

×: OPEN PATHS FOR CONJUGATE COMPLEX POLES AND ZEROS

△: OPEN PATHS FOR FREQUENCY REJECTION NETWORK

FIGURE 23b

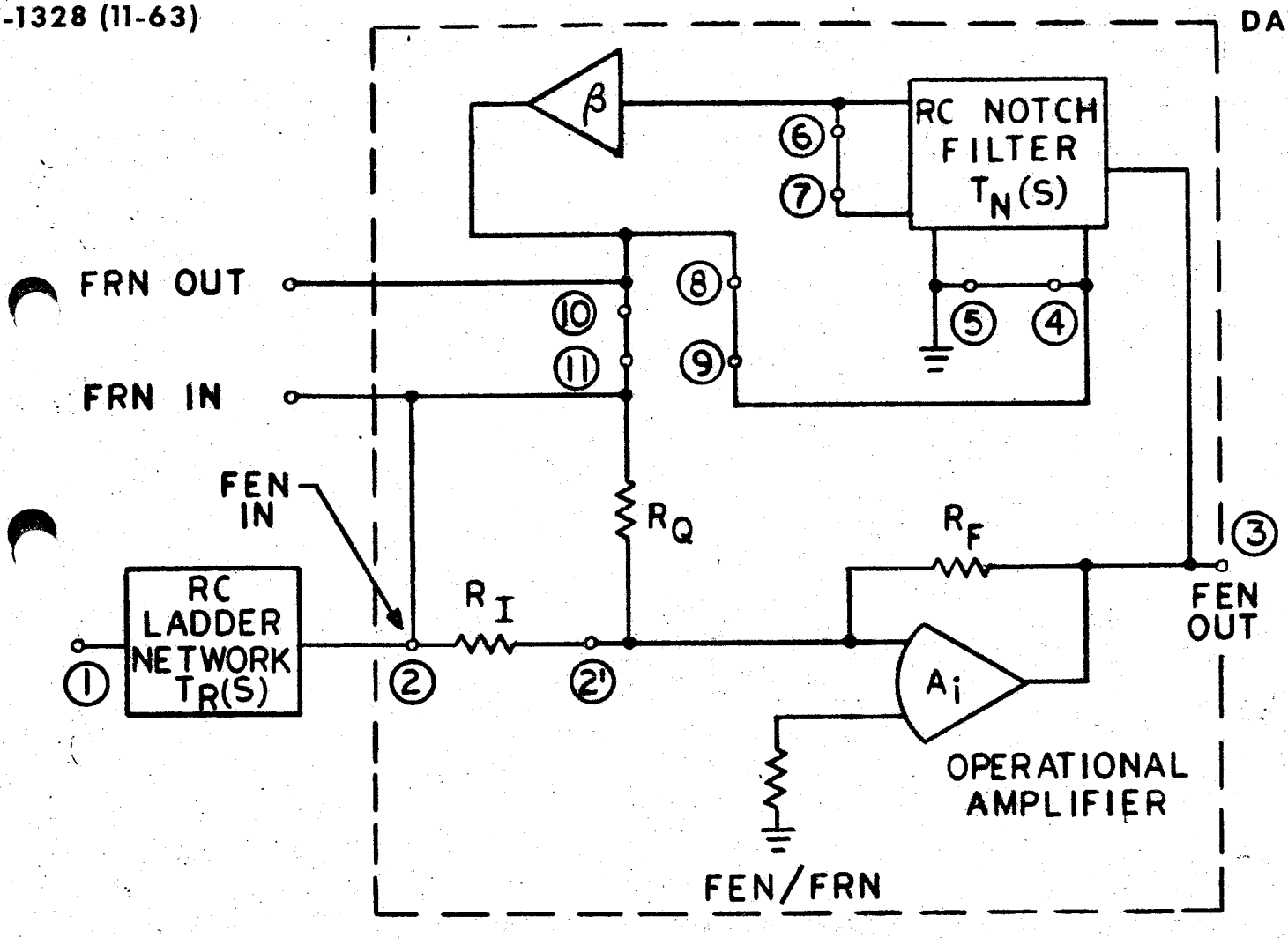

FIGURE 24 a

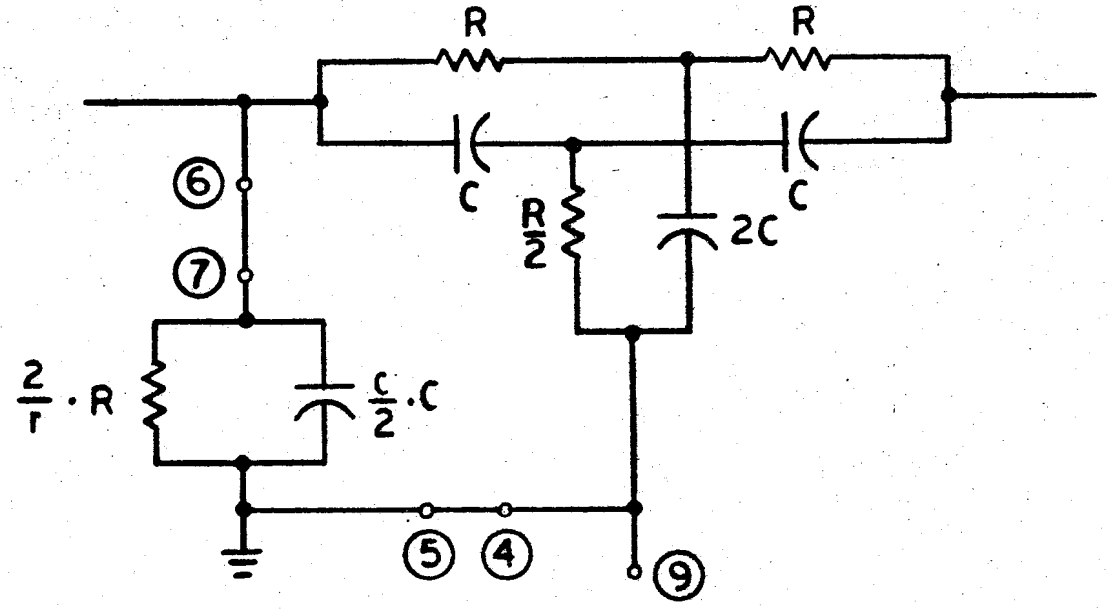

FIGURE 24 b

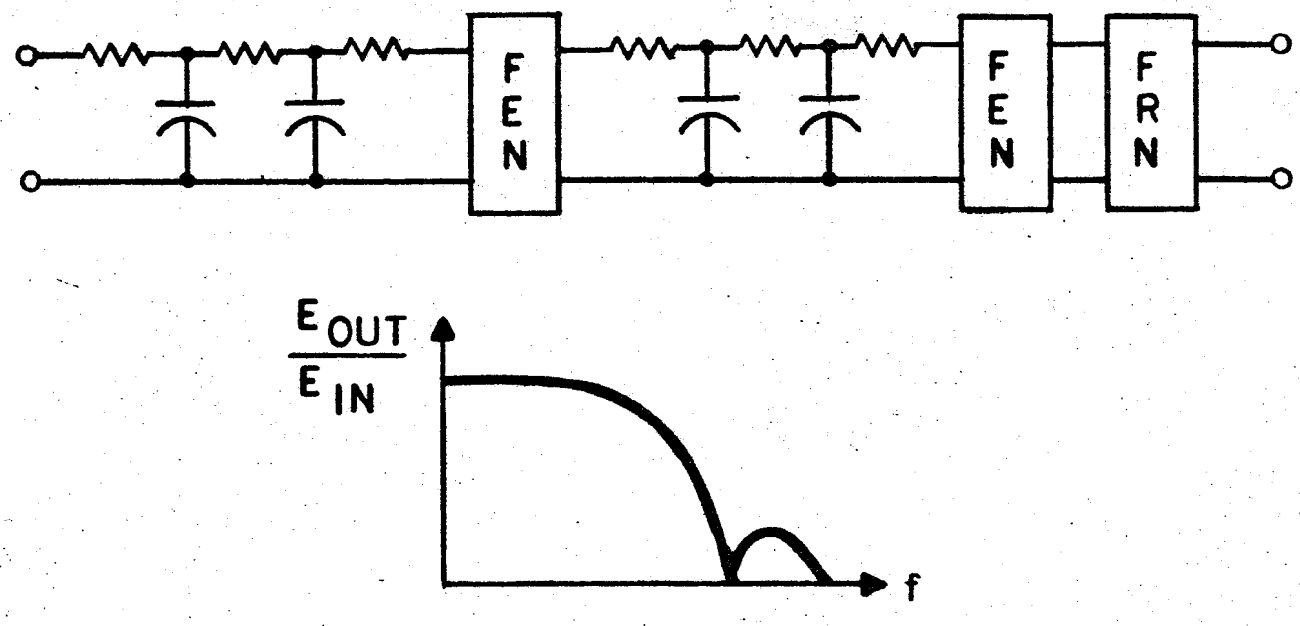

FIGURE 25 a

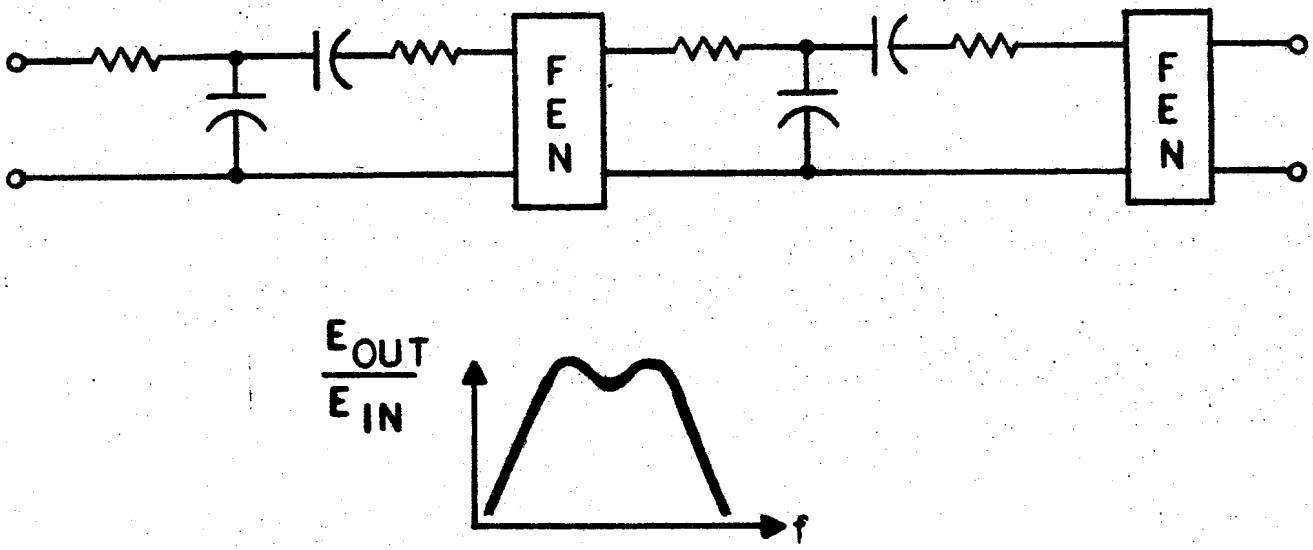

FIGURE 25 b

APPENDIX A

DEFINITION OF Q

Some confusion exists with respect to the definition of the quality factor Q of a network. This is reflected by the numerous discussions that have been published on the subject recently [A.1-A.6]. It is even more evident from the fact that the definitions vary quite widely in textbooks on network analysis and synthesis. There may be some justification for ambiguity in the field of conventional LCR networks, since a differentiation must be made between the quality factor of reactive components and the quality factor of, say, a tuned LCR-tank. In the field of inductorless active networks however, it seems unnecessary.

Let us consider the second order bandpass network whose transmission function is given by

$$T_{BP}(s) = K_{BP} \cdot \frac{s}{(s+p_1)(s+p_2)} = K_{BP} \cdot \frac{s}{s^2 + 2\sigma s + \omega_n^2} \qquad (A.1)$$

The corresponding pole-zero diagram is shown in Figure A.1, the frequency response in Figure A.2. Referring to these two figures, Q has been defined by $\omega_c/2\sigma$, $\omega_n/2\sigma$ which is identical with $1/2\zeta$, and $\omega_p/(\omega_h-\omega_\ell)$. Only when σ is very small, i.e., when the poles are very close to the $j\omega$ axis, are these terms

approximately equal. However in RC active circuit design, where passive RC networks are often considered by themselves, the expressions above can vary significantly.

It seems sufficient to distinguish between two different terms for the characterization of active RC networks, namely the inverse damping factor q and the frequency selectivity Q. They are related to one another but are only identical in special cases.

The inverse damping factor is a theoretical term that determines the location of a particular pole. It is given by:

$$q = \frac{\omega_n}{2\sigma} = \frac{1}{2\zeta} \qquad (A.2)$$

where ω_n is the undamped natural frequency, σ is the distance of the pole from the $j\omega$-axis and ζ is the cosine of the angle between the pole and the negative real axis.

The frequency selectivity Q is a practical, easily measurable term defined as:

$$Q = \frac{\omega_p}{\omega_h - \omega_\ell} \qquad (A.3)$$

ω_p is the frequency at which the steady state transmission is maximum and $(\omega_h - \omega_\ell)$ is the bandwidth between the two frequencies at which the maximum transmitted signal power is halved or the signal level reduced by 3 db. The high and low half-power

frequencies are the geometric mean of the peak frequency, namely:

$$\omega_p^2 = \omega_h \cdot \omega_\ell \qquad (A.4)$$

The theoretical term q is quite general and can be applied to any second order network for which it specifies the location of the corresponding conjugate complex pole pair (see footnote on Page 4 of main text). On the other hand, by nature of its practical definition the frequency selectivity Q is only applicable sensibly to symmetrical bandpass and bandstop networks.

A.1 Second Order Bandpass Networks

The inverse damping factor q results directly from the location of the poles of the specified transmission function and requires no further elaboration. As we shall see further on, its use can be expanded to characterize the zero location of a network. In both cases q increases as the pole or zero approaches the $j\omega$-axis.

The frequency selectivity Q has so far only been defined in physical terms and it remains to be shown that it is directly related to the inverse damping factor. To do so we must first find an expression for the frequency of peak transmission in terms of the transmission poles.

Let us consider the pole-zero diagram of the transmission function given by Equation (A.1) which is redrawn in

Figure A.3. The corresponding frequency response can be expressed in terms of the vectors shown in Figure A.3 as follows:

$$| T(j\omega) | = K_{BP} \left| \frac{\nu}{\mu_1 \mu_2} \right| \qquad (A.5)$$

The area A of the triangle formed by the three points p_1, p_2 and $s = j\omega$ can be expressed by:

$$A = \tfrac{1}{2}\mu_1 \mu_2 \sin \varphi \qquad (A.6)$$

and also by:

$$A = \tfrac{1}{2}(2\omega_c \sigma) \qquad (A.7)$$

Equating (A.6) and (A.7) we find:

$$\frac{1}{\mu_1 \mu_2} = \frac{\sin \varphi}{2\,\omega_c \sigma} \qquad (A.8)^*$$

---

* But for a constant scaling factor, this is the frequency response of a second order lowpass filter expressed as a function of the angle φ. The peak value $K_{LP}/2\omega_c\sigma$ occurs when $\varphi = 90°$. The corresponding peak frequency $[\omega_p]_{LP}$ occurs at the intersection between the $j\omega$-axis and the circle whose diameter is the line segment between the conjugate complex pole pair, (see Figure A.3). Therefore $[\omega_p]_{LP}$ equals

$$\sqrt{\omega_c^2 - \sigma^2} \ .$$

Appendix A - 5

Referring again to Figure A.3:

$$\varphi = \alpha + \beta \tag{A.9}$$

$$tg\alpha = \frac{\omega_c - \nu}{\sigma} \tag{A.10}$$

$$tg\beta = \frac{\omega_c + \nu}{\sigma} \tag{A.11}$$

from (A.9), (A.10), and (A.11):

$$tg\varphi = \frac{2\,\frac{\omega_c}{\sigma}}{1 - \left(\frac{\omega_c^2 - \nu^2}{\sigma^2}\right)} \tag{A.12}$$

Solving (A.12) for ν, we obtain

$$\nu = \left[\omega_c^2 - \sigma^2 + 2\omega_c \sigma \cdot ctg\varphi\right]^{1/2} \tag{A.13}$$

From (A.5), (A.8), and (A.13) we therefore find:

$$|T(j\omega)| = a[b + ctg\varphi]^{\frac{1}{2}} \cdot \sin\varphi \tag{A.14}$$

where

$$a = \frac{K_{BP}}{\sqrt{2\omega_c \sigma}} \tag{A.15}$$

and

$$b = \frac{\omega_c^2 - \sigma^2}{2\omega_c \sigma} \qquad (A.16)$$

To obtain the angle φ_p at which the transmission is maximum the derivative of (A.14) with respect to φ is taken and we obtain:

$$\frac{d\,|T(j\omega)|}{d\varphi} = \frac{a}{2}\left[\frac{2(b+ctg\varphi)\cos\varphi - \sin\varphi^{-1}}{(b+ctg\varphi)^{\frac{1}{2}}}\right] \qquad (A.17)$$

Setting (A.17) equal to zero we get:

$$b \cdot 2 \sin\varphi \cos\varphi + 2\cos^2\varphi - 1 = 0$$

Therefore

$$b \cdot \sin 2\varphi + \cos 2\varphi = 0$$

With (A.16) this becomes:

$$tg2\varphi = \frac{2\,\frac{\omega_c}{\sigma}}{1 - \left(\frac{\omega_c}{\sigma}\right)^2} \qquad (A.18)$$

or

$$tg\varphi_p = \frac{\omega_c}{\sigma} \qquad (A.19)$$

Substituting this value in (A.13) we find:

$$\nu_p = \omega_p = \omega_n \qquad (A.20)$$

The peak frequency of a second order bandpass filter with a conjugate complex pole pair is thus equal to the undamped natural frequency ω_n. This is shown graphically in Figure A.4. The peak transmission value follows from Equation (A.1) as:

$$\hat{T}_{BP} = \frac{K_{BP}}{2\sigma} = \frac{K_{BP}}{\omega_n} \cdot q \qquad (A.21)$$

If the two poles of the transmission function given by Equation (A.1) are negative real, the corresponding pole-zero diagram is of the type shown in Figure A.5. The frequency response, expressed in terms of the vectors shown in the figure are again given by Equation (A.5). Similarly the area A of the triangle formed by the points p_1, p_2, and $s = j\omega$ can be expressed by:

$$A = \tfrac{1}{2}\mu_1\mu_2 \sin\varphi \qquad (A.6)$$

and also by:

$$A = \tfrac{1}{2}(p_2 - p_1)\cdot\nu \qquad (A.22)$$

Letting

$$(p_2 - p_1) = \rho \qquad (A.23)$$

and equating (A.6) and (A.22) we find:

$$\frac{1}{\mu_1\mu_2} = \frac{1}{\rho \cdot \nu} \cdot \sin\varphi \qquad (A.24)$$

Substituting this expression in Equation (A.5) we get:

$$T(s) = \frac{1}{\rho} \sin\varphi \qquad (A.25)$$

T(s) can now be expressed in terms of ν. Referring to Figure A.5.

$$tg\alpha = \frac{p_1}{\nu} \qquad (A.26)$$

$$tg\beta = \frac{p_2}{\nu} \qquad (A.27)$$

and

$$\varphi = \beta - \alpha \qquad (A.28)$$

Therefore:

$$tg\varphi = \frac{\frac{p_2 - p_1}{\nu}}{1 + \frac{p_1 p_2}{\nu^2}} \qquad (A.29)$$

From (A.1) we find:

$$p_1 p_2 = \omega_n^2 \qquad (A.30)$$

and with (A.23), Equation (A.29) becomes:

$$tg\varphi = \frac{\rho\nu}{\nu^2+\omega_n^2} \qquad (A.31)$$

Since:

$$\sin\varphi = \frac{tg\varphi}{\sqrt{1+tg^2\varphi}} \qquad (A.32)$$

Equation (A.25) becomes:

$$T(s) = \frac{\nu}{\left[\left(\nu^2 + \omega_n^2\right)^2 + \rho^2\nu^2\right]^{1/2}} \qquad (A.33)$$

Taking the derivative of (A.33) and setting it equal to zero we can again solve for the value of $\nu = \nu_p$ for which Equation (A.33) has a maximum. Thus we find

$$\nu_p = \omega_p = \omega_n \qquad (A.20)$$

This is the same result as was found for the case of conjugate complex poles. The peak transmission value is therefore also given by Equation (A.21).

It may be of interest to obtain the peak frequency $\omega_p = \omega_n$ graphically. For the conjugate-complex pole case, it is of course simply the distance from either pole to the

coordinate origin. In the negative-real pole case it is the graphical solution to Equation (A.30). This is given by the familiar geometrical construction shown in Figure A.6.

Having obtained the peak frequency ω_p, the half-power bandwidth

$$BW = \omega_h - \omega_\ell \tag{A.34}$$

remains to be calculated. From Equation (A.1) the amplitude response is given by:

$$|T(j\omega)| = K_{BP} \cdot \frac{\omega}{\left[\left(\omega_n^2 - \omega^2\right)^2 + 4\sigma^2\omega^2\right]^{1/2}} \tag{A.35}$$

The half-power frequencies for this expression can be obtained by setting it equal to $\hat{T}_{BP}/\sqrt{2}$. From Equations (A.35) and (A.21) these frequencies are given by the two solutions to the quadratic equation:

$$\omega^2 + 2\sigma\omega - \omega_n^2 = 0 \tag{A.36}$$

which are:

$$\omega_h = \sqrt{\omega_n^2 + \sigma^2} + \sigma \tag{A.37}$$

and

$$\omega_\ell = \sqrt{\omega_n^2 + \sigma^2} - \sigma \qquad (A.38)$$

Forming the product of ω_h and ω_ℓ we get:

$$\omega_h \cdot \omega_\ell = \omega_n^2 \qquad (A.39)$$

which, with Equation (A.20) proves the statement of geometric symmetry expressed by Equation (A.4). The 3 db bandwidth follows from Equations (A.37) and (A.38) as:

$$BW = \omega_h - \omega_\ell = 2\sigma \qquad (A.40)$$

This expression is valid accurately whether the two transmission poles are conjugate complex or negative real. In the latter case however it is more convenient to express the bandwidth in terms of the real poles p_1 and p_2 than in terms of σ. From Equation (A.1) we find:

$$BW = 2\sigma = p_1 + p_2 \qquad (A.41)$$

Comparing Equations (A.20), (A.30) and (A.41) with Equations (A.2) and (A.3) we find that for second order networks of the general form given by Equation (A.1):

$$Q_{BP} = q = \frac{\omega_n}{2\sigma} = \frac{\sqrt{p_1 p_2}}{p_1 + p_2} \qquad (A.41)$$

Furthermore this relation applies accurately whether the two transmission poles are conjugate complex or negative real.

A.II Frequency Emphasizing Networks

The transmission function of an FEN is given by:

$$T_F(s) = K_F \cdot \frac{s^2 + 2\sigma_z s + \omega_{n_z}^2}{s^2 + 2\sigma_p s + \omega_{n_p}^2} \qquad (A.42)$$

where

$$\sigma_p < \sigma_z \qquad (A.43)$$

To derive the steady-state frequency characteristic of $T_F(s)$, it is useful to introduce the normalized angular frequency

$$\Omega = \frac{\omega}{\omega_n} \qquad (A.44)$$

and the inverse damping factor given by Equation (A.2). The amplitude response then follows as:

$$|T_F(j\Omega)| = K_F \cdot \frac{\omega_{n_z}}{\omega_{n_p}} \cdot \left[\frac{\left(\frac{1}{\Omega_z} - \Omega_z\right)^2 + \frac{1}{q_z^2}}{\left(\frac{1}{\Omega_p} - \Omega_p\right)^2 + \frac{1}{q_p^2}} \right]^{1/2} \qquad (A.45)$$

$$\frac{\left(\frac{1}{\Omega} - \Omega\right)^2 + \frac{1}{q_z^2}}{\left(\frac{1}{\Omega} - \Omega\right)^2 + \frac{1}{q_p^2}} = \frac{1}{2} \qquad (A.59)$$

Multiplying out we obtain

$$(1-\Omega^2)^2 - \Omega^2\left(\frac{1}{q_p^2} - \frac{2}{q_z^2}\right) = 0 \qquad (A.60)$$

With the substitution:

$$q_{FAN}^2 = \frac{q_p^2 q_z^2}{q_z^2 - 2q_p^2} \qquad (A.61)$$

Equation (A.60) takes on the same form as Equation (A.52) and all subsequent results are formally the same except that q_{FEN} is substituted by q_{FAN}. Therefore, by substituting Equation (A.61) into Equation (A.56), the frequency selectivity of the FAN result as:

$$Q_{FAN} = \frac{1}{\Omega_h - \Omega_1} = \frac{q_p q_z}{\sqrt{q_z^2 - 2q_p^2}} \qquad (A.62)$$

Due to the limitation given by (A.58) this expression always remains real.

where

$$q_p > q_z \tag{A.46}$$

For the symmetrical FEN, $\omega_{n_z} = \omega_{n_p}$ and Equation (A.45) becomes:

$$|T_F(j\Omega)| = K_F \cdot \left[\frac{\left(\frac{1}{\Omega} - \Omega\right)^2 + \frac{1}{q_z^2}}{\left(\frac{1}{\Omega} - \Omega\right)^2 + \frac{1}{q_p^2}} \right]^{1/2} \tag{A.47}$$

As under Section A.1, it can be shown that the peak value of (A.47) occurs at $\Omega = 1$ and is given by

$$\hat{T}_F = \frac{q_p}{q_z} K_F \tag{A.48}$$

The half-power frequencies of Equation (A.47) can be obtained by setting it equal to $\hat{T}_F/\sqrt{2}$ thus:

$$\frac{\left(\frac{1}{\Omega} - \Omega\right)^2 + \frac{1}{q_z^2}}{\left(\frac{1}{\Omega} - \Omega\right)^2 + \frac{1}{q_p^2}} = \frac{1}{2}\left(\frac{q_p}{q_z}\right)^2 \tag{A.49}$$

This can be simplified to:

$$(1-\Omega^2)^2\left(q_p^2 - 2q_z^2\right) - \Omega^2 = 0 \qquad \text{(A.50)}$$

By introducing:

$$q_{FEN}^2 = q_p^2 - 2q_z^2 \qquad \text{(A.51)}$$

Equation (50) can be further simplified as follows:

$$\Omega^2 + \frac{\Omega}{q_{FEN}} - 1 = 0 \qquad \text{(A.52)}$$

This is the normalized version of Equation (A.36). Thus, the two -3 db frequencies in normalized form are given by:

$$\Omega_h = \sqrt{\frac{1}{4q_{FEN}^2} + 1} + \frac{1}{2q_{FEN}} \qquad \text{(A.53)}$$

and

$$\Omega_\ell = \sqrt{\frac{1}{4q_{FEN}^2} + 1} - \frac{1}{2q_{FEN}} \qquad \text{(A.54)}$$

These two frequencies satisfy the condition for geometrical symmetry, namely

$$\Omega_h \cdot \Omega_\ell = 1 \qquad \text{(A.55)}$$

The frequency selectivity of the FEN results from Equations (A.53) and (A.54) as

$$Q_{FEN} = \frac{1}{\Omega_h - \Omega_l} = q_{FEN} = \sqrt{q_p^2 - 2q_z^2} \qquad (A.56)$$

Since the FEN is characterized by condition (A.46) the expression under the square root cannot, of course, become negative.

A.III Frequency Attenuating and Rejection Networks

We start out here with the same transmission function as is given by Equations (A.42) and (A.45) except that here:

$$\sigma_p > \sigma_z \qquad (A.57)$$

In terms of the inverse damping factor:

$$q_p < q_z \qquad (A.58)$$

Under these circumstances and considering only the symmetrical FAN, we get the amplitude response given by Equation (A.47). This is maximum at zero and very high frequencies where it approaches the constant value K_F. For this case, therefore, the half-power frequencies are obtained by setting Equation (A.47) equal to $K_F/\sqrt{2}$, namely:

The frequency selectivity of an FRN (i.e., Frequency Rejection Network) or notch filter is characterized by the special case of Equation (A.42) when $\sigma_z = 0$. This corresponds to Equations (A.45) and (A.47) when $q_z = \infty$. Thus we can derive the frequency selectivity of an FRN by letting q_z approach infinity in Equation (A.62). We obtain:

$$Q_{FRN} = q_p \tag{A.63}$$

A.IV Second Order Bandpass Network Incorporating High Selectivity Frequency Emphasizing Network (HSFEN)

From the main text (Section IV.2) it follows that a high Q second order bandpass network is generated by cascading an RC ladder network and an HSFEN (High Selectivity Frequency Emphasizing Network). The corresponding transmission function is of the form:

$$T(s) = K \cdot \frac{s}{s^2 + \frac{\omega_n}{q_1} s + \omega_n^2} \cdot \frac{s^2 + \frac{\omega_n}{q_2} s + \omega_n^2}{s^2 + \frac{\omega_n}{q_3} s + \omega_n^2} \tag{A.64}$$

q_1 corresponds to the poles of the RC transfer admittance and q_3 is determined by the poles of the specified selective network. Being a high Q network, q_3 is by definition much larger than q_1. Finally the characteristic of the HSFEN is that its zeros are not restricted to the negative real axis, in other words q_2 is larger than q_1. Thus:

$$q_1 < q_2 < q_3 \tag{A.65}$$

Equation (A.64) can be written as follows:

$$T(s) = T_{BP}(s) \cdot T_E(s) \tag{A.66}$$

where

$$T_{BP}(s) = V_{BP} \cdot \frac{s}{s^2 + \frac{\omega_n}{q_3} s + \omega_n^2} \tag{A.67}$$

$$T_E(s) = K_E \cdot \frac{s^2 + \frac{\omega_n}{q_2} s + \omega_n^2}{s^2 + \frac{\omega_n}{q_1} s + \omega_n^2} \tag{A.68}$$

and

$$K = K_{BP} \cdot K_E \tag{A.69}$$

$T_{BP}(s)$ is the actual transfer function desired, $T_E(s)$ constitutes an error in the resulting frequency response. Obviously if, as is the case for the MSPEN (Medium Selectivity Frequency Emphasizing Network), q_2 were equal to q_1 than the Q of the overall network would be equal to q_3. Since this is not the case here, the Q of the overall network represented by the transmission function Equation (A.64) must be calculated separately.

The normalized amplitude response corresponding to Equations (A.64) or (A.66) is given by:

$$|T(j\Omega)| = \frac{\frac{K}{\omega_n}}{\left[\left(\frac{1}{\Omega} - \Omega\right)^2 + \frac{1}{q_3^2}\right]^{1/2}} \cdot \left[\frac{\left(\frac{1}{\Omega} - \Omega\right)^2 + \frac{1}{q_2^2}}{\left(\frac{1}{\Omega} - \Omega\right)^2 + \frac{1}{q_1^2}}\right]^{1/2} \tag{A.70}$$

The peak value occurring for $\Omega = 1$ is given by

$$\hat{T} = \frac{K}{\omega_n} \cdot \frac{q_1}{q_2} \cdot q_3 \tag{A.71}$$

The -3 db (i.e., half power) frequencies can now be obtained as before. For convenience we first introduce the substitution:

$$w = \left(\frac{1}{\Omega} - \Omega\right) \tag{A.72}$$

Setting Equation (A.70) equal to $\hat{T}/\sqrt{2}$ and making the above substitution we find:

$$\frac{2}{w^2 q_3^2 + 1} \cdot \frac{w^2 q_2^2 + 1}{w^2 q_1^2 + 1} = 1 \tag{A.73}$$

This can be multipled out to give:

$$w^4 + w^2\left[\frac{q_1^2 + q_3^2 - 2q_2^2}{q_1^2 q_3^2}\right] - \frac{1}{q_1^2 q_3^2} = 0 \qquad (A.74)$$

With the new substitutions:

$$z = w^2 \qquad (A.75)$$

$$Q_1^2 = \frac{q_1^2 q_3^2}{q_1^2 + q_3^2 - 2q_2^2} \qquad (A.76)$$

and

$$Q_2^2 = q_1 q_3 \qquad (A.77)$$

Equation (74) becomes

$$z^2 + \frac{z}{Q_1^2} - \frac{1}{Q_2^4} = 0 \qquad (A.78)$$

The roots of this equation can be found by inspection. The negative root has no physical meaning. Thus we are left with the solution:

$$Z = \frac{1}{2}\left[\sqrt{\frac{1}{Q_1^4} + \frac{4}{Q_2^4}} - \frac{1}{Q_1^2}\right] \qquad (A.79)$$

From Equations (A.72) and (A.75) this becomes:

$$\left(\frac{1}{\Omega} - \Omega\right)^2 = \frac{1}{2}\left[\sqrt{\frac{1}{Q_1^4} + \frac{4}{Q_2^4}} - \frac{1}{Q_1^2}\right] \qquad (A.80)$$

Making the substitution

$$q_{HF}^2 = \frac{2}{\left[\sqrt{\frac{1}{Q_1^4} + \frac{4}{Q_2^4}} - \frac{1}{Q_1^2}\right]} \qquad (A.81)$$

Equation (A.80) becomes:

$$\Omega^2 + \frac{\Omega}{q_{HF}} - 1 = 0 \qquad (A.82)$$

This equation is formally identical with Equation (A.52). From Equations (A.56), (A.76), (A.77) and (A.81) we therefore find for the Q of the HSFEN:

$$Q_{HSFEN} = \frac{\sqrt{2}\, q_1 q_3}{\left[\sqrt{\left(q_1^2 + q_3^2 - 2q_2^2\right)^2 + 4q_1^2 q_3^2} - \left(q_1^2 + q_3^2 - 2q_2^2\right)\right]^{1/2}} \qquad (A.83)$$

as written in another form:

$$Q^2_{HSPEN} = \frac{2q_1^2q_3^2}{q_1^2 + q_3^2 - 2q_2^2} \cdot \frac{1}{\sqrt{1 + \frac{4q_1^2q_3^2}{\left(q_1^2 + q_3^2 - 2q_2^2\right)^2} - 1}} \tag{A.84}$$

As to be expected, for the limiting case that $q_1 = q_2$ the above equations give

$$Q_{HSFEN}\Big|_{q_1=q_2} = q_3 \tag{A.85}$$

In general q_1 and q_2 will be given and the value of q_3 will be required that corresponds to a specified frequency selectivity Q. Solving Equation (A.84) for q_3 we get:

$$q_3 = Q_{HSFEN}\left[\frac{\frac{Q^2_{HSFEN}}{q_1^2} + 2\left(\frac{q_2}{q_1}\right)^2 - 1}{\frac{Q^2_{HSFEN}}{q_1^2} + 1}\right]^{1/2} \tag{A.86}$$

Using the terminology of the main text (Section IV.2) we have:

$$q_1 \equiv q_R \tag{A.87a}$$

$$q_2 = q_{Na} \tag{A.87b}$$

$$q_3 = q_p \tag{A.87c}$$

Let us consider the circuit configuration of Figure 15. Assuming a symmetrical Twin-T in the HSFEN and a unity gain noninverting amplifier ($\beta = 1$) we have:

$$q_R = 0.25 \tag{A.88}$$

and

$$q_{Na} = \frac{1}{2}\,\frac{1+r}{r} \tag{A.89}$$

where

$$r = \frac{2R}{R_L} \tag{A.90}$$

Substituting Equations (A.87) to (A.90) in (A.86) we get:

$$q_p = Q_{HSFEN}\left[\frac{16\,Q^2_{HSFEN} + 8\left(\frac{1+r}{r}\right)^2 - 1}{16\,Q^2_{HSFEN} + 1}\right]^{1/2} \tag{A.91}$$

A typical value for r is 0.1 in which case $q_{Na} = 5.5$. Substituting these values into Equation (A.86) we get:

$$q_p = Q_{HSPEN}\left[\frac{16\ Q^2_{HSFEN} + 967}{16\ Q^2_{HSFEN} + 1}\right]^{1/2} \qquad (A.92)$$

Expression (A.91) has been plotted in Figure A.7a and A.7b with the resistor ratio r as parameter. For r values larger than 0.05, the required inverse damping factor q_p is approximately equal to the specified frequency selectivity Q_{HSFEN}. For smaller r values than 0.05, q_p is required to be appreciably larger than the desired frequency selectivity. This is to make up for the effective FAN that is generated when using an uncompensated HSFEN to obtain a second order bandpass filter of the type defined by Equation (A.1). In Figure A.8 the ratio of q_p to Q_{HSFEN} has been plotted on semilog paper for different values of the parameter r.

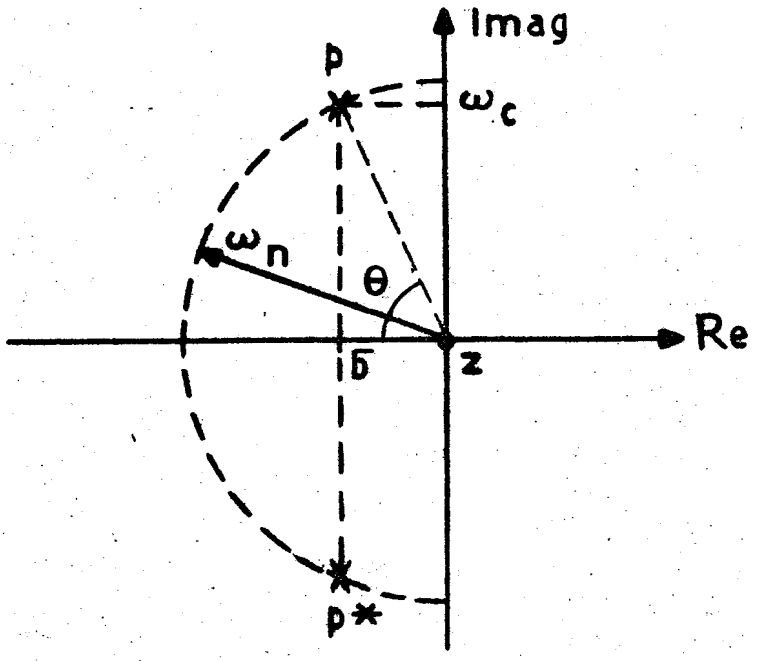

$\zeta = \cos \theta$

FIG. A. 1

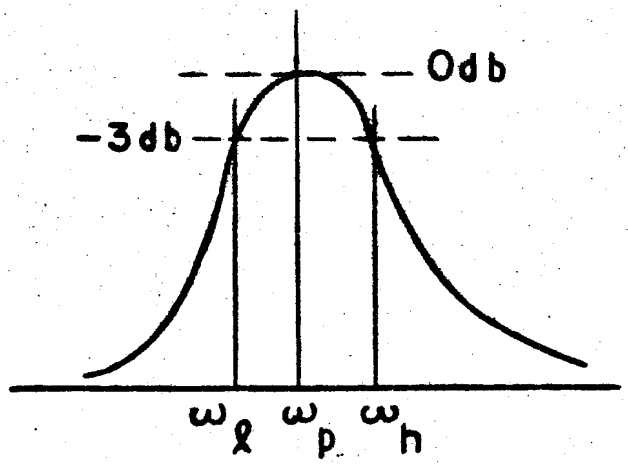

FIG. A. 2

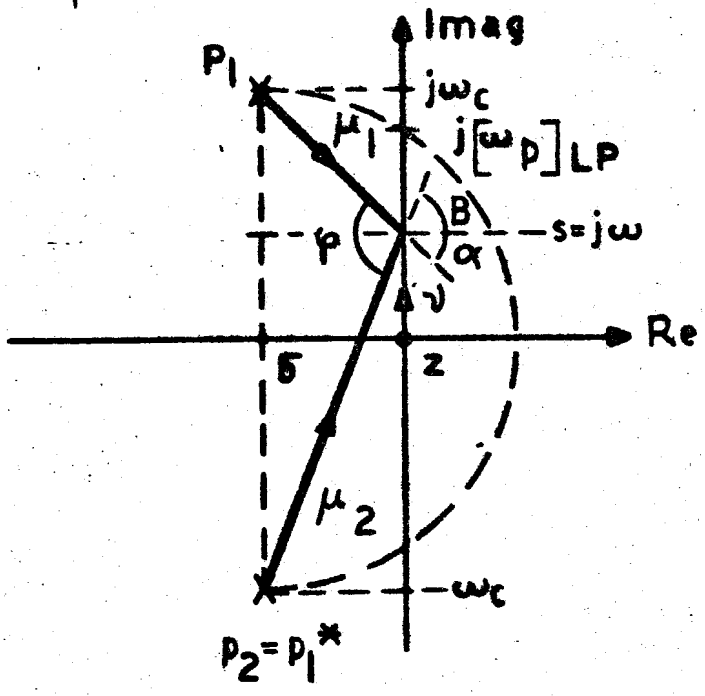
Imag
p_1
$j\omega_c$
μ_1
$j[\omega_p]_{LP}$
β
φ
α
$s=j\omega$
ν
Re
δ
z
μ_2
$-\omega_c$
$p_2=p_1^*$

FIG. A. 3

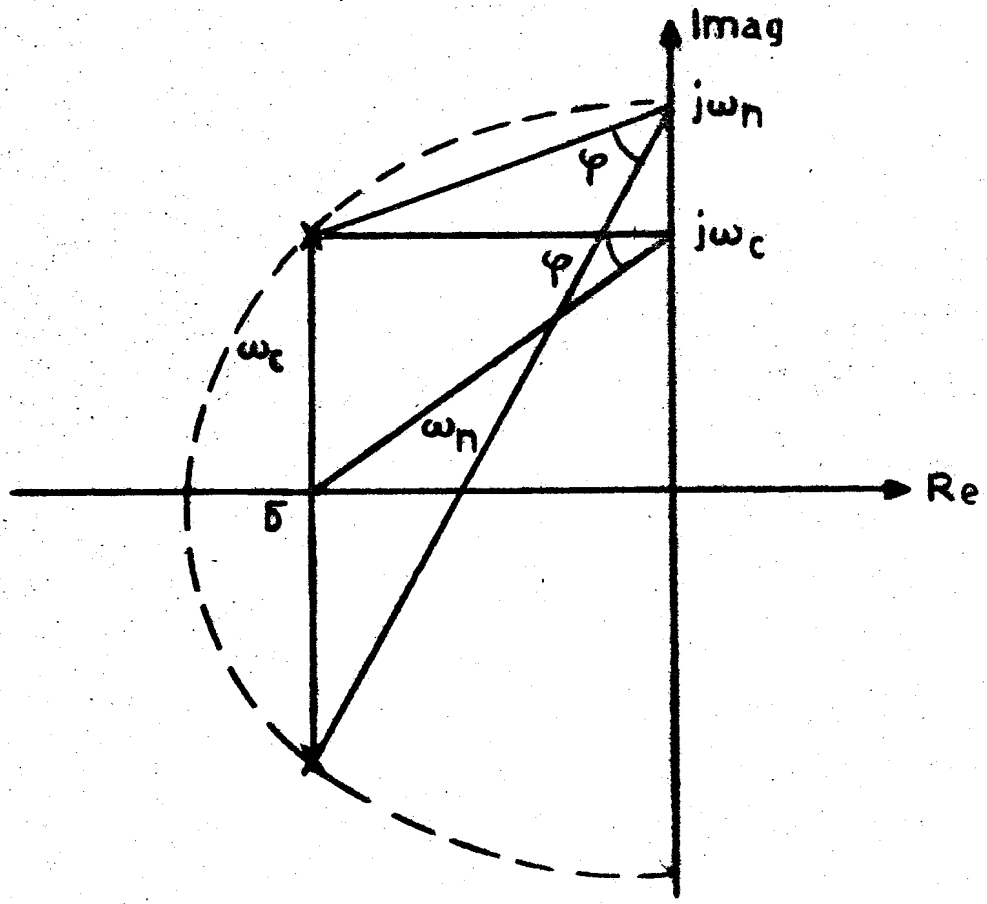
Imag
$j\omega_n$
φ
$j\omega_c$
φ
ω_c
ω_n
Re
δ

FIG. A. 4

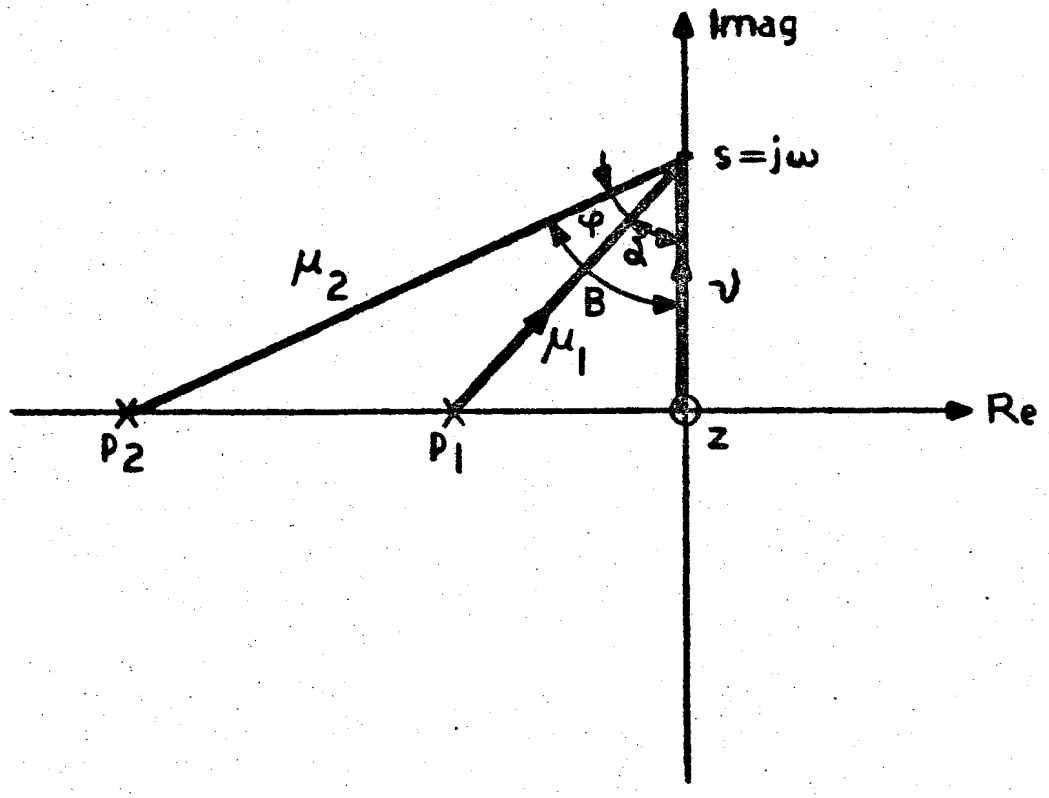

FIG. A.5

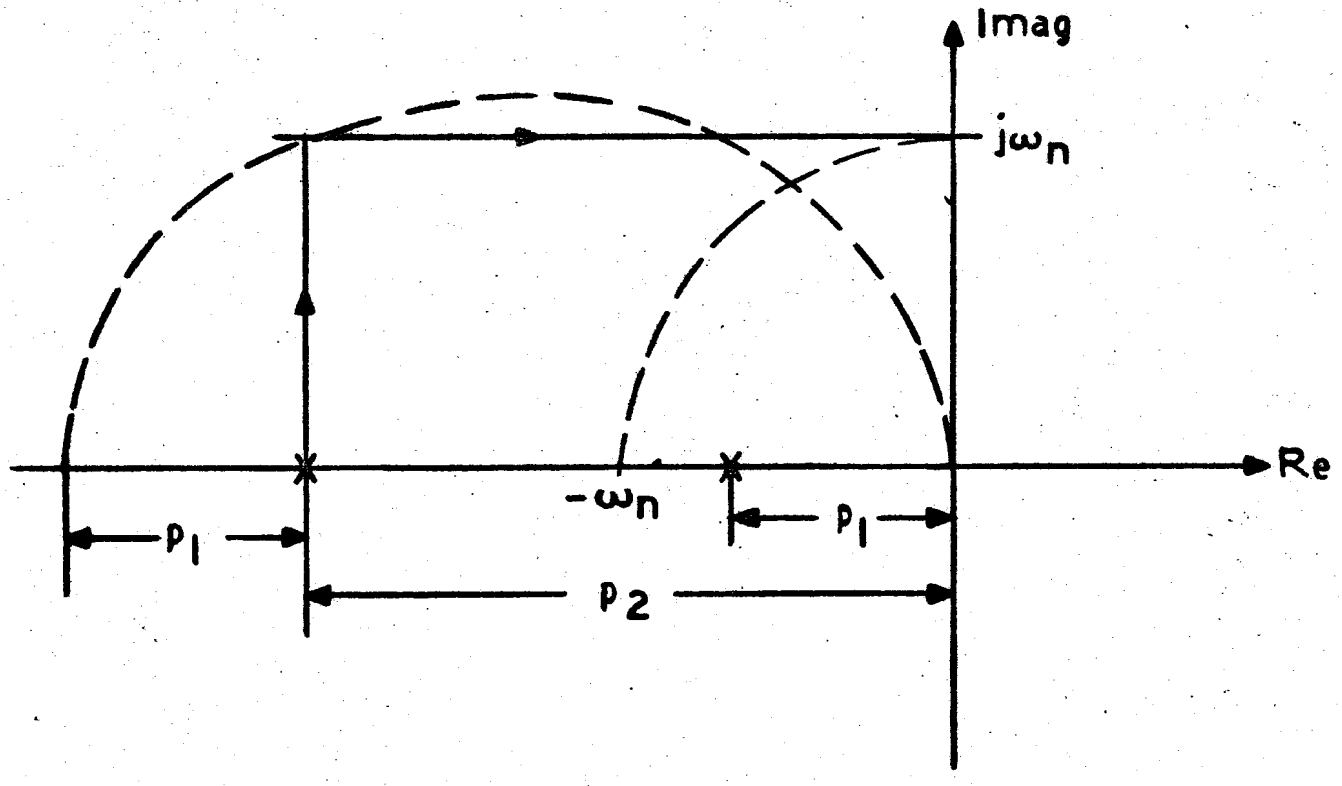

FIG. A.6

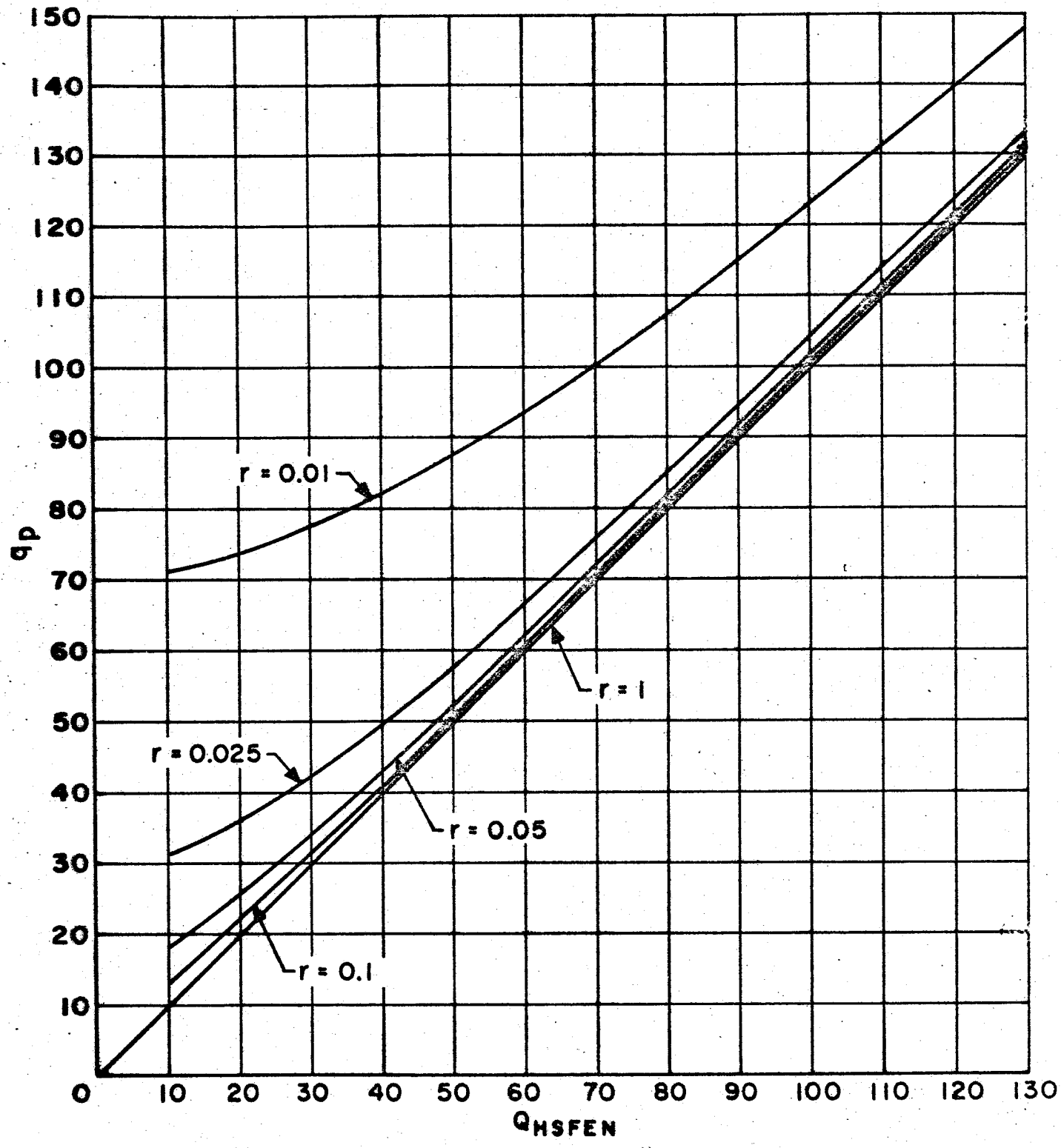
150
140
130
120
110
100
90
80
70
60
50
40
30
20
10
0
qp
r = 0.01
r = 0.025
r = 0.05
r = 0.1
r = 1
10
20
30
40
50
60
70
80
90
100
110
120
130
QHSFEN

FIG. A.7a

DATE FILE

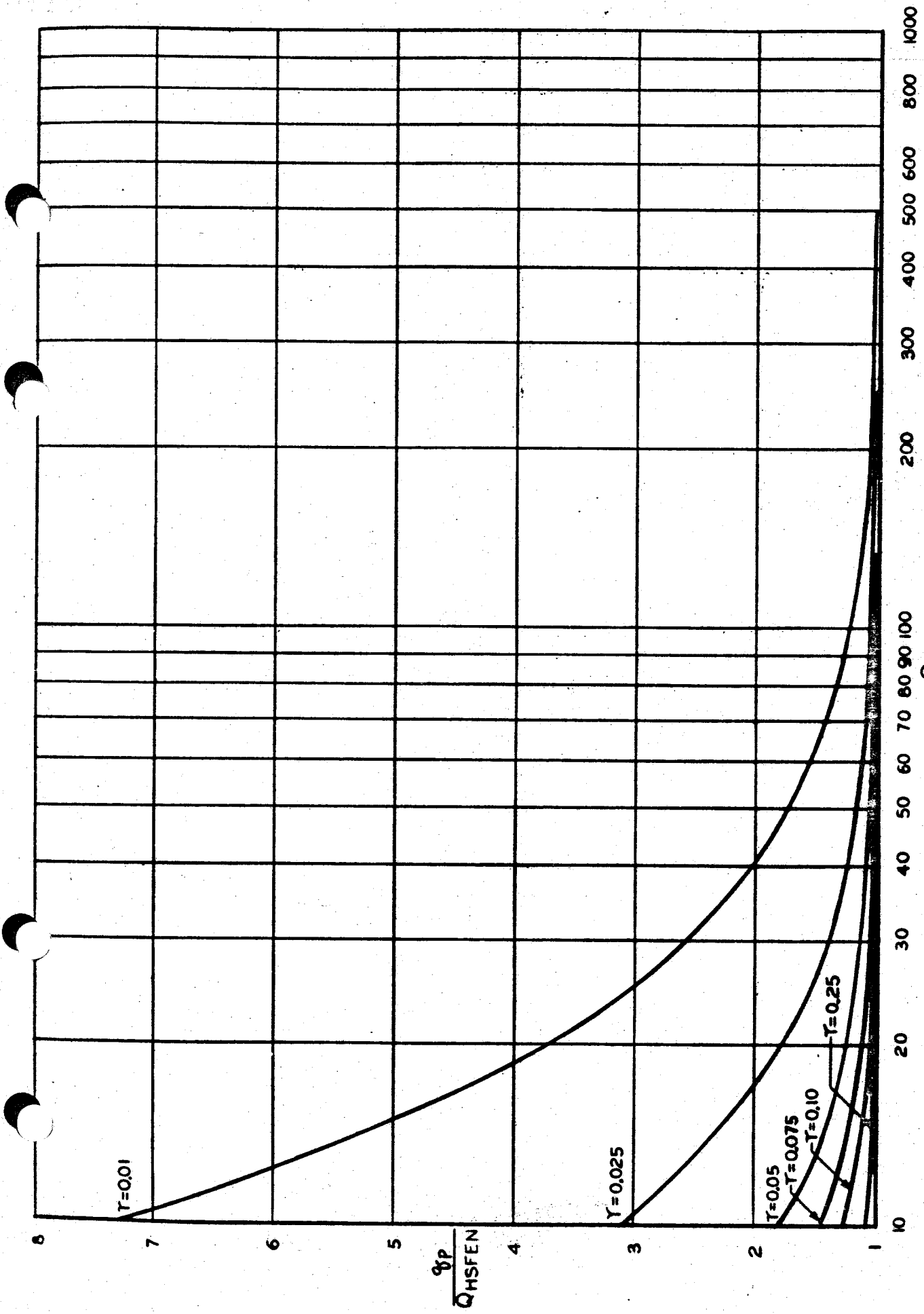

FIG. A.8

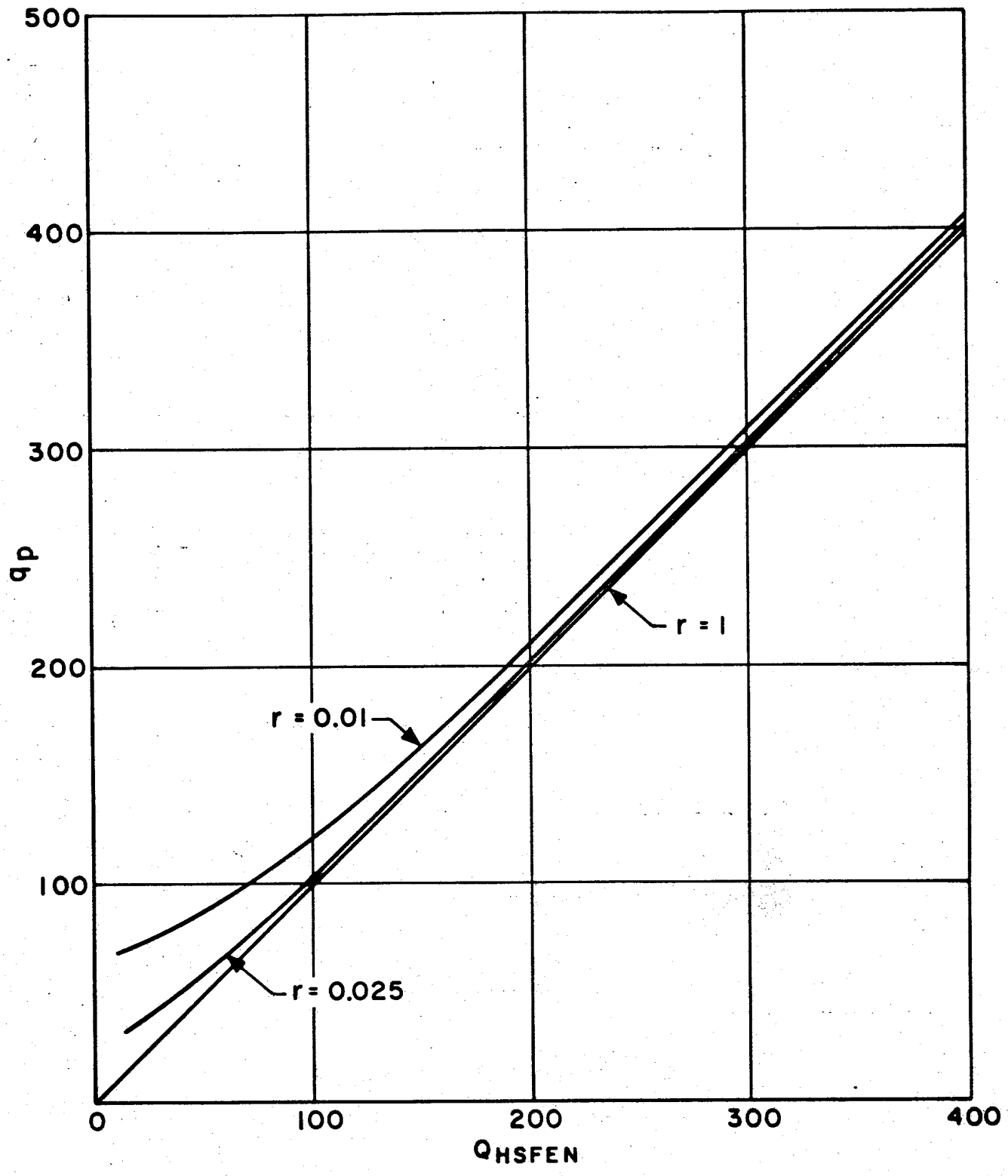

FIG. A.7b

APPENDIX B

ANALYSIS OF THE SHORT-CIRCUIT TRANSFER ADMITTANCE OF SECOND ORDER RC NETWORKS

I. General Network Configurations

A. Five Element Ladder Network

We consider here the configuration shown in Figure B.1. By straightforward ladder analysis the short-circuit transfer admittance results as:

$$-y_{21} = \left.\frac{I_0}{E_{in}}\right|_{E_0=0}$$

$$= \frac{1}{Z_1Z_2Z_3Y_1Y_2 + Z_1(Z_2+Z_3)Y_1 + Z_3(Z_1+Z_2)Y_2 + Z_1 + Z_2 + Z_3} \quad (B.1)$$

B. Three Element Ladder Network

This configuration is shown in Figure B.2. The short-circuit transfer admittance results from Equation (B.1) by setting Y_2 and Z_3 equal to zero. Thus:

$$-y_{21} = \left.\frac{I_0}{E_{in}}\right|_{E_0=0} = \frac{1}{Z_1Z_2Y_1+Z_1+Z_2} \quad (B.2)$$

or rewritten:

$$-y_{21} = \frac{1}{Z_1+Z_2} \cdot \frac{1}{1+Y_1 Z_p} \qquad (B.3)$$

where:

$$Z_p = \frac{Z_1 Z_2}{Z_1+Z_2} \, . \qquad (B.4)$$

C. Six Element, Partially Bridged Ladder Network

The configuration considered here is shown in Figure B.3. The short-circuit transfer admittance is obtained by first calculating the y-matrix of the T-network shown in Figure B.4. This is given by:

$$[y]' = \frac{1}{Y_1+Y_2+Y_3} \begin{bmatrix} Y_1(Y_2+Y_3) & -Y_1Y_2 \\ -Y_1Y_2 & Y_2(Y_1+Y_3) \end{bmatrix} \qquad (B.5)$$

Connecting the two-port shown in Figure B.5 in parallel with the T-network of Figure B.4, the y-matrix of the resulting bridged-T becomes:

$$[y] = \begin{bmatrix} \frac{Y_1(Y_2+Y_3)}{Y_1+Y_2+Y_3} + Y_4 & -\frac{Y_1Y_2}{Y_1+Y_2+Y_3} - Y_4 \\ -\frac{Y_1Y_2}{Y_1+Y_2+Y_3} - Y_4 & \frac{Y_2(Y_1+Y_3)}{Y_1+Y_2+Y_3} + Y_4 \end{bmatrix} \qquad (B.6)$$

The three elements of the pi-network shown in Figure B.6 can be expressed in terms of its short-circuit admittance ~~parameters~~ as follows:

$$y_1 = y_{11} + y_{21} \qquad (B.7)$$

$$z_2 = -\frac{1}{y_{21}} \qquad (B.8)$$

$$y_2 = y_{22} + y_{21}. \qquad (B.9)$$

With these equations the bridged-T network characterized by the y-matrix given in Equation B.6 can be transformed into the pi-network shown in Figure B.6. We find for the corresponding network elements:

$$y_1 = \frac{Y_1Y_3}{Y_1+Y_2+Y_3} \qquad (B.10)$$

$$z_2 = \frac{Y_1+Y_2+Y_3}{Y_1Y_2 + Y_4(Y_1+Y_2+Y_3)} \qquad (B.11)$$

and

$$y_2 = \frac{Y_2Y_3}{Y_1+Y_2+Y_3}. \qquad (B.12)$$

Finally, adding Z_a and Y_b as shown in Figure B.7, we obtain the four element ladder network shown in Figure B.8 for which:

$$z_1 = Z_a \tag{B.13}$$

and:

$$y_1' = Y_b + \frac{Y_1 Y_3}{Y_1+Y_2+Y_3} . \tag{B.14}$$

The elements z_2 and y_2 remain unchanged and are given by Equations (B.11) and (B.12) respectively. The short-circuit transfer admittance for this network is the same as that for the configuration shown in Figure (B.2) which is given by Equation (B.2). Therefore, substituting Equations (B.11) to (B.14) in Equation (B.2) we obtain the short-circuit transfer admittance of the configuration shown in Figure (B.3) as:

$$-y_{21} = \frac{Y_1 Y_2 + Y_4(Y_1+Y_2+Y_3)}{Z_a Y_1(Y_2+Y_3) + (Y_1+Y_2+Y_3)[Za(Y_4+Y_b) + 1]} \tag{B.15}$$

D. Nine Element, Partially Bridged Twin-T Network

We consider here the network configuration shown in Figure B.9. From Appendix D (see Figures D.2c, D.3 and Equations D.9 to D.11) we know the elements of the equivalent π-network of a perfectly nulled Twin-T to be (see Figure B.10):

$$Z_1 = \frac{R_1}{1 + \frac{\tau_1}{\tau}} \left(1 + \frac{1}{s\tau}\right) \qquad \text{(B.16)}$$

$$Z_2 = \frac{R_2}{1 + \frac{\tau_2}{\tau}} \left(1 + \frac{1}{s\tau}\right) \qquad \text{(B.17)}$$

$$Z_3 = R_s \frac{\left(1 + \frac{1}{s\tau}\right)}{s.\tau_s + \frac{1}{s\tau}} \qquad \text{(B.18)}$$

where:

$$\tau_1 = R_1 C_1$$

$$\tau_2 = R_2 C_2$$

$$\tau_s = R_s C_s$$

$$\tau = R_p C_3 = R_3 C_p$$

$$C_s = \frac{C_1 C_2}{C_1 + C_2}$$

$$C_p = C_1 + C_2$$

$$R_s = R_1 + R_2$$

$$R_p = \frac{R_1 R_2}{R_1 + R_2} .$$

The y-matrix of the π-network in Figure B.10 is given by

$$[y]' = \begin{bmatrix} \frac{1}{Z_1} + \frac{1}{Z_3} & -\frac{1}{Z_3} \\ -\frac{1}{Z_3} & \frac{1}{Z_2} + \frac{1}{Z_3} \end{bmatrix} \tag{B.19}$$

As with the preceding case under C, the effect of the admittance Y_4 across the Twin-T can be taken account of by connecting the 2-port shown in Figure B.5 in parallel with the π-network shown in Figure B.10. The resulting y-matrix is given by:

$$[y] = \begin{bmatrix} \frac{1}{Z_1} + \frac{1}{Z_3} + Y_4 & -\frac{1}{Z_3} - Y_4 \\ -\frac{1}{Z_3} - Y_4 & \frac{1}{Z_2} + \frac{1}{Z_3} - Y_4 \end{bmatrix} \tag{B.20}$$

and the modified π-network in terms of the network elements shown in Figure B.6 can be obtained from Equations (B.7 to B.9) as follows:

$$y_1 = \frac{1}{Z_1} \tag{B.21}$$

$$y_2 = \frac{1}{Z_2} \tag{B.22}$$

$$z_2 = \frac{Z_3}{1+Z_3 Y_4} . \tag{B.23}$$

From here the steps follow exactly those under C., i.e., Za and Y_b (see Figure B.9) are added to the π-network of Figure B.6 and we obtain the ladder network shown in Figure B.8 for which:

$$z_1 = Za \tag{B.24}$$

and

$$y_1' = Y_b + \frac{1}{Z_1}. \tag{B.25}$$

The elements y_2 and z_2 are given by Equations (B.22) and (B.23), and the short-circuit transfer admittance results as:

$$-y_{21} = \frac{1}{z_1 z_2 y_1' + z_1 + z_2}. \tag{B.26}$$

Substituting Equations (B.16), (B.18), and (B.22) to (B.25) in Equation B.26 we get:

$$-y_{21} = \frac{1}{Za} \cdot \frac{s^2\tau\tau_s + s\tau R_s Y_4 + R_s Y_4 + 1}{s^2\tau\tau_s + s\tau R_s\left[Y_b + Y_4 + \frac{1}{R_1}\left(1 + \frac{\tau_1}{\tau}\right) + \frac{1}{Za}\right] + R_s(Y_b + Y_4) + \frac{R_s}{Za} + 1}. \tag{B.27}$$

II. Some Network Examples

Some examples are given here of how the preceding general network configurations were used to derive the short-circuit transfer admittances of the representative second order RC networks listed in Table 1.

Example 1. We consider here the network shown in Figure B.11. It belongs to the category of circuits analyzed under I.C., of this appendix. In terms of the elements of the general network of this kind shown in Figure B.3 we have:

$$Za = R_a \tag{B.28a}$$

$$Zb = \frac{1}{R_b} \tag{B.28b}$$

$$Y_1 = \frac{1}{R_1} \tag{B.28c}$$

$$Y_2 = \frac{1}{R_2} \tag{B.28d}$$

$$Y_3 = sC_3 \tag{B.28e}$$

$$Y_4 = \frac{1}{R_4} + sC_4. \tag{B.28f}$$

Substituting these values into Expression (B.15) the following short-circuit transfer admittance is obtained:

$$-y_{21} = \frac{1}{R_a} \cdot \frac{s^2 + s\left\{\frac{R_p C_3 + R_4 C_4}{R_4 R_p C_3 C_4}\right\} + \frac{1}{R_p R_q C_3 C_4}}{s^2 + s\left\{\frac{R_4 C_4 + R_p\left(1 + \frac{R_4}{R_1} + \frac{R_4}{R_m}\right) C_3}{R_4 R_p C_3 C_4}\right\} + \frac{1 + \frac{R_q}{R_m}}{R_p R_q C_3 C_4}} \qquad \text{(B.29)}$$

where:

$$R_p = \frac{R_1 R_2}{R_1 + R_2} \qquad \text{(B.30a)}$$

$$R_m = \frac{R_a R_b}{R_a + R_b} \qquad \text{(B.30b)}$$

$$R_q = \frac{R_4 (R_1 + R_2)}{R_1 + R_2 + R_4} \; . \qquad \text{(B.30c)}$$

This case is tabulated under 5a) in Table 1.

Example 2. Here the circuit configuration shown in Figure B.12 is considered. In terms of the elements of its general equivalent shown in Figure B.9 we have here:

$$Za = R_1 \qquad \text{(B.31a)}$$

$$Y_b = \frac{1}{R_2} \qquad \text{(B.31b)}$$

(Cont)

$$R_1 = R \tag{B.31c}$$

$$R_2 = \rho \cdot R \tag{B.31d}$$

$$R_3 = \frac{\rho}{1+\rho} R \tag{B.31e}$$

$$C_1 = C \tag{B.31f}$$

$$C_2 = \frac{C}{\rho} \tag{B.31g}$$

$$C_3 = \frac{1+\rho}{\rho} \tag{B.31h}$$

$$Y_4 = sC_1. \tag{B.31i}$$

Substituting these values in the expression for the corresponding short-circuit admittance matrix as given under I.D. in Equation (B.27) we get:

$$-y_{21} = \frac{1}{R_1} \frac{s^2 + s \cdot \frac{\alpha}{(1+\alpha)RC} + \frac{1}{(1+\alpha)R^2C^2}}{s^2 + s \frac{\alpha + \beta + 2(1+\rho)}{(1+\alpha)RC} + \frac{1+\beta}{(1+\alpha)R^2C^2}} \tag{B.32}$$

where:

$$\alpha = \frac{C_1(1+\rho)}{C} \tag{B.33a}$$

$$\beta = R(1+\rho)\left[\frac{R_1R_2}{R_1+R_2}\right]^{-1}. \tag{B.33b}$$

The network discussed in this example is tabulated under 5e) in Table 1. In precisely the same way all the other networks in Table 1 were obtained by using the transfer admittance expressions derived for the general configurations considered under I. of this appendix.

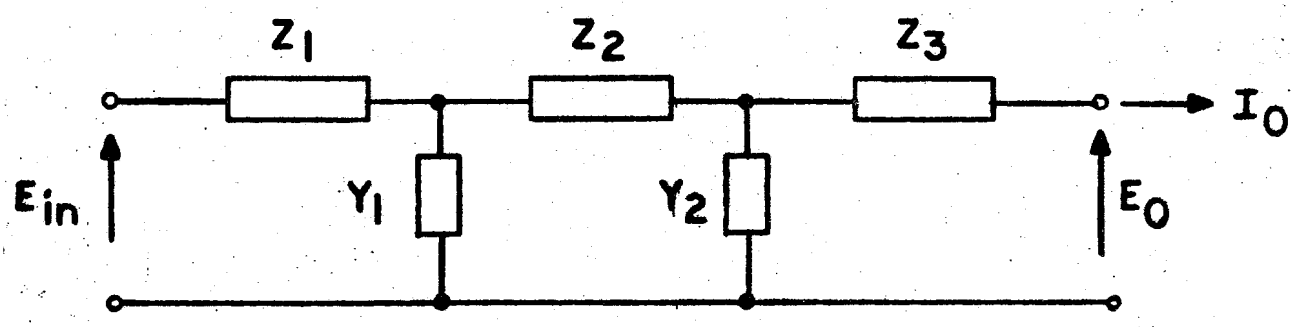

FIG. B. 1

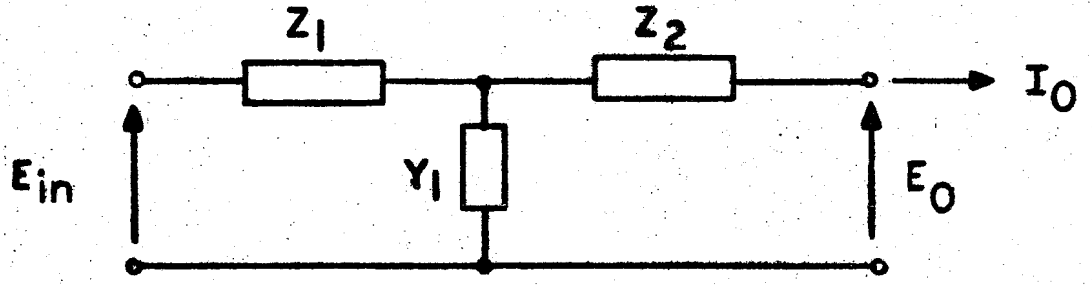

FIG. B.2

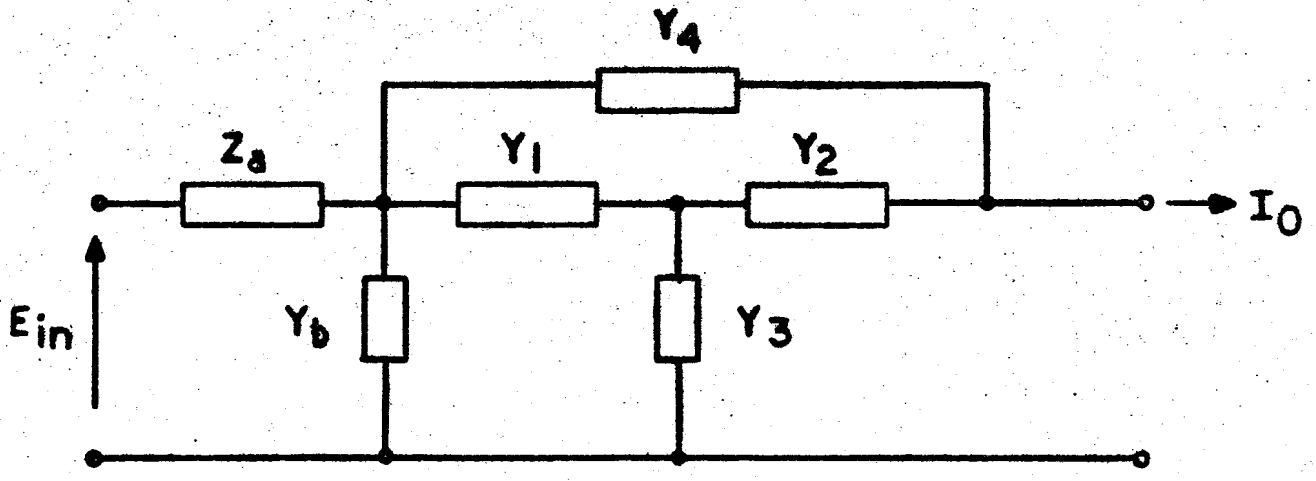

FIG. B.3

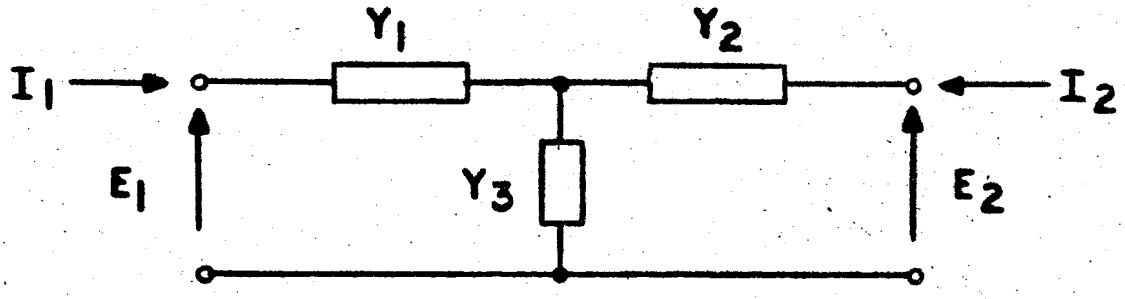

FIG. B. 4

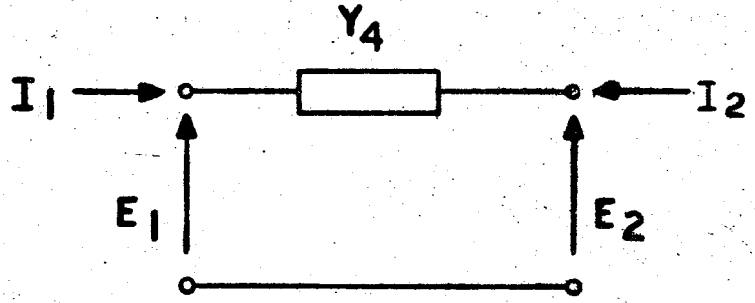

FIG. B. 5

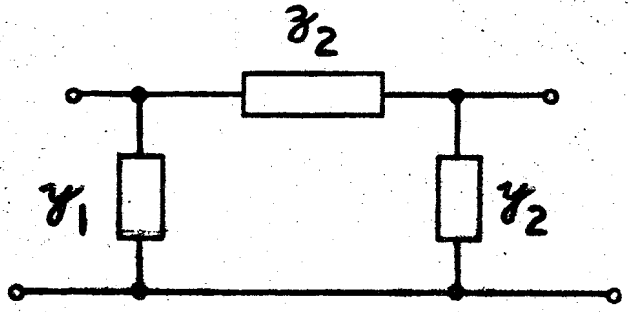

FIG. B. 6

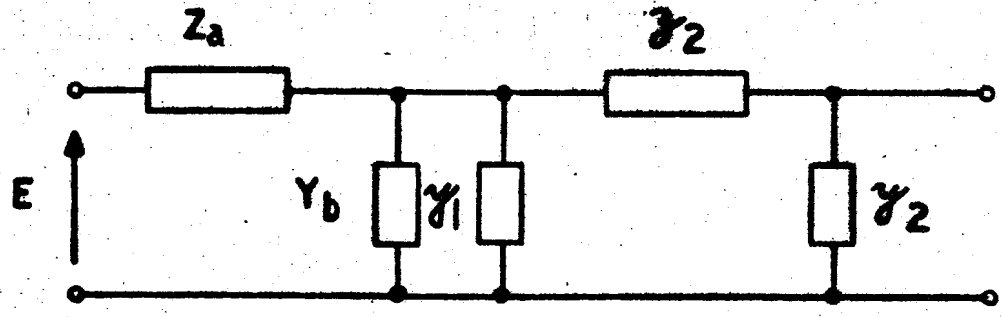

FIG. B. 7

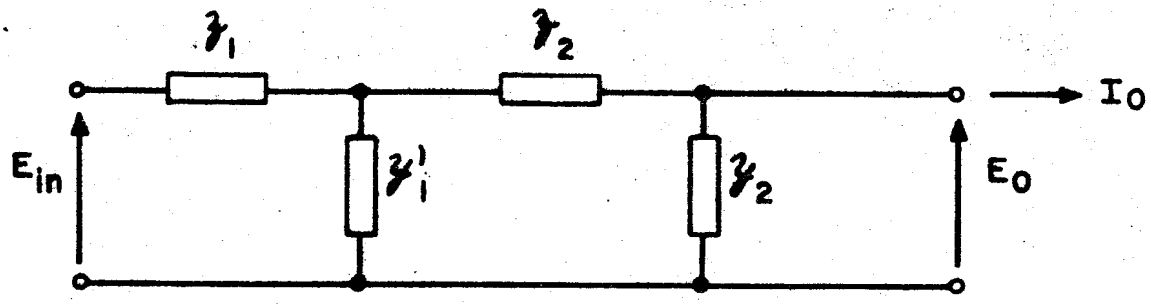

FIG. B.8

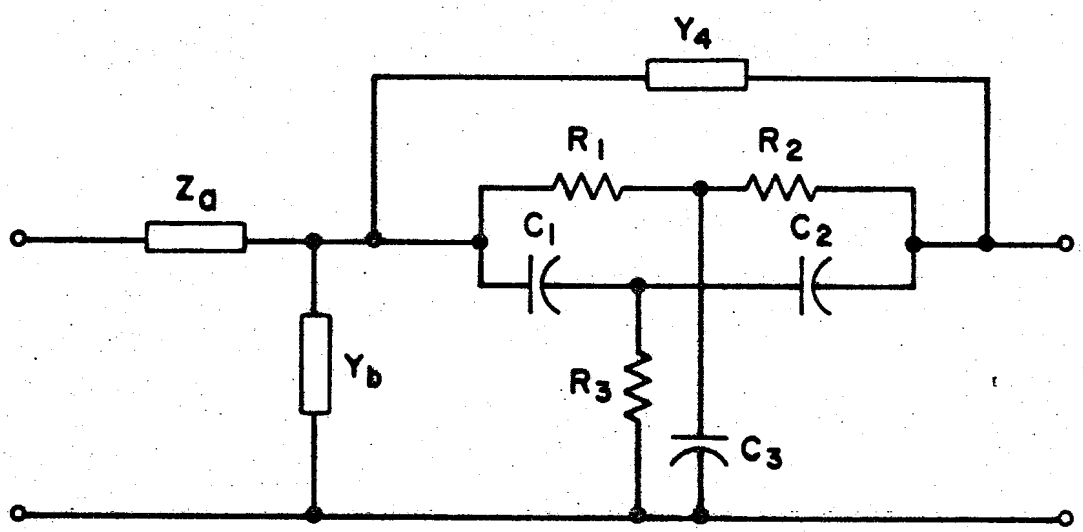

FIG. B.9

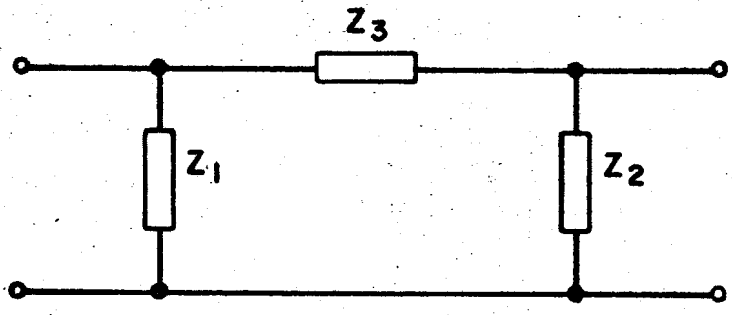

FIG. B.10

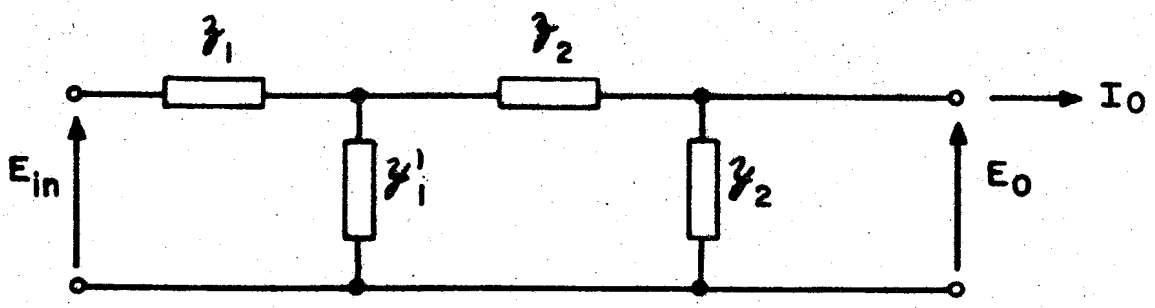

FIG. B.8

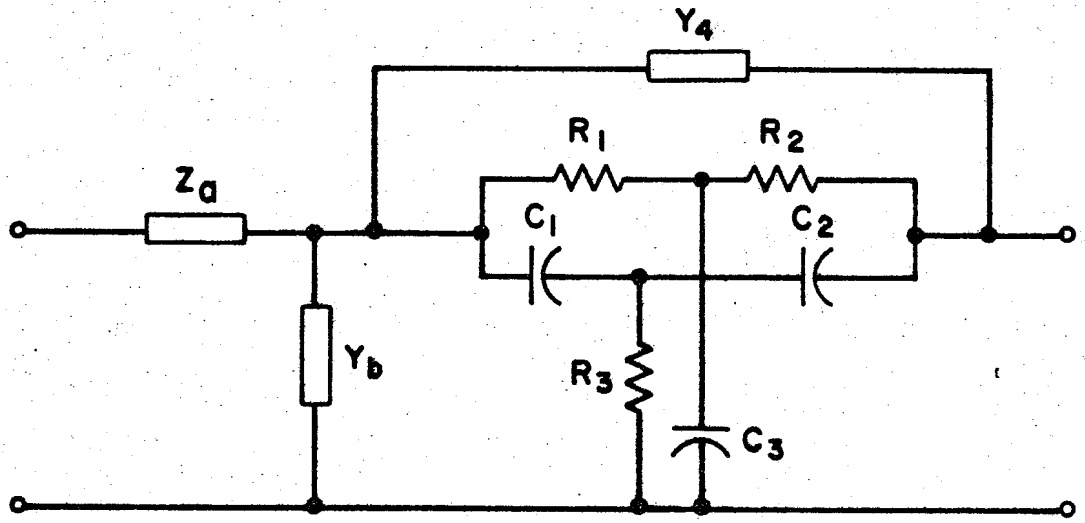

FIG. B.9

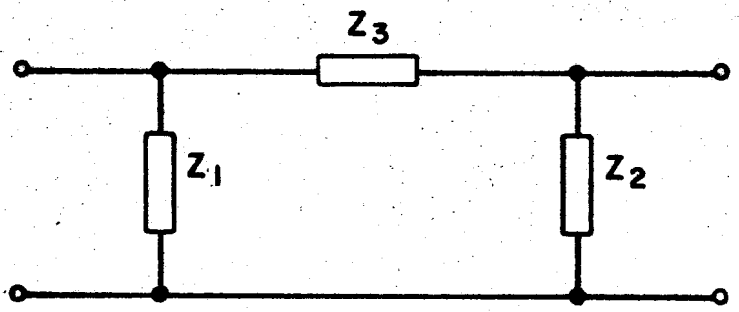

FIG. B.10

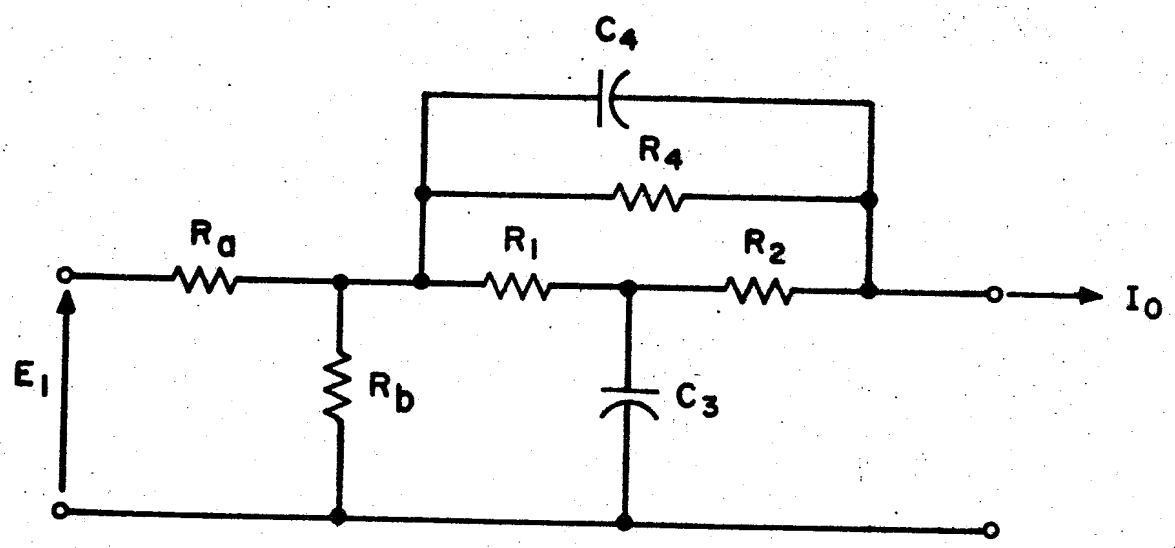

FIG. B.11

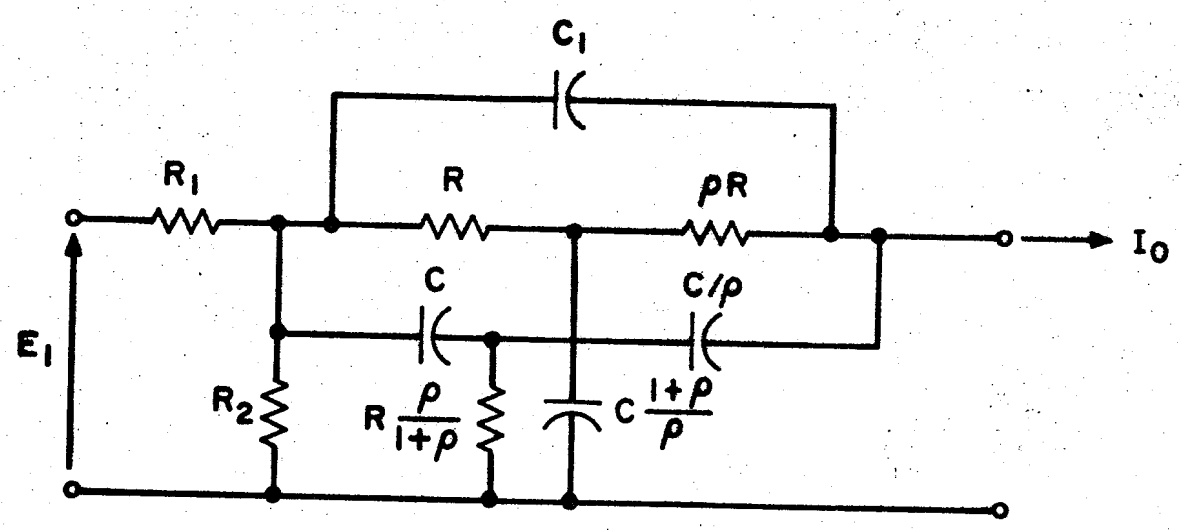

FIG. B.12

APPENDIX C

SYMMETRICAL AND POTENTIALLY SYMMETRICAL NETWORKS

Consider the cascade connection of the two networks shown in Figure 1. By multiplying out the transmission parameters of the two networks and converting these to open-circuit impedance parameters the overall z-matrix results as:

$$[z]_{ab} = \frac{1}{z_{22a}+z_{11b}} \cdot \begin{bmatrix} z_{11a}z_{11b} + \Delta z_a & z_{12a}z_{12b} \\ z_{21a}z_{21b} & z_{22a}z_{22b} + \Delta z_b \end{bmatrix} \qquad (C.1)$$

If the two networks N_a and N_b are identical and connected in mirror-image symmetry with respect to a vertical center line as shown in Figure 2, then the total network is said to be structurally and electrically symmetrical. The open circuit impedance matrix for a physically symmetrical network in terms of the z-parameters of one of the symmetrical network halves thus results as:

$$[z]_s = \begin{bmatrix} z_{11} - \frac{z_{21}^2}{2z_{22}} & \frac{z_{12}^2}{2z_{22}} \\ \frac{z_{21}^2}{2z_{22}} & z_{11} - \frac{z_{21}^2}{2z_{22}} \end{bmatrix} \qquad (C.2)$$

Therefore

$$z_{11s} = z_{22s} \tag{C.3}$$

for a symmetrical network. If the symmetrical network is also passive, then

$$z_{12s} = z_{21s} \tag{C.4}$$

The open-circuit impedance parameters of the network can be easily obtained in terms of the open- and short-circuit impedances of half of the total symmetrical network by applying Bartlett's theorem. This says that

$$Z_{11s} + Z_{21s} = z_{oc} \tag{C.5}$$

and

$$Z_{11s} - Z_{21s} = z_{sc} \tag{C.6}$$

Thus the z matrix of a symmetrical network can be expressed as

$$[Z]_s = \begin{bmatrix} \frac{z_{oc}+z_{sc}}{2} & \frac{z_{oc}-z_{sc}}{2} \\ \frac{z_{oc}-z_{sc}}{2} & \frac{z_{oc}+z_{sc}}{2} \end{bmatrix} \tag{C.7}$$

Substituting the expressions given by (C.2) into (C.5) and (C.6), we can therefore also write

$$Z_{11s} + Z_{21s} = z_{11} \tag{C.8}$$

$$Z_{11s} - Z_{21s} = \frac{\Delta z}{z_{22}} = \frac{1}{y_{11}} \tag{C.9}$$

A potentially symmetrical network can be defined in terms of a structurally symmetrical network whose right half has been impedance scaled by a constant factor ρ. This is shown in Figure 3. With Equation (C.1) and referring to Figure 3, the corresponding open-circuit impedance matrix then becomes:

$$[Z]_{ps} = \begin{bmatrix} z_{11} - \frac{1}{1+\rho} \cdot \frac{z_{21}^2}{z_{22}} & \frac{\rho}{1+\rho} \cdot \frac{z_{21}^2}{z_{22}} \\ \frac{\rho}{1+\rho} \cdot \frac{z_{21}^2}{z_{22}} & \rho z_{11} - \frac{\rho^2}{1+\rho} \frac{z_{21}^2}{z_{22}} \end{bmatrix} \tag{C.10}$$

Utilizing the expressions given by Equation (C.2), the open-circuit impedance matrix of the potentially symmetrical network can be given in terms of the impedance parameters of the symmetrical network, namely:

$$[Z]_{ps} = \begin{bmatrix} z_{11s} + \left(\frac{\rho-1}{\rho+1}\right)z_{21s} & \frac{2\rho}{1+\rho}\, z_{21s} \\ \frac{2\rho}{1+\rho}\, z_{21s} & \rho\left[z_{11s} - \left(\frac{\rho-1}{\rho+1}\right)z_{21s}\right] \end{bmatrix} \qquad (C.11)$$

Finally, using Bartlett's theorem, the impedance matrix in terms of the open- and short-circuit impedances of one half of the symmetrical network becomes

$$[Z]_{ps} = \begin{bmatrix} \frac{\rho z_{oc}+z_{sc}}{1+\rho} & \frac{\rho}{1+\rho}\,(z_{oc}-z_{sc}) \\ \frac{\rho}{1+\rho}\,(z_{oc}-z_{sc}) & \frac{\rho}{1+\rho}\,(z_{oc}+\rho z_{sc}) \end{bmatrix} \qquad (C.12)$$

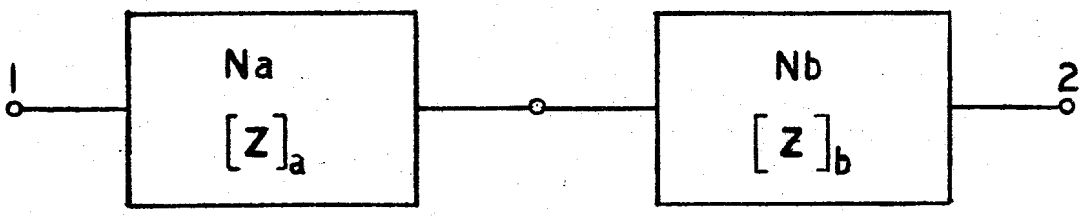

FIGURE C.1.

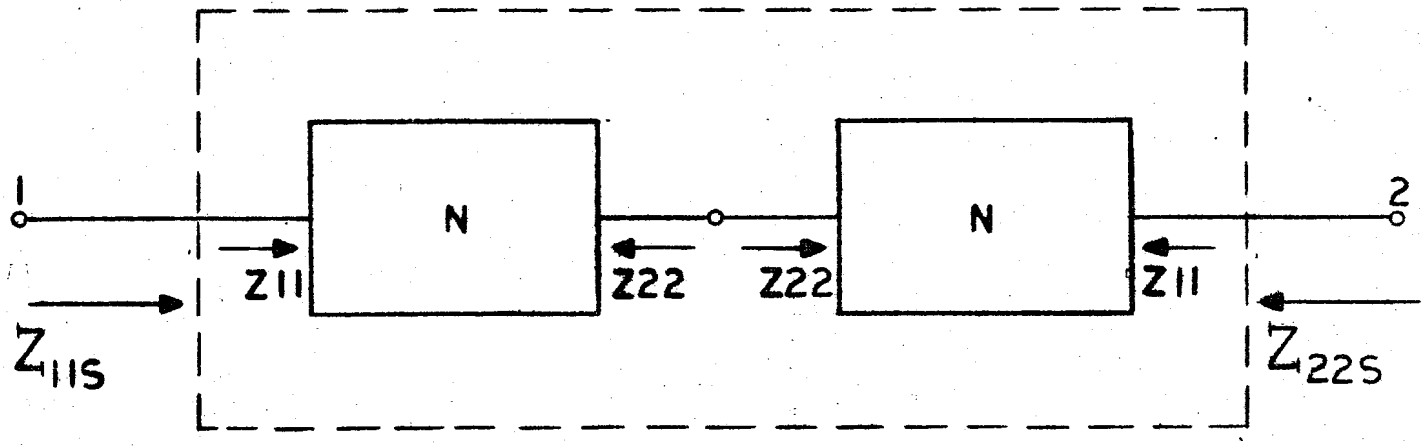

FIGURE C.2.

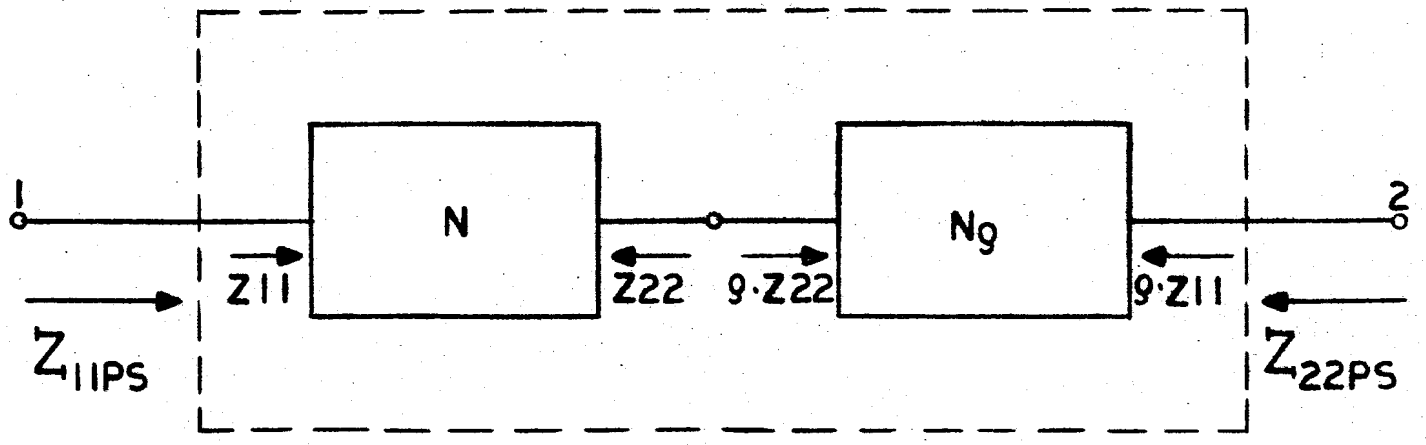

FIGURE C.3

APPENDIX D

ANALYSIS OF A TWIN-T INFINITE NULL NETWORK

The voltage transfer function for the general Twin-T shown in Figure D.1 is given by

$$T_N(s) = \frac{E_2}{E_1}(s) = \frac{N_N(R_1,R_2,R_3,C_1,C_2,C_3,s)}{D_N(R_1,R_2,R_3,C_1,C_2,C_3,s)} \qquad (D.1)$$

where

$$N_N(s) = R_1R_2R_3C_1C_2C_3s^3 + (R_2R_3C_1C_2+R_1R_3C_1C_2)s^2 + (R_3C_1+R_3C_2)s + 1 \qquad (D.2)$$

and

$$D_N(s) = R_1R_2R_3C_1C_2C_3s^3 + (R_2R_3C_1C_2+R_1R_3C_1C_2+R_1R_3C_2C_3+R_1R_2C_2C_3+R_1R_3C_1C_3)s^2 + (R_1C_2+R_2C_2+R_3C_2+R_3C_1+R_1C_3)s + 1 \qquad (D.3)$$

In order for $T_N(s)$ to represent a null network it must equal zero at a frequency $s = j\omega_N$. Thus at this frequency

$$N_N(R_1,R_2,R_3,C_1,C_2,C_3,j\omega_N) = 0 \qquad (D.4)$$

From (D.2) and (D.4) we therefore obtain two conditions for a perfect null to occur at ω_N. They are

$$\omega_N^2 = \frac{1}{R_1 R_2 C_s C_3} = \frac{1}{R_s R_3 C_1 C_2} \qquad (D.5)$$

and

$$\frac{C_3}{R_3} = \frac{C_p}{R_p} \qquad (D.6)$$

where

$$C_s = \frac{C_1 C_2}{C_1 + C_2}$$

$$C_p = C_1 + C_2$$

$$R_s = R_1 + R_2$$

and

$$R_p = \frac{R_1 R_2}{R_1 + R_2}$$

Substituting (D.5) and (D.6) into (D.1) and after some straightforward manipulations, the general voltage transfer function for the Twin-T follows, namely

$$T_N(s) = \frac{s^2 + \omega_N^2}{s^2 + 2\sigma_N s + \omega_N^2} \qquad (D.7)$$

where ω_N is given by (D.5), and

$$2\sigma_N = \omega_N^2 \cdot R_1 C_3 + \frac{1}{R_3 C_1} = \frac{1}{R_2 C_s} + \frac{1}{R_3 C_1} \qquad (D.8)$$

Comparing (D.7) with (D.1), (D.2), and (D.3) we see that the transfer function of a general Twin-T is simplified by a pole-zero cancellation when it satisfies the two conditions for a perfect null given by Equations (D.5) and (D.6).

It is often useful to know the general equivalent π-network for the Twin-T. This can be simply obtained by converting each of the two T-networks into their equivalent π-networks. This is shown in Figure D.2a and b, assuming sinusoidal input signals. The two resulting π-networks can then be connected in parallel (as shown in Figure D.2c), and the resulting impedance directly calculated. With the two conditions for a perfect null given by Equations (D.5) and (D.6) we get a simple π-network as shown in Figure D.3. The corresponding impedances are given by

$$Z_a = \frac{R_1}{1 + \frac{\tau_1}{\tau}} \left(1 + \frac{1}{s\tau}\right) \qquad (D.9)$$

$$Z_b = \frac{R_2}{1 + \frac{\tau_2}{\tau}} \left(1 + \frac{1}{s\tau}\right) \qquad (D.10)$$

and

$$Z_c = R_s \frac{\left(1 + \frac{1}{s\tau}\right)}{s\tau_s + \frac{1}{s\tau}} \qquad (D.11)$$

where

$$\tau_1 = R_1C_1$$

$$\tau_2 = R_2C_2$$

$$\tau_s = R_sC_s$$

$$\tau = R_pC_3 = R_3C_p$$

In terms of these impedances the open-circuit impedance matrix for the Twin-T simply follows as

$$[z] = \frac{1}{Z_a+Z_b+Z_c} \begin{bmatrix} Z_a(Z_b+Z_c) & Z_aZ_b \\ Z_aZ_b & Z_b(Z_a+Z_c) \end{bmatrix} \qquad (D.12)$$

So far we have considered a general Twin-T that has an infinite null at a specified frequency ω_N. Because the general transfer function given by (D.7) has the form of a quadratic fraction, it has geometric symmetry around ω_N.

The most frequently used Twin-T is structurally (and electrically) symmetrical. For this case

$$\tau_1 = \tau_2 = \tau_s = \tau = RC \qquad (D.13)$$

$$R_3 = R/2 \qquad (D.14)$$

and

$$C_3 = 2C \tag{D.15}$$

The impedances of Figure D.3 then become

$$Z_a = Z_b = \frac{R}{2}\left(1 + \frac{1}{s\tau}\right) \tag{D.16}$$

and

$$Z_c = 2R\,\frac{(1+s\tau)}{1+s^2\tau^2} \tag{D.17}$$

The open-circuit impedance matrix consequently becomes

$$[z]_s = \frac{R}{4}\begin{bmatrix} \frac{1+4s\tau+s^2\tau^2}{s\tau(1+s\tau)} & \frac{1+s^2\tau^2}{s\tau(1+s\tau)} \\ \frac{1+s^2\tau^2}{s\tau(1+s\tau)} & \frac{1+4s\tau+s^2\tau^2}{s\tau(1+s\tau)} \end{bmatrix} \tag{D.18}$$

The voltage transfer function for the symmetrical Twin-T then follows as

$$T_{N_s}(s) = \frac{z_{21s}}{z_{11s}} = \frac{s^2\tau^2+1}{s^2\tau^2+4\tau s+1} \tag{D.19}$$

Comparing with Equations (D.5), (D.7), (D.8), and (D.13), we have

$$\omega_{N_s} = \frac{1}{RC} \tag{D.20}$$

$$2\sigma_{N_s} = \frac{4}{RC} \qquad (D.21)$$

and the inverse damping factor defined by Equation (E.13)

$$q_{N_s} = 0.25 \qquad (D.22)$$

It can be shown [D.1, D.2] that the selectivity, i.e., the inverse damping factor can be increased by modifying the symmetrical Twin-T into a potentially symmetrical network (see Appendix C). This is possible with any structurally symmetrical network for which Bartlett's bisection theorem holds. A symmetrical network can be converted into a potentially symmetrical network by impedance scaling one half of the network by some factor ρ. This is shown for the Twin-T in Figure D.5. We can now utilize the results of Equation (C.11), Appendix C, in which the z-matrix of a potentially symmetrical network is expressed in terms of the z-parameters of a symmetrical network and the conversion ratio ρ. With Equation (D.18) we therefore obtain

$$[z]_{ps} = \frac{\rho}{1+\rho} \cdot \frac{R}{2} \begin{bmatrix} \frac{s^2\tau^2 + 2\left(1+\frac{1}{\rho}\right)s\tau + 1}{s\tau(1+s\tau)} & \frac{1+s^2\tau^2}{s\tau(1+s\tau)} \\ \frac{1+s^2\tau^2}{s\tau(1+s\tau)} & \frac{s^2\tau^2 + 2(1+\rho)s\tau + 1}{s\tau(1+s\tau)} \end{bmatrix} \qquad (D.23)$$

The voltage transfer function thus results as

$$T_{Nps} = \frac{z_{21ps}}{z_{11ps}} = \frac{s^2\tau^2+1}{s^2\tau^2 + 2\left(1 + \frac{1}{\rho}\right)s\tau + 1} \qquad (D.24)$$

In terms of the expression given by Equation (D.7) we find that

$$\omega_{Nps} = \frac{1}{RC} \qquad (D.25)$$

$$2\sigma_{Nps} = \frac{2}{RC}\left(\frac{\rho+1}{\rho}\right) \qquad (D.26)$$

and

$$q_{Nps} = \frac{1}{2}\frac{\rho}{1+\rho} \qquad (D.27)$$

ρ gives a measure of the Twin-T symmetry. For the extreme asymmetrical case for which $\rho \gg 1$, $q_{N_{ps}}$ takes on its maximum value, namely:

$$q_{N_{ps}}\Big|_{\rho\to\infty} \to \frac{1}{2} \qquad (D.28)$$

This is in agreement with the constraint on passive RC networks expressed by Equation (69). (D.28) also indicates that the most frequency selective Twin-T network is the extreme asymmetrical one. This is a well-known fact that was first demonstrated by A. Wolf (see Reference D.2).

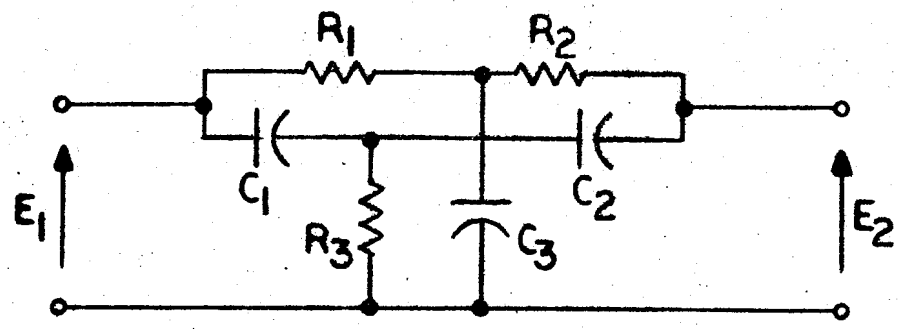

FIG. D.1

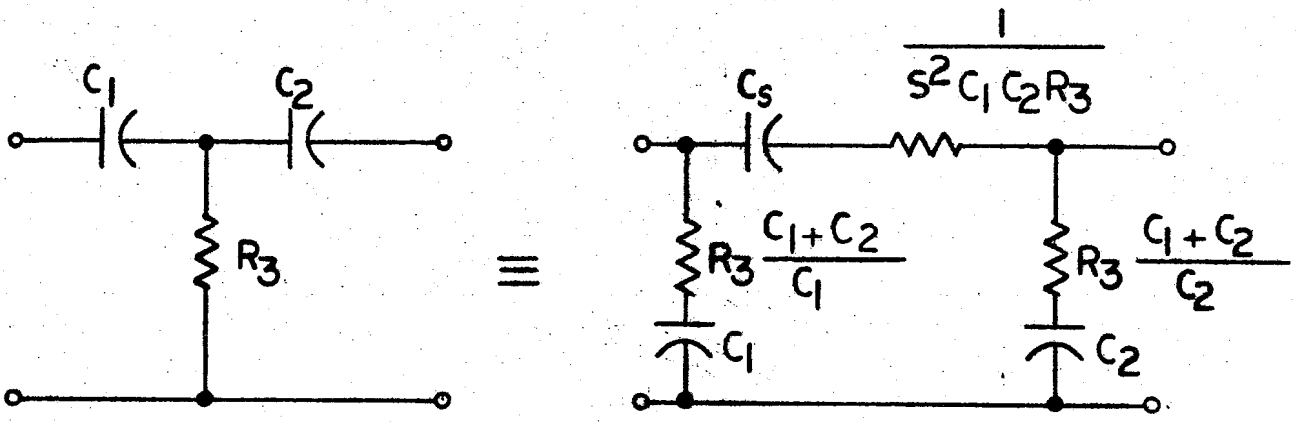

FIG. D.2a

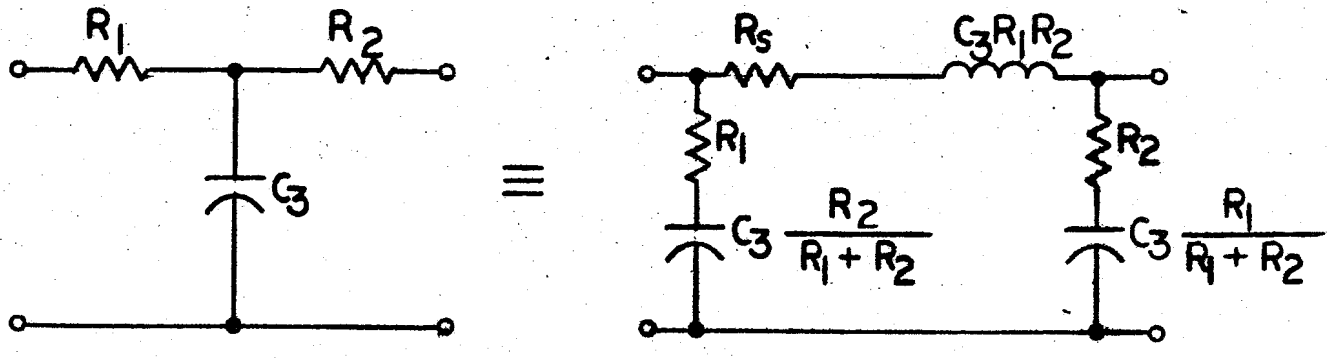

FIG. D.2b

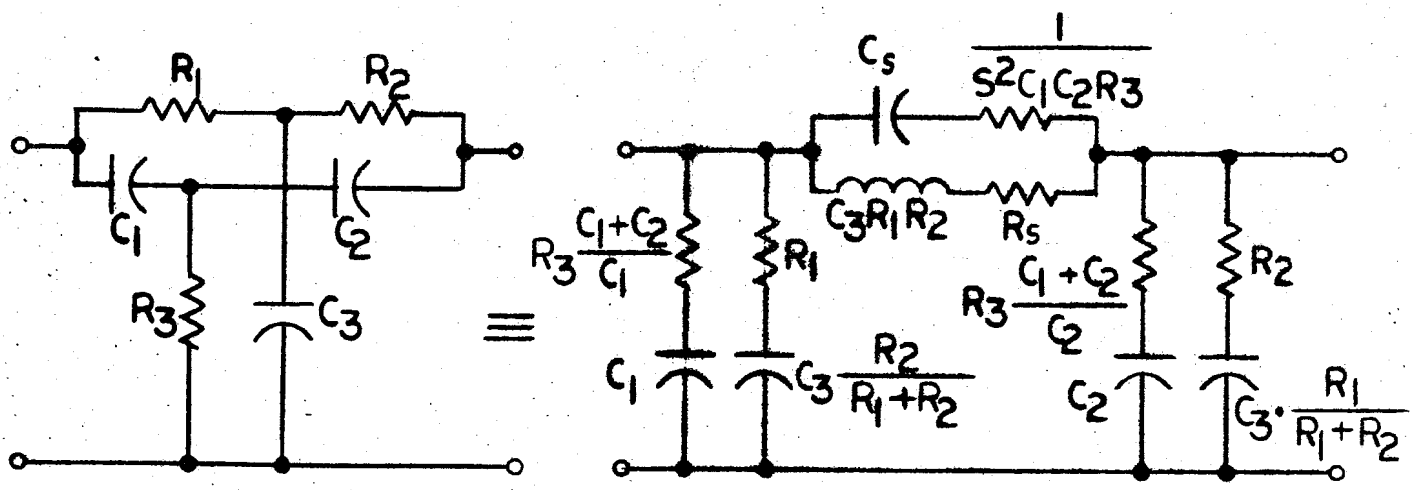

FIG. D. 2c

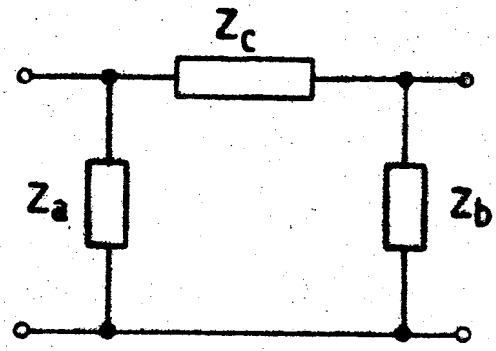

FIG. D. 3

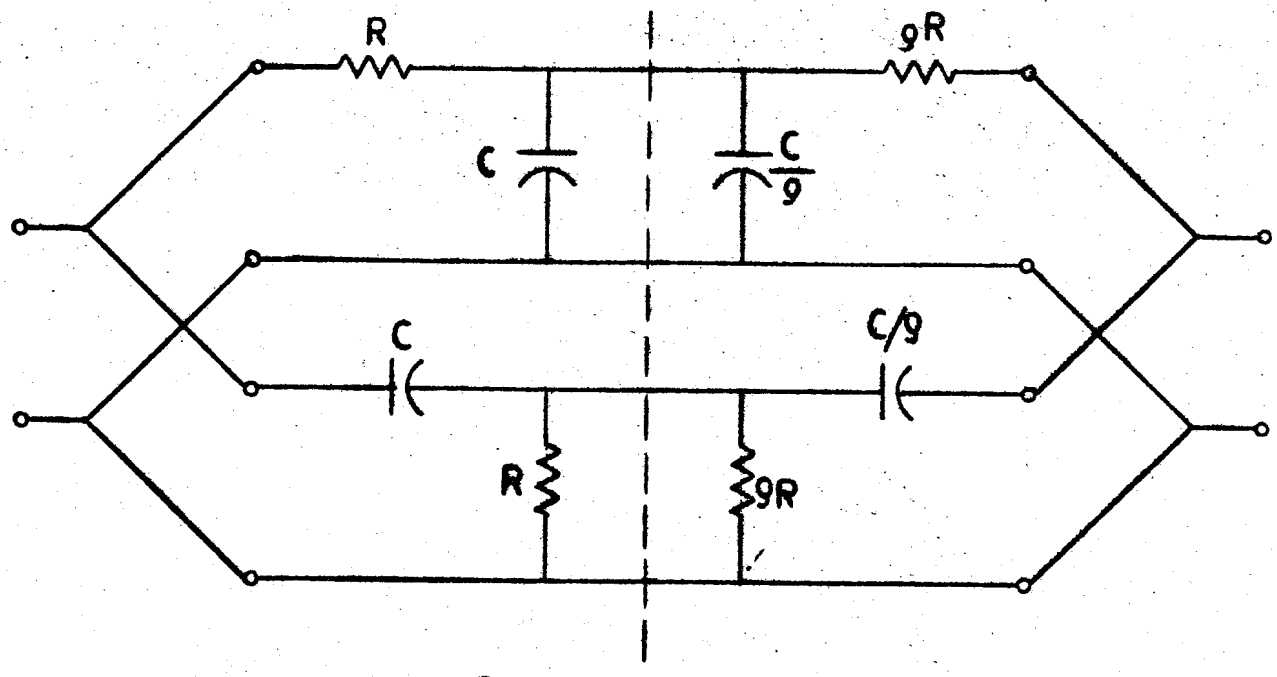

FIG. D.4

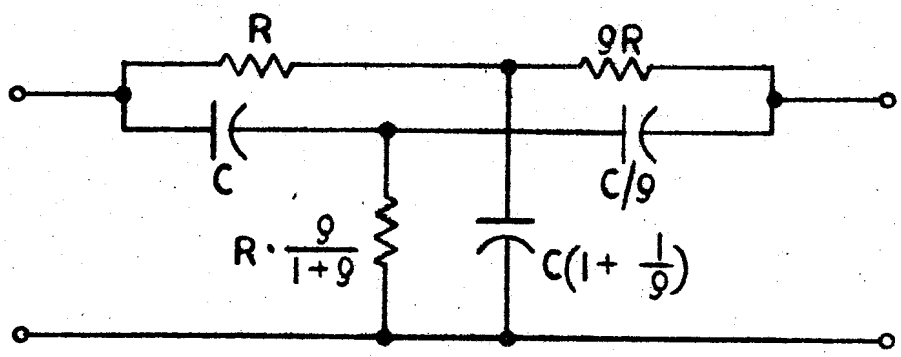

FIG. D.5

APPENDIX E

SALLEN AND KEY INFINITE-NULL NETWORK WITH AMPLIFIER GAIN LARGER OR EQUAL TO UNITY

Noninverting operational amplifiers are presently available commercially in semiconductor integrated form. They present an almost ideal equivalent to the grounded voltage amplifier as required by Sallen and Key's method of active filter design [E.1]. The only problem is that Sallen and Key require gains of less than unity whereas with noninverting operational amplifiers only gains of unity or higher can be obtained. Design and synthesis methods have been developed that expand Sallen and Key's method to include noninverting voltage amplifiers of gain equal to or larger than unity [E.2, E.3]. However, these methods do not allow for a simple adjustment of the inverse damping factor of the network that is independent of the natural frequency. Because this independence is required for the synthesis method described here, another modification of Sallen and Key's method employing noninverting operational amplifiers has been developed here.

The basic configuration used is shown in Figure E.1. It consists of a voltage amplifier β, a three terminal RC network T(s) and a two terminal RC network Y(s). Referring to Figure E.1, we can write the following mesh equations

$$E_1 = z_{11}I_1 + z_{12}I_2 \qquad (E.1)$$

$$E_2 = z_{21}I_1 + z_{22}I_2 \qquad (E.2)$$

$$I_2 = -EY \qquad (E.3)$$

$$E = E_2 + E_{out} \qquad (E.4)$$

$$E_{out} = E \cdot \beta \qquad (E.5)$$

$$E_{in} = E_1 + E_{out} \qquad (E.6)$$

Solving these equations for the voltage transfer function, we get

$$\frac{E_{out}}{E_{in}} = T_0(s) = \frac{\beta \cdot \frac{z_{21}}{z_{11}}}{1 + \beta\left(\frac{z_{21}}{z_{11}} - 1\right) + Y\frac{|z|}{z_{11}}} \qquad (E.7)$$

where

$$|z| = z_{11}z_{22} - z_{12}z_{21}$$

With a unity gain voltage amplifier, E.7 simplifies to

$$T_{0(s)}\Big|_{\beta=1} = \frac{z_{21}}{z_{21}+Y|z|} \qquad (E.8)$$

Appendix E - 3

A potentially symmetrical Twin-T network is used for the three terminal network T(s). From Appendix D, Equation (D.22), the corresponding z matrix is given by

$$[z] = \frac{\rho}{1+\rho} \cdot \frac{R}{2} \begin{bmatrix} \dfrac{s^2\tau^2 + 2\left(1+\frac{1}{\rho}\right)s\tau + 1}{s\tau(1+s\tau)} & \dfrac{1+s^2\tau^2}{s\tau(1+s\tau)} \\ \dfrac{1+s^2\tau^2}{s\tau(1+s\tau)} & \dfrac{s^2\tau^2 + 2(1+\rho)s\tau + 1}{s\tau(1+s\tau)} \end{bmatrix} \tag{E.9}$$

where ρ is a measure of the Twin-T symmetry and $\tau = RC$ (see Figure D.5). From (E.9), we obtain

$$\frac{z_{21}}{z_{11}} = \frac{1+s^2\tau^2}{s^2\tau^2 + 2\left(1+\frac{1}{\rho}\right)s\tau + 1} \tag{E.10}$$

and

$$|z| = 2\rho\left(\frac{R}{2}\right)^2 \cdot \frac{1}{s\tau} \tag{E.11}$$

With (E.10) and (E.11) the voltage transfer function E.7 therefore becomes

$$T_0(s) = K_N \frac{s^2+\omega_{n_1}^2}{s^2+2\sigma_2 s+\omega_{n_2}^2} \tag{E.12}$$

where

$$\omega_{n_1} = \frac{1}{RC} \tag{E.13}$$

$$\omega_{n_2} = \omega_{n_1}\sqrt{1 + (1+\rho)RY} \tag{E.14}$$

$$2\sigma_2 = \omega_{n_1}\left[2\left(1-\beta\right)\left(1 + \frac{1}{\rho}\right) + (1+\rho)RY\right] \tag{E.15}$$

$$K_N = \beta \tag{E.16}$$

and the inverse damping factor

$$q_N = \frac{\frac{\rho}{1+\rho}\sqrt{1 + (1+\rho)RY}}{2 + \rho RY - 2\beta} \tag{E.17}$$

In terms of the inverse damping factor of the passive potentially symmetrical twin T as given by Equation (D.27) in Appendix D, E.17 becomes

$$q_N = q_{Nps} \cdot \frac{\sqrt{1 + (1+\rho)RY}}{1 + \frac{\rho RY}{2} - \beta} \tag{E.18}$$

Equation (E.12) represents the voltage transfer function of an infinite null network as described under II.3 of the main text. Equations (E.13), (E.14), and (E.18) provide us with sufficient design information to realize this transfer function with the circuit configuration of Figure E.1.

Let us now consider the special case for which Y consists of a resistor R_L and a capacitor C_L in parallel, i.e.

$$Y = \frac{1}{R_L} + sC_L \tag{E.19}$$

Substituting Equation (E.19) into (E.12) and using a prime on the parameters to characterize this case, we find that

$$\omega'_{n_1} = \frac{1}{RC} \tag{E.20}$$

$$\omega'_{n_2} = \omega'_{n_1}\left[\frac{1+r}{1+c}\right]^{1/2} \tag{E.21}$$

$$2\sigma'_2 = \frac{\omega'_{n_1}}{q_{N_{ps}}} \frac{1 + (r+c)q_{N_{ps}} - \beta}{1+c} \tag{E.22}$$

$$K'_N = \frac{\beta}{1+c} \tag{E.23}$$

where

$$r = (1+\rho)\frac{R}{R_L} \tag{E.24}$$

and

$$c = (1+\rho)\frac{C_L}{C} \tag{E.25}$$

The inverse damping factor is accordingly

$$q_N' = q_{N_{ps}} \frac{[(1+r)(1+c)]^{\frac{1}{2}}}{1 + (r+c)q_{N_{ps}} - \beta} \qquad (E.26)$$

It is clear from Equations (E.21) and (E.26) that a given ratio of $\omega_{n_2}'/\omega_{n_1}'$ can be obtained by an appropriate ratio of $(1+r)/(1+c)$ and that any specified value of q_N results from the appropriate selection of the gain β.*

Since we have one degree of freedom too many for the realization of Equations (E.21) and (E.26), we can use it to make certain that the required gain β will not be less than unity. In this way, a noninverting operational amplifier can be used for β. With (E.21), Equation (E.26) can be written as

$$y = q_{N_{ps}} \frac{(1+c)x}{1 + (r+c)q_{N_{ps}} - \beta} \qquad (E.27)$$

where

$$x = \frac{\omega_{n_2}'}{\omega_{n_1}'} \qquad (E.28)$$

---

* It can be seen from Equation (E.26) as well as the general Equations (E.17) and (E.18) that q_N is not restricted to any maximum level. This is as it should be since q_N is the inverse damping factor of an <u>active</u> RC network.

and

$$y = q'_N \tag{E.29}$$

are introduced for convenience.

Eliminating r and solving for β, we get

$$\beta = 1 + q_{N_{ps}} \left\{ [x^2(1+c) + c] - \left[\frac{x}{y} (1+c) + 1 \right] \right\} \tag{E.30}$$

For $\beta \geq 1$ we get the following condition from this expression

$$x^2(1+c) + c \geq \frac{x}{q_N} (1+c) + 1 \tag{E.31}$$

Solving for c we find that

$$c \geq \frac{y(1-x^2) + x}{y(x^2+1) - x} \tag{E.32}$$

In the same way we find that

$$r \leq \frac{y(x^2-1) + x}{y(x^2+1) - x} \tag{E.33}$$

Within the constraints established by Equations (E.32) and (E.33) either r or c can be chosen arbitrarily, and the other then determined by Equation (E.21). The required β follows from Equation (E.30), and is guaranteed to be larger or equal to unity.

For the case that $\beta = 1$, i.e., a unity gain amplifier is used, the inverse damping factor simplifies to

$$y\,|_{\beta=1} = \frac{[(1+r)(1+c)]^{\frac{1}{2}}}{r+c} \qquad (E.34)$$

For this case the inequalities given by (E.32) and (E.33) take on equal signs, namely

$$c = \frac{y(1-x^2) + x}{y(x^2+1) - x} \qquad (E.35)$$

and

$$r = \frac{y(x^2-1) + x}{y(x^2+1) - x} \qquad (E.36)$$

The obtainable frequency ratio $x = \omega'_{n_2}/\omega'_{n_1}$ and inverse damping factor $y = q'_N$ is now limited to that range of values for which r and c remain larger than zero, i.e., are realizable by passive resistors and capacitors. This range of permissible values is readily obtainable. Considering the resistor ratio r first, it can be expressed as the ratio of two functions of two variables, namely

$$r = \frac{N(x,y)}{D(x,y)} \qquad (E.37)$$

For physical realizability x and y can only take on positive values. For r to be positive N and D must both be either positive or negative. The boundaries are readily obtained by setting N respectively D equal to zero. For N = 0 we get

$$y = \frac{x}{1-x^2} \qquad \text{(E.38)}$$

For D = 0

$$y = \frac{x}{x^2+1} \qquad \text{(E.39)}$$

Both boundaries are plotted in Figure E.2a and the corresponding regions within which r is positive are shown. Using the same notation for the capacitor ratio c the boundary corresponding to N = 0 is given by

$$y = \frac{x}{x^2-1} \qquad \text{(E.40)}$$

The boundary corresponding to D = 0 is the same as that for r [see Equation (E.39)]. These boundaries are plotted in Figure E.2b and the regions within which c is positive are shown. Since r and c must both be larger or equal to zero the attainable range of x and y values must lie in the overlapping region shown in Figure E.2c. Furthermore, since any values corresponding to $y < 0.5$ can be obtained with passive networks, the region of interest is bounded by the curves corresponding

to r = 0, c = 0, and y = 0.5. Thus by eliminating one degree of freedom and setting $\beta = 1$, the range of realizable frequency ratios x and inverse damping factors y is limited. The boundaries r = 0 and c = 0 correspond to the network with only a capacitor C_L or a resistor R_L respectively. In these two cases there is no independence at all between x and y. These two variables are then related according to Equations (E.38) and (E.40) respectively.

One configuration that is often very useful results when we let r equal c. From Equations (E.24) and (E.25) this means that

$$R_L C_L = RC \qquad \text{(E.41)}$$

From Figure E.2c we see that this corresponds to the case when the frequency ratio x equals unity. This is the only value of x for which the range of y values, attainable by varying r in a configuration in which $\beta = 1$, is unlimited. The relation between y and r for this case follows directly from Equation (E.25) or (E.36), namely

$$y \Big|_{\substack{\beta=1 \\ x=1}} = \frac{1+r}{2r} \qquad \text{(E.42)}$$

This expression is plotted in Figure E.3. With (E.24) it can be expressed in terms of the actual network resistors R and R_L, the inverse damping factor of a potentially symmetrical Twin-T, q_{NPS} and the asymmetry coefficient ρ, namely

$$y\Big|_{\substack{\beta=1\\x=1}} = q_{N_{ps}} \frac{R_L + (1+\rho)R}{\rho R} \qquad (E.43)$$

Finally, using a symmetrical twin T, we get

$$y\Big|_{\substack{\beta=1\\x=1\\\rho=1}} = \frac{1}{4} \frac{R_L+2R}{R} \qquad (E.44)$$

and

$$K_N\Big|_{\substack{\beta=1\\x=1\\\rho=1}} = \frac{R_L}{R_L+2R} \qquad (E.45)$$

For the case that $\beta = 1$ and $r = c$, the pole location of $T_o(s)$ (see Equation (E.12)) depends on the resistance ratio r only. This dependence results directly from the root locus of $T_o(s)$. It can be derived very simply from Equation (E.8) which can be written as

$$T_o(s)\Big|_{\beta=1} = \frac{1}{1 + Y \left[\frac{z}{z_{21}}\right]} \qquad (E.46)$$

From Equations (E.19), (E.24), (E.25), and (E.41), we then find

$$Y\Big|_{r=c} = \frac{r}{(1+\rho)R}(1+s\tau) \qquad (E.47)$$

and with Equations (E.9) and (E.11)

$$T_o(s)\Big|_{\substack{\beta=1\\ r=c}} = \frac{1}{1 + r\,\dfrac{(s+\omega_n)^2}{s^2+\omega_n}} \qquad \text{(E.48)}$$

where

$$\omega_n = \frac{1}{\tau} = \frac{1}{RC}$$

The root locus of Equation (E.48) results by inspection and is shown in Figure E.4. Clearly this network configuration (i.e., $\beta = 1$ and $r = c$) is only practicable for small values of r as the transmission decreases with increasing r and in the limit goes to zero.

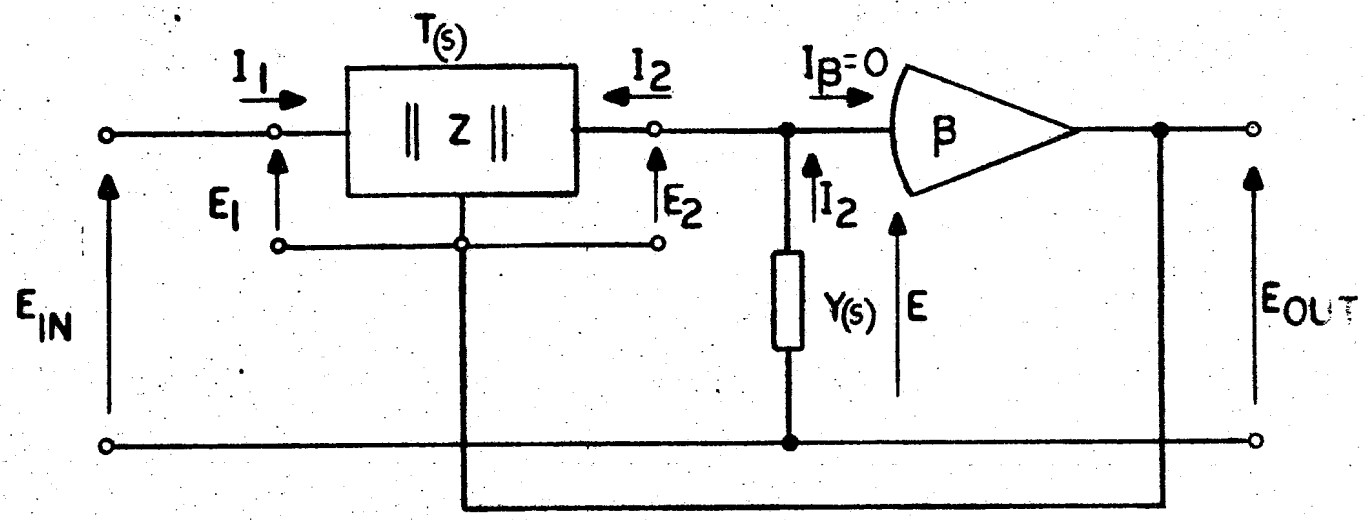

FIGURE E.1.

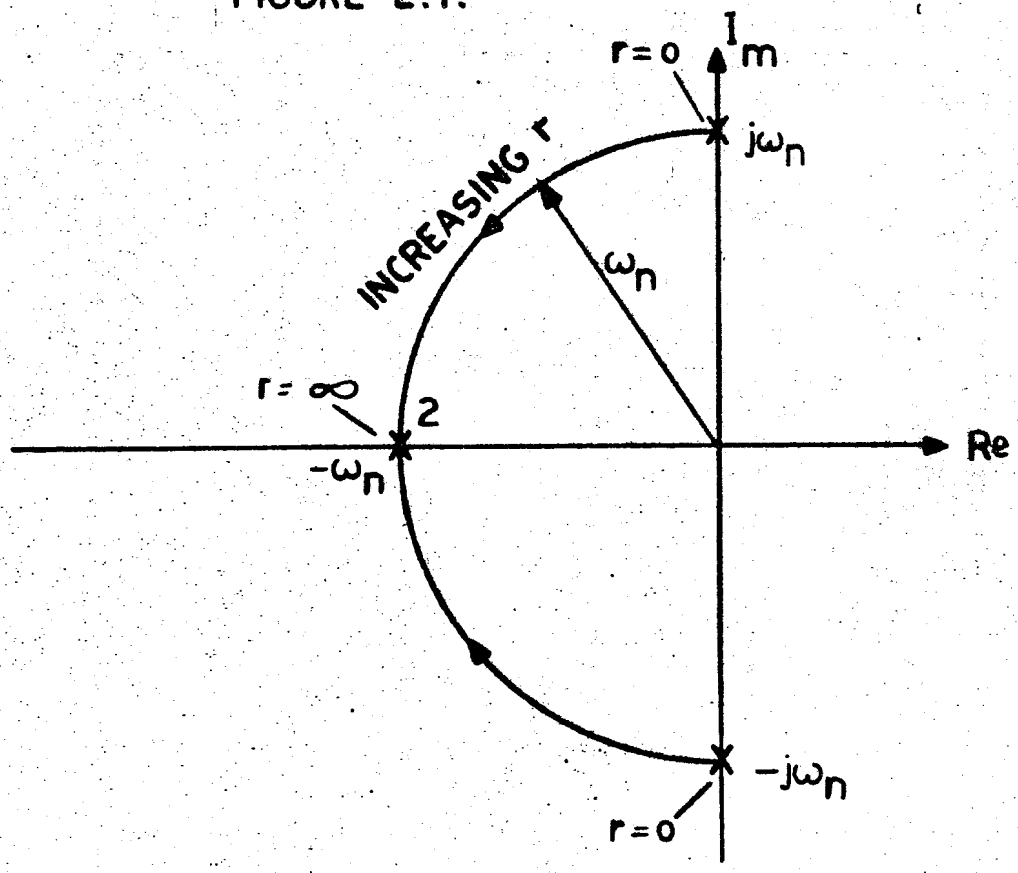

FIGURE E.4.

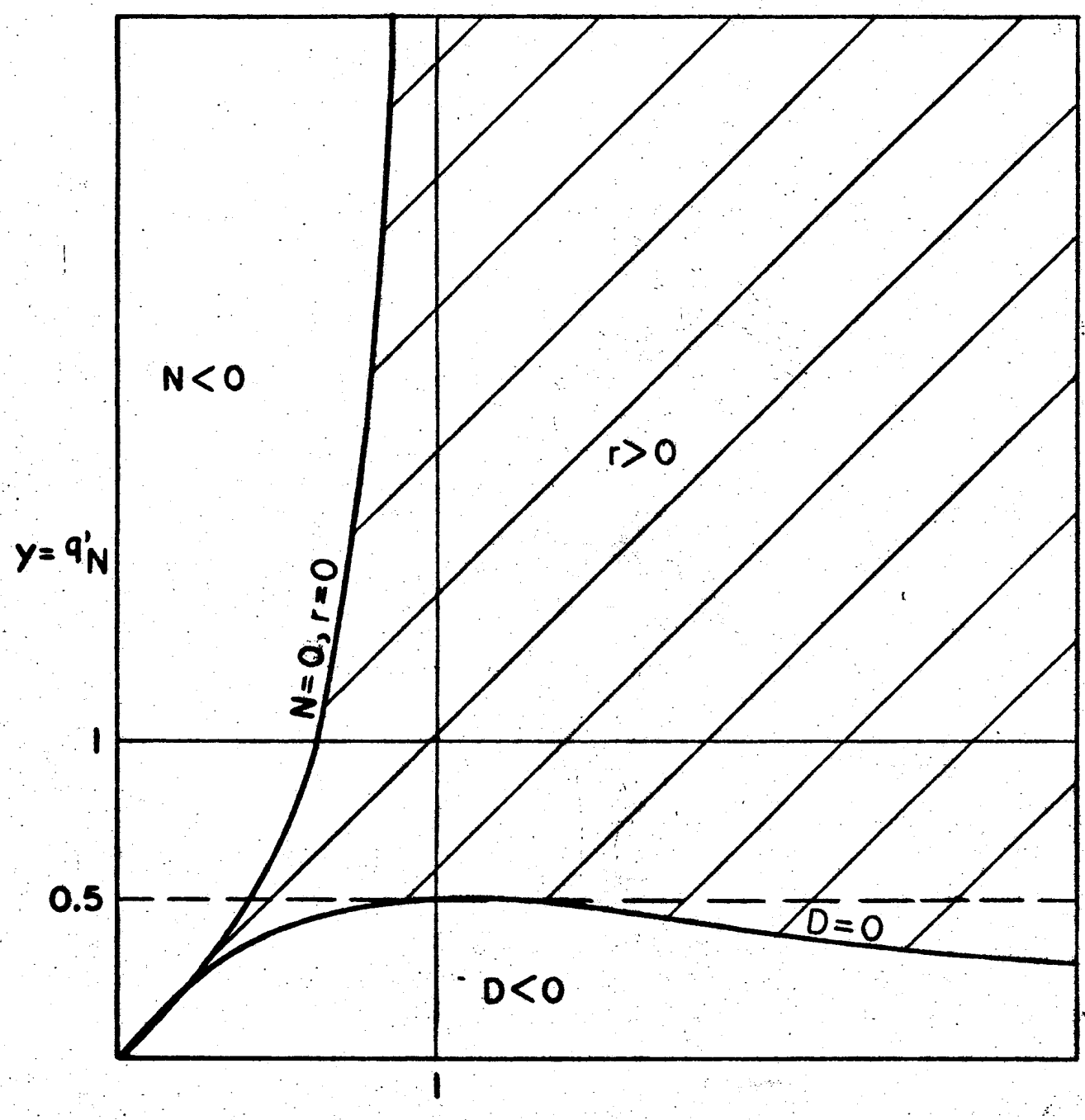

FIGURE E. 2a

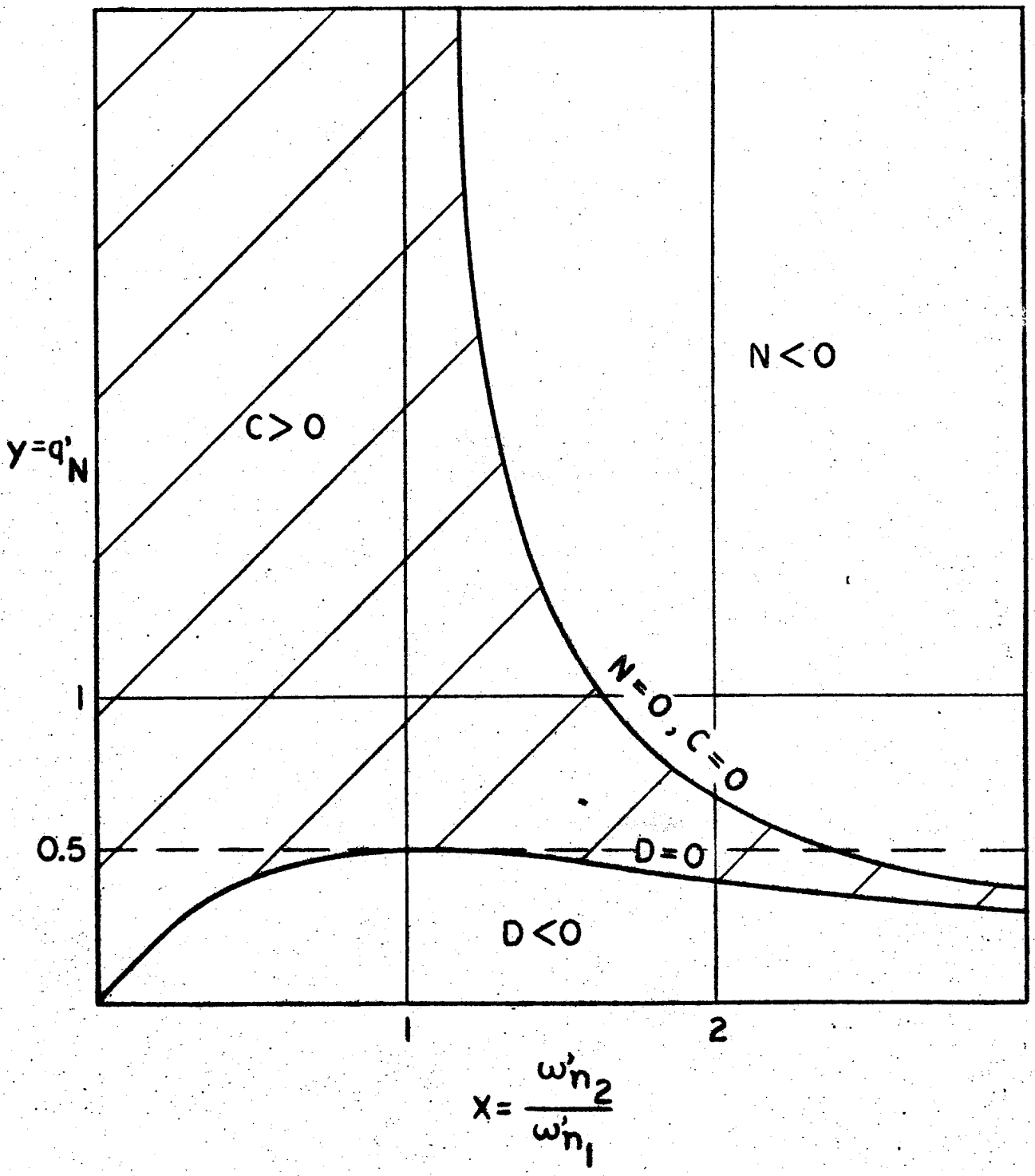

FIGURE E.2b

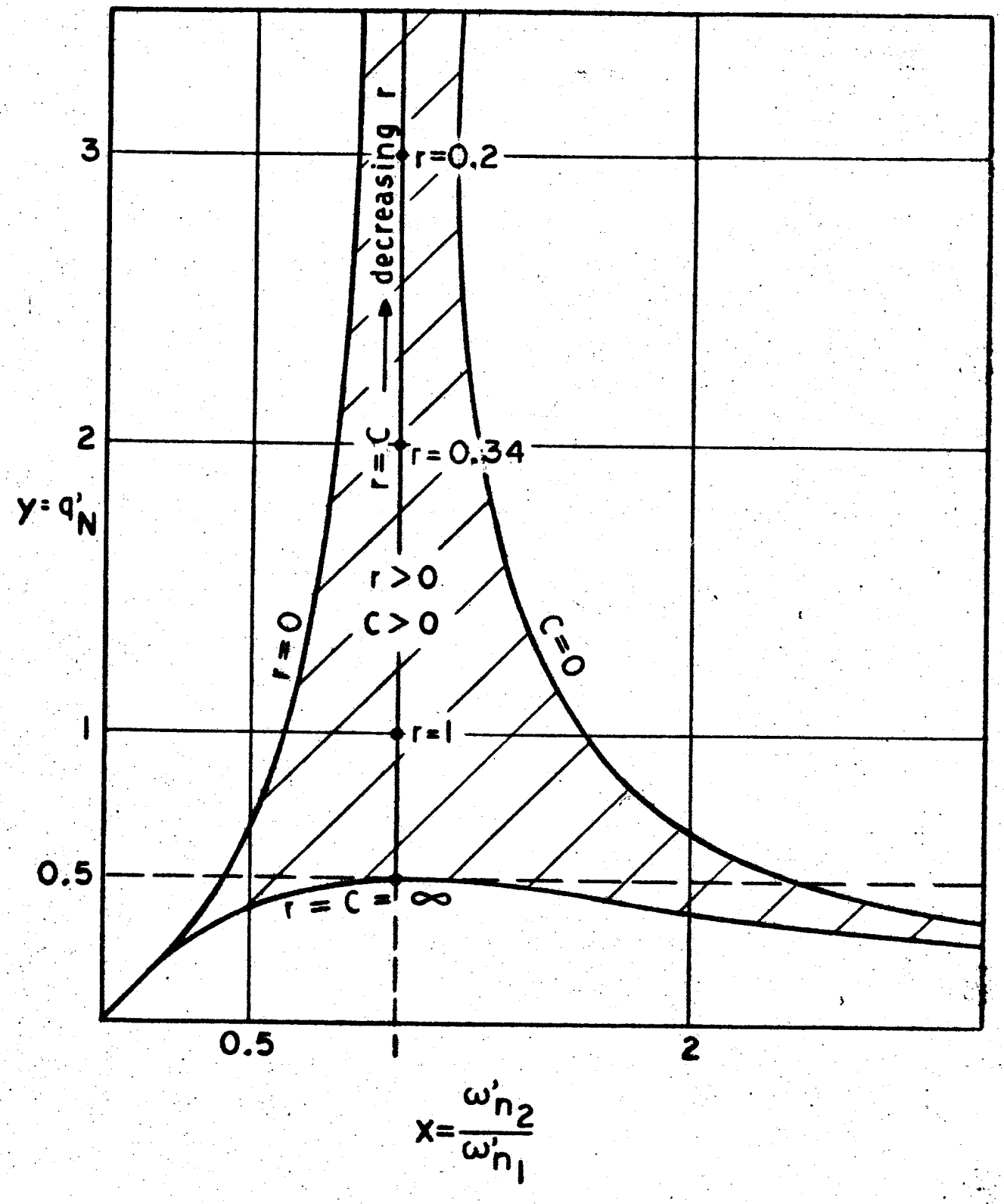
3
2
1
0.5
$y = q'_N$
r=0.2
decreasing r
r=C
r=0.34
r>0
C>0
r=0
C=0
r=1
r=C=∞
0.5
1
2
$x = \frac{\omega'_{n_2}}{\omega'_{n_1}}$

FIGURE E.2c

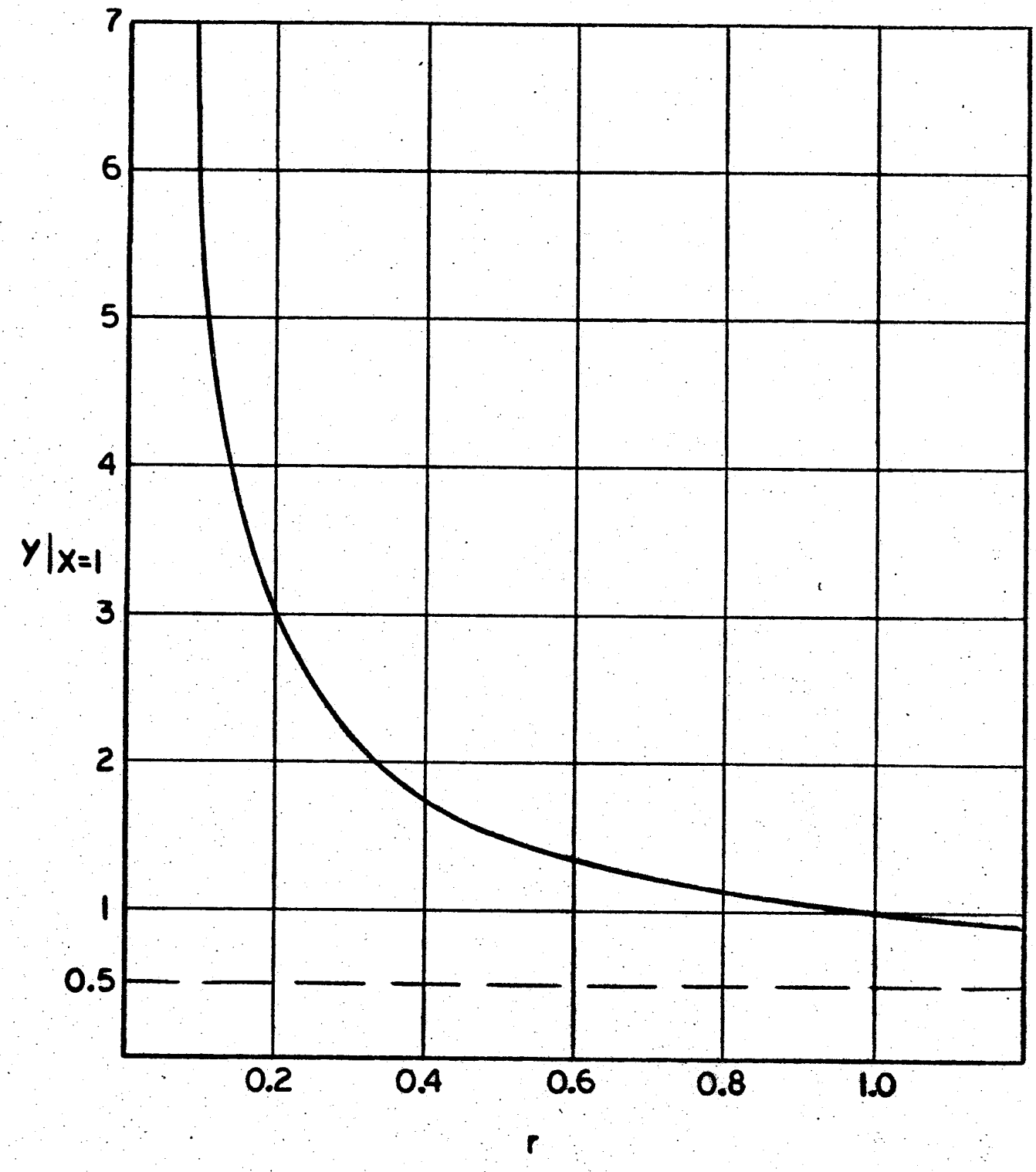

FIGURE E.3

REFERENCES FOR APPENDICES

[A.1]: D. A. H. Brown: The Equivalent Q of RC Networks, Electron. Eng., Vol. 25, pp. 294-298, July, 1953.

[A.2]: D. Morris: Q as a Mathematical Parameter, Electron. Eng., Vol. 26, pp. 306-307, July, 1954.

[A.3]: S. C. Dutta Roy: The Definition of Q of RC Networks, Proc. IEEE, Vol. 52, p. 421, April, 1964.

[A.4]: W. D. Fuller, P. S. Castro: A Microsystem Bandpass Amplifier, Lockheed Missiles and Space Division Rept. No. 703110, October 5, 1960.

[A.5]: D. G. O. Morris: Q and Selectivity, Correspondence, Proc. IEEE, Vol. 53, pp. 87, January, 1965.

[A.6]: S. C. Dutta Roy: On the Design of Parallel -T Resistance Capacitance Networks for Maximum Selectivity, J. Inst. Telecom. Engrs., Vol. 8, No. 5, pp. 218, September, 1962.

[D.1]: A. P. Bolle, Theory of Twin-T, RC-Networks and their Application to Oscillators, Journ. Brit. Inst. Radio Engrs., December, 1953, pp. 571-587.

[D.2]: A. Wolf, Note on a Parallel-T Resistance Capacitance Network, Proc. IRE, Vol. 34, September, 1964, p. 659.

[E.1]: R. P. Sallen, and E. L. Key, A Practical Method of Designing RC Active Filters, IRE Trans. Circuit Theory, Vol. CT-2, No. 1, March, 1955, pp. 74-85.

References For Appendices - 2

[E.2]: D. Hazony, R. D. Joseph, Transfer Matrix Systhesis with One Amplifier but no Inductors, Proc. of the Eighth Midwest Symposium on Circuit Theory, Paper 29, June, 1965. Also summarized in Proc. IEEE (Corr.), Vol. 52, No. 12, December, 1964, p. 1748.

[E.3]: N. Balabanian, B. Patel, Active Realization of Complex Zeros, IEEE Trans. Circuit Theory, Vol. CT-10, June, 1963, pp. 299-300.

TABLE I : TRANSFER ADMITTANCE OF SOME 2ND ORDER RC TWO PORTS

TRANSFER ADMITTANCE	RC NETWORK	PARAMETER-COMPONENT RELATIONS
1) LOW-PASS FILTER $K_R \cdot \frac{1}{s^2 + \frac{\omega_p}{q_R} s + \omega_p^2}$	(a) 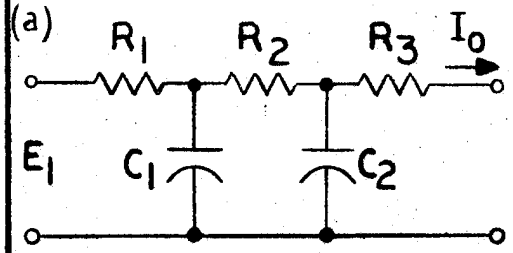 	$K_R = \frac{1}{R_1 R_2 R_3 C_1 C_2}$; $\omega_p^2 = \frac{R_1 + R_2 + R_3}{R_1 R_2 R_3 C_1 C_2}$ $q_R = \frac{\sqrt{R_1 R_2 R_3 (R_1 + R_2 + R_3) C_1 C_2}}{R_1 (R_2 + R_3) C_1 + R_3 (R_1 + R_2) C_2}$
	(b) 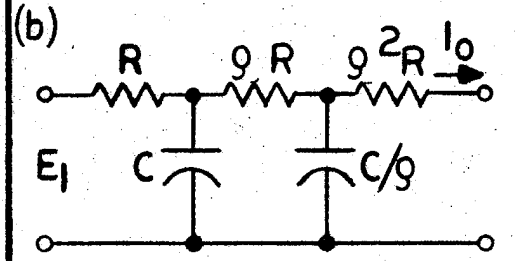 	$K_R = \frac{1}{\vartheta^2 R^3 C^2}$; $\omega_p^2 = \frac{1}{R^2 C^2} \left(\frac{1 + \vartheta + \vartheta^2}{\vartheta^2} \right)$; $q_R = \frac{1}{2} \frac{\sqrt{1 + \vartheta + \vartheta^2}}{1 + \vartheta}$
	(c) 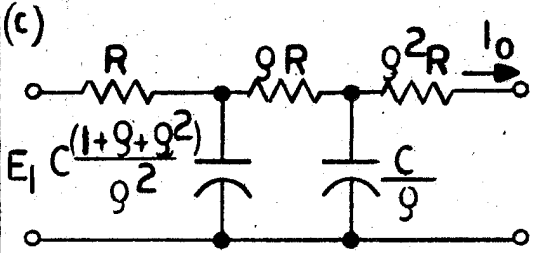 	$K_R = \frac{1}{R^3 C^2 (1 + \vartheta + \vartheta^2)}$; $\omega_p^2 = \frac{1}{R^2 C^2}$; $q_R = \frac{\vartheta}{1 + \vartheta} \cdot \frac{1 + \vartheta + \vartheta^2}{1 + \vartheta + 2\vartheta^2}$

TABLE I CONT'D

TRANSFER ADMITTANCE	RC NETWORK	PARAMETER-COMPONENT RELATIONS
2) HIGH-PASS FILTER $K_R \cdot \frac{s^2}{s^2 + \frac{\omega_p}{q_R} s + \omega_p^2}$	(a) 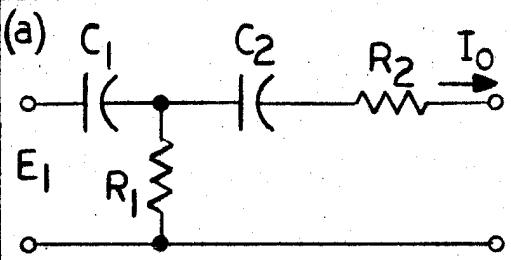	$K_R = \frac{1}{R_2}$; $\omega_p^2 = \frac{1}{R_1 R_2 C_1 C_2}$; $q_R = \frac{\sqrt{R_1 R_2 C_1 C_2}}{R_1(C_1 + C_2) + R_2 C_2}$
	(b) 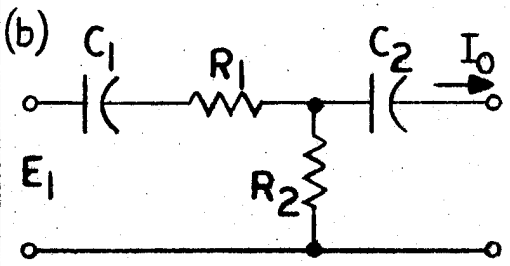	$K_R = \frac{1}{R_1}$; $\omega_p^2 = \frac{1}{R_1 R_2 C_1 C_2}$; $q_R = \frac{\sqrt{R_1 R_2 C_1 C_2}}{(R_1 + R_2) C_1 + R_2 C_2}$
	(c) 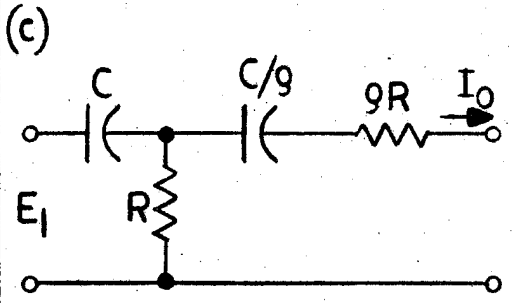	$K_R = \frac{1}{9R}$; $\omega_p^2 = \frac{1}{R^2 C^2}$; $q_R = \frac{9}{1+29}$

TABLE I CONT'D

TRANSFER ADMITTANCE	RC NETWORK	PARAMETER – COMPONENT RELATIONS
	(d) 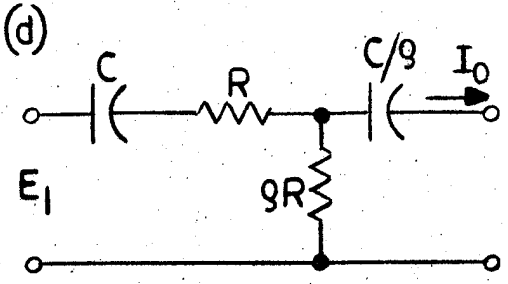	$K_R = \frac{1}{R}$; $\omega_p^2 = \frac{1}{R^2C^2}$; $q_R = \frac{1}{2+9}$
3) BAND-PASS FILTER $K_R \cdot \frac{S}{S^2 + \frac{\omega_p}{q_R}S + \omega_p^2}$	(a) 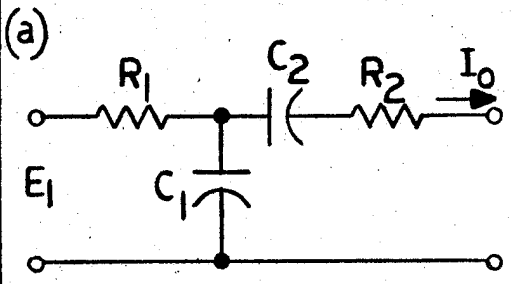	$K_R = \frac{1}{R_1R_2C_1}$; $\omega_p^2 = \frac{1}{R_1R_2C_1C_2}$; $q_R = \frac{\sqrt{R_1R_2C_1C_2}}{R_1(C_1+C_2)+R_2C_2}$
	(b) 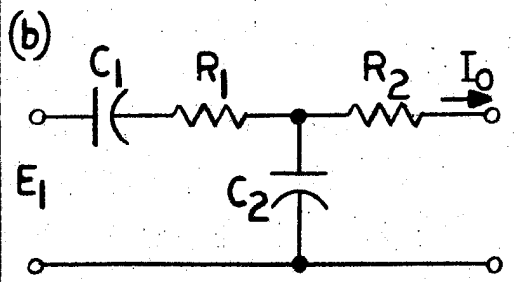	$K_R = \frac{1}{R_1R_2C_2}$; $\omega_p^2 = \frac{1}{R_1R_2C_1C_2}$; $q_R = \frac{\sqrt{R_1R_2C_1C_2}}{(R_1+R_2)C_1+R_2C_2}$

TABLE I CON'T

TRANSFER ADMITTANCE	RC NETWORK	PARAMETER-COMPONENT RELATIONS
	(c) 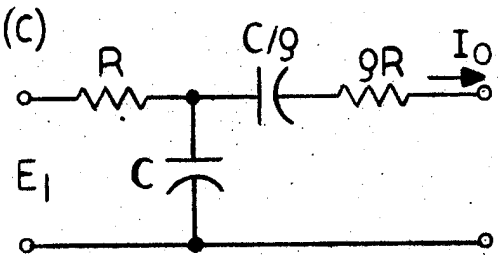	$K_R = \frac{1}{9R^2C}$; $\omega_p^2 = \frac{1}{R^2C^2}$; $q_R = \frac{9}{1+2g}$
	(d) 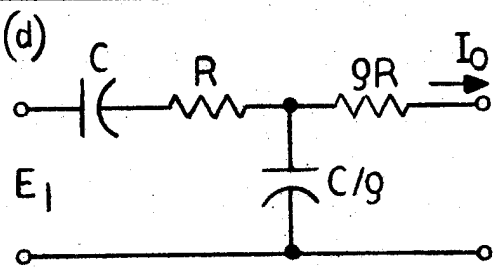	$K_R = \frac{1}{R^2C}$; $\omega_p^2 = \frac{1}{R^2C^2}$; $q_R = \frac{1}{2+g}$
4) RESONATOR $K_R \cdot \frac{S+\omega_Z}{S^2+\frac{\omega_P}{q_R}S+\omega_p^2}$	(a) 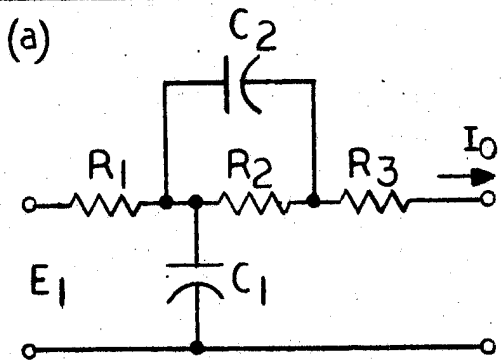	$K_R = \frac{1}{R_1R_3C_1}$; $\omega_z = \frac{1}{R_2C_2}$; $\omega_p^2 = \frac{R_1+R_2+R_3}{R_1R_2R_3} \cdot \frac{1}{C_1C_2}$ $q_R = \frac{\sqrt{R_1R_2R_3(R_1+R_2+R_3)C_1C_2}}{(R_2+R_3)R_1C_1+(R_1+R_3)R_2C_2}$

E-1328 (11-63)

DATE FILE

TABLE I CON'T

TRANSFER ADMITTANCE	RC NETWORK	PARAMETER-COMPONENT RELATIONS
	(b) 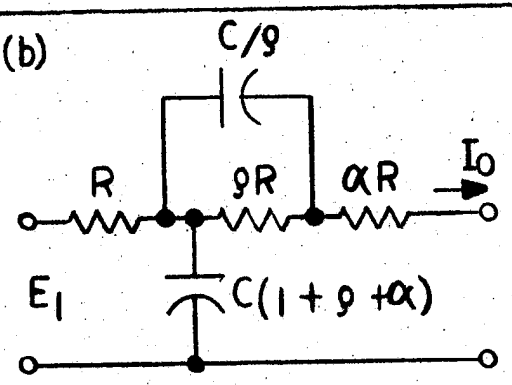	$K_R = \frac{1}{\alpha(1+\vartheta+\alpha)R^2C}$; $\omega_Z = \frac{1}{RC}$; $\omega_p^2 = \frac{1}{\alpha R^2C^2}$ $q_R = \frac{\sqrt{\alpha}(1+\vartheta+\alpha)}{(\vartheta+\alpha)(1+\vartheta+\alpha)+1+\alpha}$
5) CONJUGATE - COMPLEX POLES AND ZEROS $K_R \frac{s^2+\frac{\omega_Z}{q_Z}s+\omega_Z^2}{s^2+\frac{\omega_p}{q_R}s+\omega_p^2}$	(a) 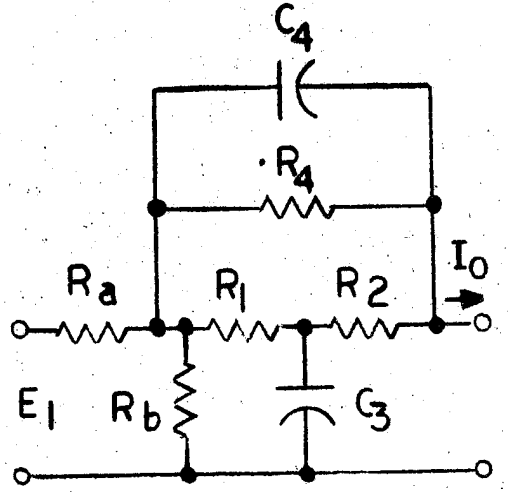	$K_R = \frac{1}{R_a}$; $\omega_Z^2 = \frac{1}{R_pR_qC_3C_4}$; $q_Z = \frac{\sqrt{(1+\frac{R_4}{R_1+R_2})R_pR_4C_3C_4}}{R_pC_3+R_4C_4}$ $\omega_p^2 = \frac{1}{R_pR_qC_3C_4}(1+\frac{R_q}{R_m})$; $q_R = \frac{\sqrt{(1+\frac{R_4}{R_1+R_2})(1+\frac{R_q}{R_m})R_pR_4C_3C_4}}{R_4C_4+R_pC_3\left[1+\frac{R_4}{R_1}+\frac{R_4}{R_m}\right]}$ WHERE: $R_p = \frac{R_1R_2}{R_1+R_2}$; $R_m = \frac{R_aR_b}{R_a+R_b}$; $R_q = \frac{R_4(R_1+R_2)}{R_1+R_2+R_4}$

E-1328 (11-63)

DATE FILE

TABLE I CONT'D

TRANSFER ADMITTANCE	RC NETWORK	PARAMETER-COMPONENT RELATIONS
5)	(b) 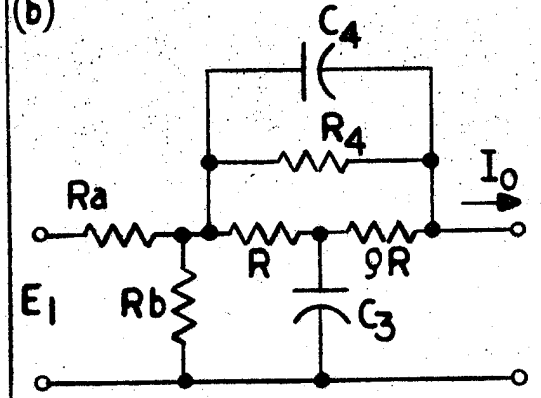	$K_R = \frac{1}{Ra}$; $\omega_Z^2 = \frac{1+9+R_4/R}{9RR_4C_3C_4}$; $q_Z = \frac{\sqrt{9(1+9+R_4/R)RR_4C_3C_4}}{9RC_3+(1+9)R_4C_4}$ $\omega_p^2 = \frac{1+9+R_4/R}{9RR_4C_3C_4}\left(1+\frac{Rq}{Rm}\right)$ $\qquad Rq = \frac{R_4(1+9)}{(1+9)+R_4/R}$ $q_R = \frac{\sqrt{(1+9+R_4/R)(1+Rq/Rm)9RR_4C_3C_4}}{(1+9)R_4C_4 + 9RC_3\left[1+R_4/R+R_4/Rm\right]}$ $\qquad Rm = \frac{RaRb}{Ra+Rb}$
	(c) 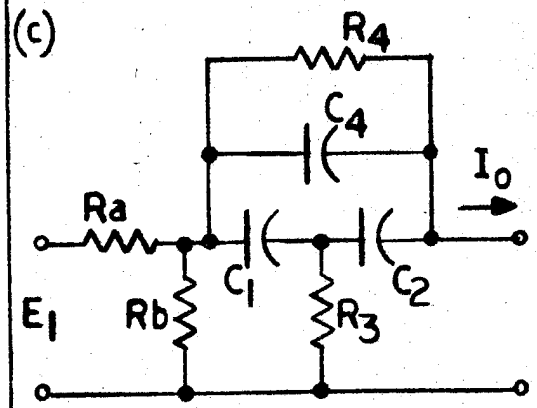	$K_R = \frac{1}{Ra}$; $\omega_Z^2 = \frac{1}{R_3R_4CpCq}$; $q_Z = \frac{\sqrt{R_3R_4CpCq}}{R_3Cp+R_4C_4}$ $\omega_p^2 = \frac{1}{R_3R_4CpCq}\frac{R_4/Rm}{}$; $q_p = \frac{\sqrt{(1+R_4/Rm)R_3R_4CpCq}}{(1+R_4/Rm)R_3Cp+R_4(C_1+C_4)}$ WHERE : $Cp = C_1+C_2$; $Cq = C_4 + \frac{C_1C_2}{C_1+C_2}$; $Rm = \frac{RaRb}{Ra+Rb}$

TABLE I CONT'D

TRANSFER ADMITTANCE	RC NETWORK	PARAMETER - COMPONENT RELATIONS
5)	(d) 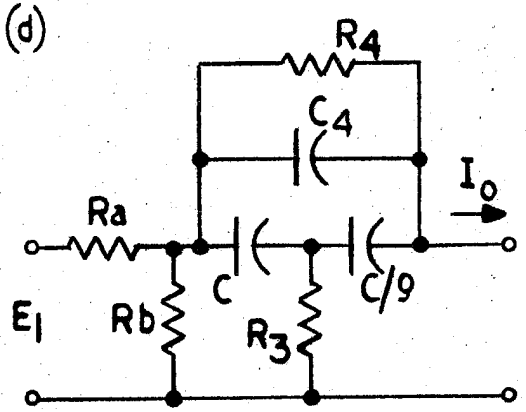	$K_R = \frac{1}{Ra}$; $\omega_z^2 = \frac{9}{R_3R_4C^2}$; $q_z = \frac{\sqrt{9R_3R_4}\,C}{9R_4C_4 + (1+9)R_3C}$ $\omega_p^2 = \frac{9}{R_3R_4C^2}(1 + R_4/Rm)$; $q_p = \frac{\sqrt{9(1+R_4/Rm)}\,C}{(1+9)(1+R_4/Rm)R_3C + 9R_4(C+C_4)}$

TABLE I CON'T

TRANSFER ADMITTANCE	RC NETWORK	PARAMETER-COMPONENT RELATIONS
5)	(e) 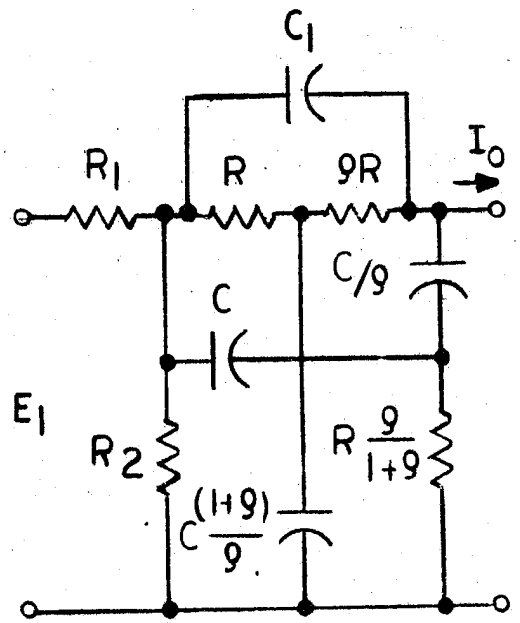	$K_R = \frac{1}{R_1}$; $\omega_Z^2 = \frac{1}{R^2C^2[1+\alpha]}$; $q_Z = \frac{\sqrt{1+\alpha}}{\alpha}$ $\omega_p^2 = \frac{1+\beta}{R^2C^2[1+\alpha]}$; $q_R = \frac{\sqrt{(1+\alpha)(1+\beta)}}{\alpha+\beta+2(1+9)}$ WHERE: $\alpha = \frac{C_1(1+9)}{C}$ $\beta = R(1+9)/\frac{R_1R_2}{R_1+R_2}$

E-1328 (11-63)

DATE FILE

E-1328 (11-63)

TABLE 2: EXAMPLES OF BASIC 2ND ORDER FILTERS USING FEN'S

FILTER TYPE	VOLTAGE TRANSFER RATIO	NETWORK
1) LOW-PASS [1c]*	$\frac{E_2}{E_1} = K \cdot \frac{1}{s^2 + 2.66\omega_p s + \omega_p^2} \cdot \frac{s^2 + 2.66\omega_p s + \omega_p^2}{s^2 + \frac{\omega_p}{q_p} s + \omega_p^2}$ WHERE: $q_R = 0.375$	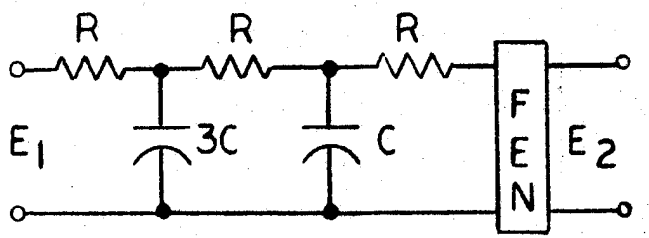
2) HIGH-PASS [2c]	$\frac{E_2}{E_1} = K \cdot \frac{s^2}{s^2 + 2.1\omega_p s + \omega_p^2} \cdot \frac{s^2 + 2.1\omega_p s + \omega_p^2}{s^2 + \frac{\omega_p}{q_p} s + \omega_p^2}$ WHERE: $q_R = 0.475$	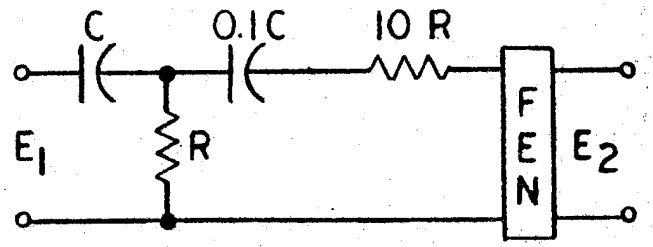
3) BAND-PASS [3c]	$\frac{E_2}{E_1} = K \cdot \frac{s}{s^2 + 2.2\omega_p s + \omega_p^2} \cdot \frac{s^2 + 2.2\omega_p s + \omega_p^2}{s^2 + \frac{\omega_p}{q_p} s + \omega_p^2}$ WHERE: $q_R = 0.455$	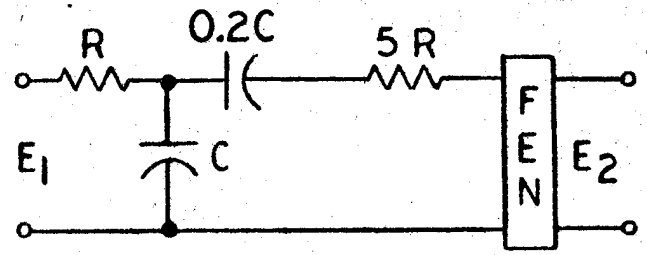
4) FREQUENCY REJECTION [6]	$\frac{E_2}{E_1} = K \cdot \frac{s^2 + \omega_z^2}{s^2 + 3.54\omega_p s + \omega_p^2} \cdot \frac{s^2 + 3.54\omega_p s + \omega_p^2}{s^2 + \frac{\omega_p}{q_p} s + \omega_p^2}$ WHERE: $R = \frac{1}{2} \frac{Ra\ Rb}{Ra + Rb}$ AND $q_R = 0.283$	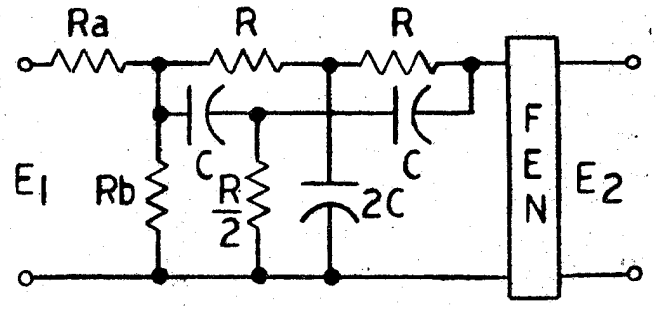

* NUMBER IN PARENTHESES REFERS TO RC CONFIGURATION IN TABLE I.

DATE FILE

TABLE 2: EXAMPLES OF BASIC 2ND ORDER FILTERS USING FEN'S

FILTER TYPE	VOLTAGE TRANSFER RATIO	NETWORK
1) LOW-PASS [1c]*	$\frac{E_2}{E_1} = K \cdot \frac{1}{s^2 + 2.66\omega_p s + \omega_p^2} \cdot \frac{s^2 + 2.66\omega_p s + \omega_p^2}{s^2 + \frac{\omega_p}{q_p} s + \omega_p^2}$ WHERE: $q_R = 0.375$	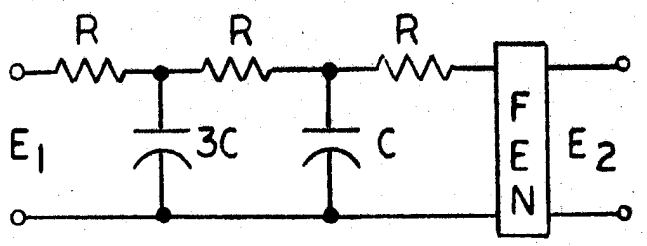
2) HIGH-PASS [2c]	$\frac{E_2}{E_1} = K \cdot \frac{s^2}{s^2 + 2.1\omega_p s + \omega_p^2} \cdot \frac{s^2 + 2.1\omega_p s + \omega_p^2}{s^2 + \frac{\omega_p}{q_p} s + \omega_p^2}$ WHERE: $q_R = 0.475$	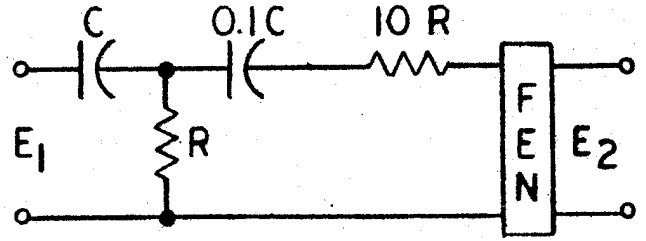
3) BAND-PASS [3c]	$\frac{E_2}{E_1} = K \cdot \frac{s}{s^2 + 2.2\omega_p s + \omega_p^2} \cdot \frac{s^2 + 2.2\omega_p s + \omega_p^2}{s^2 + \frac{\omega_p}{q_p} s + \omega_p^2}$ WHERE: $q_R = 0.455$	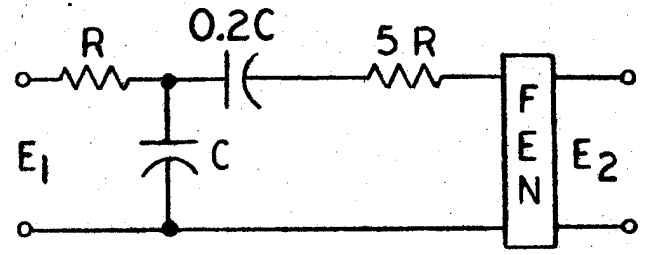
4) FREQUENCY REJECTION [6]	$\frac{E_2}{E_1} = K \cdot \frac{s^2 + \omega_z^2}{s^2 + 3.54\omega_p s + \omega_p^2} \cdot \frac{s^2 + 3.54\omega_p s + \omega_p^2}{s^2 + \frac{\omega_p}{q_p} s + \omega_p^2}$ WHERE: $R = \frac{1}{2} \frac{Ra\ Rb}{Ra + Rb}$ AND $q_R = 0.283$	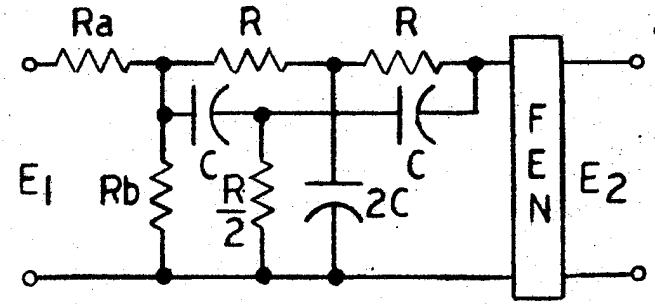

* NUMBER IN PARENTHESES REFERS TO RC CONFIGURATION IN TABLE 1.

TABLE 2 CONT

FILTER TYPE	VOLTAGE TRANSFER RATIO	NETWORK
5) CONJUGATE COMPLEX POLES AND ZEROS [5a]	$K \cdot \frac{s^2 + 1.63\,\omega_z s + \omega_z^2}{s^2 + 2.52\,\omega_p s + \omega_p^2} \cdot \frac{s^2 + 2.52\,\omega_p s + \omega_p^2}{s^2 + \frac{\omega_p}{q_p} s + \omega_p^2}$ WHERE: $R = \frac{R_a R_b}{R_a + R_b}$ AND $q_R = 0.396$	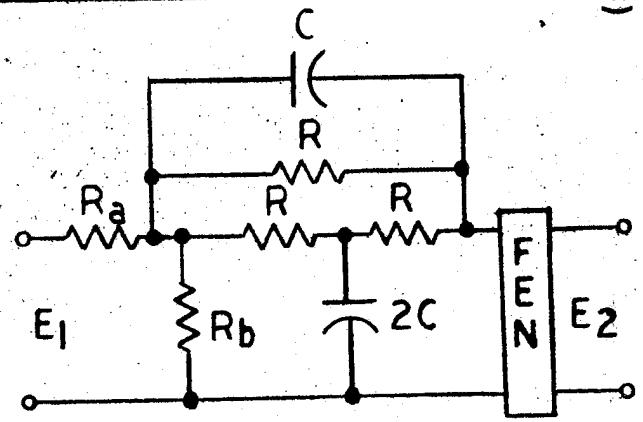
6) RESONATOR [4b]	$K \cdot \frac{s + \omega_z}{s^2 + 3.35\omega_p s + \omega_p^2} \cdot \frac{s^2 + 3.35\omega_p s + \omega_p^2}{s^2 + \frac{\omega_p}{q_p} s + \omega_p^2}$ WHERE: $q_R = 0.296$; $\omega_p = \frac{1}{2}\omega_z$	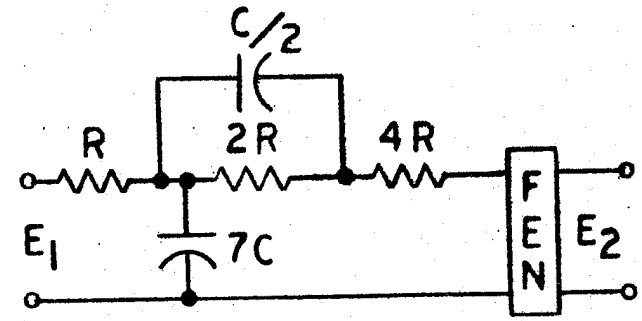

TABLE 3

CHARACTERISTICS OF TANTALUM THIN FILM PASSIVE COMPONENTS		
	Routine	Available
RESISTORS (Ta_2N)		
Range	10 Ω-250 KΩ	1 Ω-5 mΩ
Precision	0.1%	0.02%
Aging (20 years)	1%	0.05%
Temp Coeff. $\frac{dR/R}{°C}$	-70 ±30 ppm/°C	-200 to 1000 ppm/°C
Tunability	+20% ±0.1%	+50% ±0.1%
Tracking	±5 ppm/°C	
CAPACITORS ($Au/NiCr/Ta_2O_5/Ta$)		
Max C/Substrate	0.05 μf	1 μf
Precision	2 - 5%	1%
Stability (Humidity and Aging)	0.5%	0.1%
Temp Coeff. $\frac{dC/C}{C}$	200 ppm/°C	
Guaranteed Matching of Temp Coeff.		±30 ppm/°C

TABLE 4

COMPARISON OF LCR AND TA THIN FILM FREQUENCY STABILITY

Property	Ta Thin Film Resistors and Capacitors		Ferrite Core Ind and Polystyrene Cap	Permalloy Powder Core Ind and Polystyrene Cap (Hermetically Sealed)
	Routine	Available		
Inductor Precision			3 to 5%	0.1%
Aging			< 1.0%	0.1%
Temp Coeff			+410 ppm/°C	135 ±45 ppm/°C
Capacitor Precision	2 to 5%	1%	2 to 5%	2 to 5%
Aging	0.5%	0.1%	0.3 to 0.35%	0.1%
Temp Coeff	200 ppm/°C	-	-130 ±20 ppm/°C	-130 ±20 ppm/°C
Resistor Precision	0.1%	0.02%		
Aging	1%	0.05%		
Temp Coeff	-70 ±30 ppm/°C	-200 to 1000 ppm/°C		
Guaranteed Matching of Temp Coeff	±30 ppm/°C		±150 ppm/°C	±70 ppm/°C
Relative Frequency Drift over 50°C Temp Range	0.15% (±1.5 cps per 1000 cps)		0.38% (±3.8 cps per 1000 cps)	0.18% (±1.8 cps per 1000 cps)

TABLE 5

FEN/FRN PARAMETER ADJUSTEMENTS (See Figure 24).

	FEN	FRN
Input/Output Terminals, Type 1	2/3	11/10
Input/Output Terminals, Type II	2'/3	11/10
Open between terminals	-	11&10
Loop Gain (damping factor Q) determined by	R_Q,r	β,r
Forward Gain determined by	R_I	R_Q
Peak Frequency determined by	f_{Null} of $T_2(s)$	-
Null Frequency determined by	-	f_{Null} of $T_2(s)$
Pole - Zero Frequency Ratio determined by	-	r,c,β
High-Q operation - Noninverting VCVS - Open between terminals	Op. Amp. 4&5	Op. Amp. 4&5
Low-Q operation - Noninverting VCVS - Open between terminals	Darlington Pair 8&9 6&7	Darlington Pair 4&5

TABLE 5

FEN/FRN PARAMETER ADJUSTEMENTS (See Figure 24).

	FEN	FRN
Input/Output Terminals, Type 1	2/3	11/10
Input/Output Terminals, Type II	2'/3	11/10
Open between terminals	-	11&10
Loop Gain (damping factor Q) determined by	R_Q,r	β,r
Forward Gain determined by	R_I	R_Q
Peak Frequency determined by	f_{Null} of $T_2(s)$	-
Null Frequency determined by	-	f_{Null} of $T_2(s)$
Pole - Zero Frequency Ratio determined by	-	r,c,β
High-Q operation		
- Noninverting VCVS	Op. Amp.	Op. Amp.
- Open between terminals	4&5	4&5
Low-Q operation		
- Noninverting VCVS	Darlington Pair 8&9	Darlington Pair 4&5
- Open between terminals	6&7	